MODELING OF PERMEABILITY REDUCING VERTICAL CONFORMANCE TREATMENTS

by

JYUN-SYUNG TSAU, B.S.

THESIS

Presented to the Faculty of the Graduate School of

The University of Texas at Austin

in Partial Fulfillment

of the Requirements

for the degree of

MASTERS OF SCIENCE IN ENGINEERING

THE UNIVERSITY OF TEXAS AT AUSTIN

December 1985

ACKNOWLEDGEMENTS

The author wishes to express his sincere thanks and appreciation to his supervising professors, Dr. Alfred D. Hill and Dr. Kamy Sepehrnoori, for their guidance, assistance and encouragement throughout this study. In particular, their unending patience and understanding are deeply appreciated.

The financial support for this research, furnished by the University of Texas Center for Enhanced Oil and Gas Recovery Research, is gratefully acknowledged.

Special appreciation is expressed to his lovely wife, Su-Hwa, for her understanding, constant support during the course of this work.

Jyun-Syung Tsau

The University of Texas at Austin
December, 1985

ABSTRACT

Chemical treatments (usually polymer gels) are commonly used to improve the vertical conformance of oil reservoirs by selectively reducing the permeability in some zones near the well. The results of such treatments have been sporadic and unpredictable. The objective of this study is to define those reservoir characteristics which lead to successful treatments and to provide guidelines for the application of conformance treatments by modeling them with a reservoir simulator.

The computer simulator is the BOAST model, a multiphase, three-dimensional finite difference model written by Fanchi J. R. et al. and released by the Department of Energy. It was modified in areas such as the restart procedure , the rate allocation scheme, condition of well constraint, interpretation of relative permeability and implicit rate calculation to meet the objectives of this study.

Several cases have been run to identify the reservoir properties that strongly influence the outcome of a conformance treatment. These are the vertical permeability, the permeability thickness product contrast between layers, the permeability contrast, and the level of permeability reduction near the injection well. The results presented interpret the test cases and provide a basis for possible implementation of a successful conformance treatment.

Finallly, a field case is presented in which actual reservoir properties were used to study a conformance treatment.

TABLE OF CONTENTS

TABLE OF CONTENTS (CONT'D.)

LIST OF TABLES

LIST OF TABLES (CONT'D.)

LIST OF TABLES (CONT'D.)

LIST OF FIGURES

LIST OF FIGURES (CONT'D.)

LIST OF FIGURES (CONT'D.)

LIST OF FIGURES (CONT'D.)

LIST OF FIGURES (CONT'D.)

LIST OF FIGURES (CONT'D.)

CHAPTER I

INTRODUCTION

Because of the availability and relative ease of injection, water is frequently used in a flooding program to recover oil. However, since most reservoirs are normally composed of strata possessing wide variations in permeability which give different levels of entry for water, when water is injected , it is not distributed uniformly and seeks the path of least resistance to flow. Often, the main conductor of this injected water, called a thief zone, becomes depleted sooner than the less permeable zones and allows more water flow at a higher rate. Consequently, more and more water is injected through the thief zone while significant oil remains in the low permeability zone, resulting in a waterflood that is not efficient.

Various treatments have been developed to redistribute the water injected to the zones containing most of the remaining oil when water no longer effectively displaces the oil during the life of waterflooding. These treatments generally attempt to restrict water flow into the main conductors of water by plugging these layers in the wellbore or deeper into the matrix.

When treatments are performed within the wellbore, the sandface is simply shut-off by mechanical techniques shch as placing rubber sleeve over the thief zone or setting packer above and below the thief zone[1-3]. When treatments are implemented deeper into the matrix, plugging materials shch as granular leather, fibrous materials[4-5], polymers and gels can be used to reduce the permeability of thief zones[6-11].

Chemical treatment(usually polymer gels) are commonly used to reduce the permeability of main conductors of water due to its attractive properties that allow them to be injected a considerable distance into the formation.

In this thesis, we are concerned more about polymer gel treatment near the wellbore than the other treatment methods. However, due to the complexity of reservoirs, the results of field cases are often sporadic and unpredictable. Accordingly, attempts were made to investigate those reservoir characteristics which will lead to successful treatment.

In this chapter, the vertical conformance and permeability variation will be discussed first, followed by a literature survey of vertical conformance treatment and related simulation studies. Finally, the objective of this thesis is presented.

1.1 Vertical Conformance

Reservoir permeability variations result in different amount of water being injected into vertically distributed layers. This relative distribution is often qualitatively described as vertical conformance. In homogeneous reservoir, the water is uniformly distributed and as a consequence, exhibits a perfect vertical conformance. On the other hand, a heterogeneous reservoir has poor vertical conformance, hence the water is distributed in a nonuniform fashion.

In the predictions of waterflooding performance, the heterogeneity of a reservoir is often mesured quantitatively. Dykstra and Parsons[12] defined a coefficient of permeability variation, V , to measure the degree of heterogeneity. The coefficient ranges from zero for homogeneous to one for reservoir with extreme contrast in permeability among layers. Schmalz and Rahme[13] proposed the Lorenz coefficient of heterogeneity to characterize the permeability distribution. Analogous to permeability variation V, the value of the Lorenz coefficient ranges from zero to one, with a uniform permeability reservoir having Lorenz coefficient of zero. Other approaches used to distinguish the heterogeneity quantitatively were done by Stiles[14] and Miller and Lente[15].

1.2 Literature Survey of Vertical Conformance Treatments

Vertical conformance treatment methods are used to improve the vertical conformance of reservoirs. Its essential concept is to reduce the permeability of the thief zone and divert water into the zone containing most of the remaining oil. Materials such as polymers and gels which have chemical properties that allow them to be injected a considerable distance into the formation are applied. Systems which have been used include: polyacrylamide gels[6-7], crosslinked biopolymer[8], silica gels[9], lignosulfonate gels [10], and gelled furfuryl alcohol [11].

Various treatment methods are used in the oil industry. The polyacrylamide treatment(PAA) is most commonly used, for it possesses some attractive properties.

Polyacrylamide is used as a water reduction agent in production well and a mobility control agent in the injection well because of its ability to reduce the permeability of porous rock [16]. It is also used as a blocking agent due to its ability to be crosslinked by some multivalent ions such as aluminum [17], or chromium [18] to form a stable gel. When PAA solution is crosslinked in situ to form gels, the rock permeability is reduced deliberately and therefore the following water injected after PAA placement will be diverted. Furthermore, the gellation time can be controlled through adjusting the pH of the solution [17] or the flow rate [18]; this allows the mixture of polymer and crosslinking agents to travel deep inside the reservoir before gellation. The ability to considerably reduce rock permeability and to penetrate in-depth are reasons why PAA is commonly used in treatments.

When a polymer gel treatment is applied , either the thief zone is isolated so that the high permeability zone is the only entry for the polymer[19-20], or all zones are open to enable the polymer to seek the path of least resistance to flow[21]. In addition, due to the reactivity between crosslinking agent and polymers, either alternative slug[17,22] or simultaneous injection method may be applied[23] . When those reactions occur very fast, the polymers and crosslinking agents are injected with either small water spacers or a reducing agent in between so that the gellation is prevented until polymer and the crosslinking agent mix in the formation. On the other hand, polymer and crosslinking agents may be injected simultaneously, usually with the gellation chemically delayed until after the polymer is placed in the formation.

The properties of PAA with crosslinking agents can be determined through laboratory tests and controlled by field operations, but the results of such a treatment are not always as successful as expected. Thus, there is a need to examine the factors that might affect the results of the treatment through the use of simulation.

1.3 Literature Survey of Related Simulation Work

Some studies have been done by modeling the result on reservoir performance of profile control treatments. Luis F. Silva[24] et al. in 1971 presented a method for predicting waterflooding performance in the presence of reservoir stratification and formation plugging, using a two-phase three-dimensional reservoir simulator. In the case study of formation plugging, the high permeability strata was shut off as if a vertical conformance treatment had been applied. They noted the ineffectiveness of formation plugging when crossflow exists in the reservoir. This implies that for near wellbore treatments to improve oil recovery over a normal waterflooding, there must be virtually no crossflow in the reservoir.

M. K. Abdo et al[8]. employed a two-dimensional polymer, salinity, and surfactant model to study the effects of profile control by complexed biopolymer. They showed that in a reservoir with non-communicating layers, the selective placement of a viscous complexed biopolymer into the high permeability zone will cause an immediate response in the oil production rate, thus making the waterflood more effective. In the case of communicating layers, the oil production increase following polymer treatment is delayed and is less in magnitude than the non-communicating case. Based on their conclusions, it is possible to minimize the effect of communication as long as a more severe permeability reduction or a more in-depth treatment by the polymer is placed.

1.4 Objective of This Study

In the previous simulation studies, the vertical permeability and an assumed shut-off layer were investigated in conformance treatment. But the level of permeability reduction affected by polyacrylamide was not fully simulated. Also, the vertical flow in the reservoir is limited only to two extreme cases, non-communicating and fully communicating cases. In this study, the following parameters were varied widely to more fully determine the reservoir and treatment characteristics necessary for a successful treatment: vertical permeability, level of permeability reduction, permeability contrast between layers, and permeability-thickness product contrast between layers.

To model this system, a black oil model was used to simulate a waterflood in a multi-layer reservoir with contrasting permeabilities in the various layers. At some point during the waterflood, the permeability of the high permeability zone is altered in the grid block at the injection well as if it were treated by polyacrylamide. The waterflood is then continued to an economic limit, and the results of oil recovery are compared with and without the hypothetical treatment.

1.5 Outline of This Study

A comprehensive model of polymer treatment was developed by using BOAST program in this work, and six chapters are included.

Chapter I is the introduction.

Chapter II describes the mathematical model used.

Chapter III discusses the selection of an appropriate black-oil model for use. The intercomp BETA II model and the DOE BOAST model were compared. BOAST was selected primarily because its codes could be modified to suit our needs.

Chapter IV discusses the assumptions and modifications needed to simulate a polymer conformance treatment with a black-oil model.

Chapter V covers the results and discussion of the simulation runs. Several parameters that were thought important to the outcome of a conformance treatment were varied to determine their effect. The parameters that were investigated include the permeability contrast between zones, the vertical permeability, the zone thickness ratio, and the level of permeability reduction which is assumed to occur during treatment.

Chapter VI is a field case study in which actual reservoir properties were used to study the effect of conformance treatment. The results of the treatment were interpreted in the end of this chapter.

Chapter VII is the conclusion and recommendations of future areas where there is the need for further investigation concerning conformance treatments.

CHAPTER II

MATHEMATICAL MODEL OF THE VERTICAL CONFORMANCE TREATMENT

A comprehensive polymer treatment can be modeled by a black oil model if the actual PAA placement is simplified by artificially reducing the permeability around the wellbore in the simulation . Thus, the mathematical model for this study is based on the derivation of a black oil model.

2.1 Description of Mathematical Model

The basic form of mass conservation equation for isothermal fluid flow in porous media is

$$\partial W_i/\partial t + \vec{\nabla}\cdot \vec{N}_i = R_i \tag{2.1}$$

where W_i is accumulation term defined by

$$W_i = \sum_{j=1}^{M} \phi \rho_j S_j w_{ij} + (1-\phi)\rho_s w_{is} \tag{2.2}$$

$\vec{N}_i$ is the flux term, defined by

$$\vec{N}_i = \sum_{j=1}^{M} (\rho_j w_{ij} \vec{u}_j - \phi \rho_j S_j \vec{K}_{ij} \vec{\nabla} w_{ij}) \tag{2.3}$$

$\vec{R}_i$ is the source term, defined by

$$\vec{R}_i = \sum_{j=1}^{M} \phi S_j \Upsilon_j + (1-\phi)\Upsilon_{is} \tag{2.4}$$

In a three phase, three component system, based on the following assumptions, eq.(2.1) can be split into equations representing each component. These assumptions are:

(1) No mass transfer between oil and water or between water and gas.

(2) Aqueous phase contains only water.

(3) Oleic phase does not contain water.

(4) Gaseous phase contains only gas.

(5) The system is isothermal .

(6) No chemical reaction between fluids nor between fluid and rock.

(7) No adsorption.

(8) Darcy flow applicable.

Subsequently, according to the mass fraction definition

$$\sum_{i=1}^{N} w_{ij} = 1 \tag{2.5}$$

let i = 1 represent water

2 represent oil

3 represent gas

and j = 1 represent aqueous phase

2 represent oleic phase

3 represent gaseous phase

Then, from assumption (1) and (2)

$$w_{11} = 0;\ w_{21} = 0,\ w_{31} = 0$$

was obtained;

from assumption (1) and (3)

$$w_{12} = 0,\ w_{32} + w_{22} = 1$$

from assumption(1) and (4)

$$w_{33} = 1,\ w_{13} = 0,\ w_{23} = 0$$

and from assumption(2),(3),(4)

$$w_{is} = 0$$

In addition, assumption (6) makes eq.(2.4)

$$R_i = 0$$

Then, for each component, including the production conservation equation for each component is:

For water

$$\partial/\partial t(\phi \rho_1 S_1) + \vec{\nabla}\cdot(\rho_1 \vec{u}_1) = q_1 \qquad (2.6)$$

For oil

$$\partial/\partial t(\phi \rho_2 S_2) + \vec{\nabla}\cdot(\rho_2 w_{22} \vec{u}_2) = q_2 \qquad (2.7)$$

For gas

$$\partial/\partial t(\phi \rho_3 S_3 + \phi \rho_2 w_{32} S_2) + \vec{\nabla}\cdot(\rho_3 \vec{u}_3 + \rho_2 w_{32} \vec{u}_2) = q_3 \qquad (2.8)$$

According to the definition

w_{22} = mass of oil / mass of oleic phase

= (mass of oil / standard volume of oil)/

[(mass of oleic phase / volume of oleic phase) ×

(volume of oleic phase / standard volume of oil)]

$= (\rho_2)_{sc}/\rho_2 B_2$

Similarly,

$$w_{33} = (\rho_3)_{sc} R_s/\rho_2 B_2$$

And because the mass fraction of oil in oleic phase is equal to unity when reservoir condition approaches to standard condition, then

$$w_{22} = 1$$

and

$$\lim_{T,p \to T_{sc},p_{sc}} \rho_2 B_2 = (\rho_2)_{sc}/w_{22} = (\rho_2)_{sc}$$

and since gas is no longer soluble in oil when the condition is at standard condition:

$$\lim_{T,p \to T_{sc},p_{sc}} w_{32} = 0$$

Consequently, formation volume factors are brought into mass conservation equations and eqs.(2.6),(2.7),(2.8) become

$$\partial/\partial t(\phi S_1/B_1) + \vec{\nabla}\cdot(\vec{u}_1/B_1) = q_1 \quad (2.9)$$

$$\partial/\partial t(\phi S_2/B_2) + \vec{\nabla}\cdot(\vec{u}_2/B_2) = q_2 \quad (2.10)$$

$$\partial/\partial t(\phi S_3/B_3 + \phi S_2 R_S) + \vec{\nabla}\cdot(\vec{u}_3/B_3 + R_S\vec{u}_2/B_2) = q_3 \quad (2.11)$$

From the assumption (8), the flux term is written as

$$\vec{u}_j = -\lambda_j \bar{k}\cdot(\vec{\nabla}p_j - \rho_j g\vec{\nabla}D) \quad (2.12)$$

Substitute it into eqs.(2.9),(2.10),(2.11) and change the notation of subscripts 1,2,3 into w(water),o(oil),g(gas) respectively, the final form of equation(2.1) becomes

$$\partial/\partial t(\phi S_w/B_w) - \vec{\nabla}\cdot[\,\bar{k}\,\lambda_w/B_w(\vec{\nabla}p_w - \rho_w g\vec{\nabla}D)\,] = q_w \quad (2.13)$$

$$\partial/\partial t(\phi S_o/B_o) - \vec{\nabla}\cdot[\,\bar{k}\,\lambda_o/B_o(\vec{\nabla}p_o - \rho_o g\vec{\nabla}D)\,] = q_o \quad (2.14)$$

$$\partial/\partial t(\phi S_g/B_g + \phi S_o R_S/B_o) + \vec{\nabla}\cdot[\,\bar{k}\,\lambda_g/B_g(\vec{\nabla}p_g - \rho_g g\vec{\nabla}D)$$
$$+ R_S\bar{k}\,\lambda_o/B_o(\vec{\nabla}p_o - \rho_o\vec{\nabla}D)\,] = q_g + R_S q_o \quad (2.15)$$

In order to solve these equations simultaneously, we also need to introduce the concept of capillary pressure.

$$P_{cow} = p_o - p_w \quad (2.16)$$

$$P_{cgo} = p_g - p_o \quad (2.17)$$

The difference P_{cow} and P_{cgo} are the capillary pressure of oil-to-water and gas-to-oil phases,respectively.

The saturation terms sum to unity

$$S_o + S_w + S_g = 1 \quad (2.18)$$

The compressibility terms are defined as

$$C_r = (1/\phi)(\partial\phi/\partial p_o)$$

$$C_g = -(1/B_g)(\partial B_g/\partial p_o)$$

$$C_w = -(1/B_w)(\partial B_w/\partial p_o)$$

$$C_o = (1/B_o)(\partial B_o/\partial p_o) + (B_g/B_o)(\partial R_s/\partial p_o)$$

$$C_t = C_r + C_o S_o + C_w S_w + C_g S_g$$

The final working equation for three-phase compressible fluid flow is rearranged from equations (2.13),(2.14),(2.15),(2.16), and (2.17) to

$$\begin{aligned}
&(B_o - R_s B_g)[\,(\vec{\nabla}\cdot\bar{K}\,\lambda_o/B_o)(\vec{\nabla}p_o - \rho_o g\vec{\nabla}D) - q_o\,] + \\
&B_w\,[\,(\vec{\nabla}\cdot\bar{K}\,\lambda_w/B_w)(\vec{\nabla}p_w - \rho_w g\vec{\nabla}D - p_{cow}) - q_w\,] + \\
&B_g\vec{\nabla}\cdot\bar{K}\,[\,\lambda_g/B_g(\vec{\nabla}p_o - \rho_g\bar{D} - p_{cgo}) + R_s\lambda_o/B_o \\
&(\vec{\nabla}p_o - \rho_o g\vec{\nabla}D) - q_g\,] = \phi C_t\partial p_o/\partial t
\end{aligned} \tag{2.19}$$

2.2 Finite Difference Equations

Using a block-centered grid system with backward difference in time, the partial differential equations of (2.13),(2.14) and (2.19) are approximated by the finite difference method as

$$\begin{aligned}
&[\,\Delta A_w^n \Delta p^{n+1} - \Delta A_w^n\,\Delta(\rho_w D + p_{cow})^n - q_w V_B\,]_{ijk} \\
&= 1/\Delta t\,[\,(V_p S_w/B_w)^{n+1} - (V_p S_w/B_w)^n\,]_{ijk}
\end{aligned} \tag{2.20}$$

$$\begin{aligned}
&[\,\Delta A_o^n \Delta p^{n+1} - \Delta A_o^n\,\Delta(\rho_o D)^n - q_o V_B\,]_{ijk} \\
&= 1/\Delta t\,[\,(V_p S_o/B_o)^{n+1} - (V_p S_o/B_o)^n\,]_{ijk}
\end{aligned} \tag{2.21}$$

and

$$\begin{aligned}
&(B_o - B_g^n R_s)_{ijk}\,[\,\Delta A_o^n \Delta p^{n+1} - \Delta A_o^n\,\Delta(\rho_o D)^n - q_o V_B\,]_{ijk} \\
&+ (B_w^n)_{ijk}\,[\,\Delta A_w^n \Delta p^{n+1} - \Delta A_w^n\,\Delta(\rho_w D + p_{cow})^n - q_w V_B\,]_{ijk} \\
&+ (B_g^n)_{ijk}\,[\,\Delta A_g^n \Delta p^{n+1} + \Delta R_s^n A_o^n \Delta p^{n+1} + \Delta A_g^n\,\Delta(\rho_g D + p_{cgo})^n \\
&- \Delta R_s A_o^n \Delta\rho_o - q_g V_B\,]_{ijk} \\
&= (V_p C_t/\Delta t)_{ijk}^n (p^{n+1} - p^n)_{ijk}
\end{aligned} \tag{2.22}$$

where superscript n denotes properties evaluated at old time level and n+1 at new time level. The subscripts i,j,k denote the position of node in the grid block system and is shown as Fig.1.

Fig. 1 NODE REPRESENTTATION OF GRID
BLOCKS IN THREE DIMENSIONAL CASE

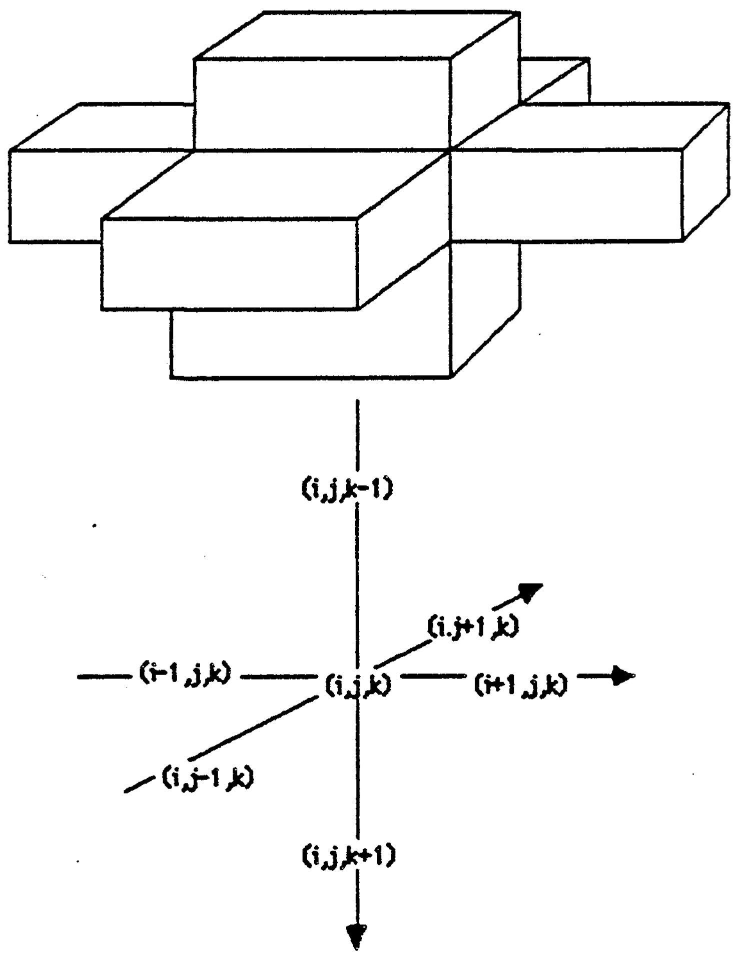

The linear difference operator used here is defined as

$$\Delta A \Delta p = \Delta_X A \Delta_X p + \Delta_Y A \Delta_Y p + \Delta_Z A \Delta_Z p$$

and

$$\Delta_X A \Delta_X = A_{i-1/2,j,k}(p_{i-1,j,k} - p_{i,j,k}) + A_{i+1/2,j,k}(p_{i+1/2,j,k} - p_{i,j,k})$$

The transmissibility A is defined as

$$A_{i-1/2,j,k} = \frac{2\,(\Delta x \Delta y)_{i,j,k}\; k_{i-1/2,j,k}\; \lambda_{i-1/2,j,k}}{(\Delta x_{i,j,k} + \Delta x_{i-1,j,k})}$$

where the interblock permeability is obtained by harmonic average as

$$k_{i-1/2,j,k} = \frac{2\,(k_{i,j,k})(k_{i-1,j,k})}{[\Delta x_{i-1,j,k}(k_{i,j,k}) + \Delta x_{i,j,k}(k_{i-1,j,k})]} \times \frac{1}{(\Delta x_{i,j,k} + \Delta x_{i-1,j,k})}$$

2.3 Description of Reservoir Modeling in Vertical Conformance Treatment

As discussed in Chapter 1, a factor to affect the vertical conformance treatment might be the crossflow between layers of reservoir. A two dimension cross-sectional model is chosen so that concentration on the crossflow might be singled out in our study.

The finite-difference technique of numerical solution of differential equations requires that the portion of the reservoir for our study be divided into grid blocks as shown in Fig.2. In this model, two wells are imposed on each extreme side of the system, one of them being an injection well, the other a production well. Since we do not take polyacrylamide into account in the programming when simulating the treatment, the equivalent effect is set by artificially reducing the permeability of the grid block which contains an

FIG.2 RESERVOIR GRID SYSTEM

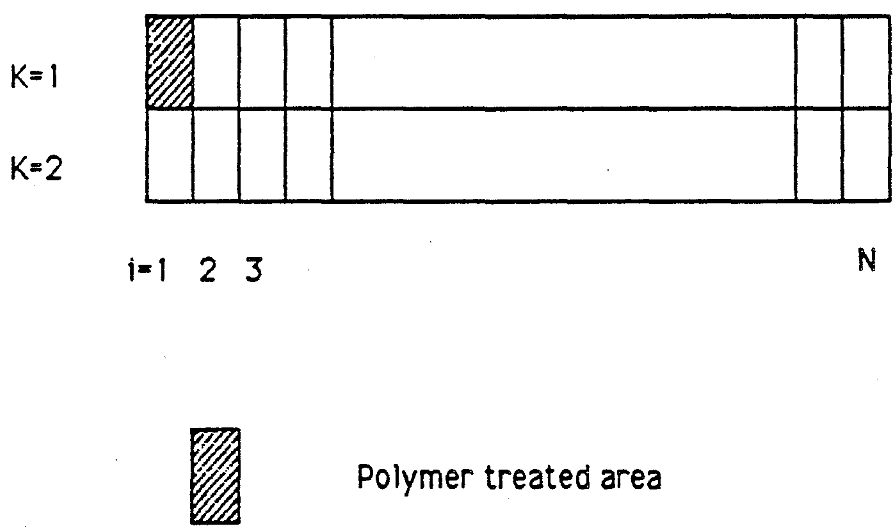

injection well to a factor as though the permeability near the wellbore were reduced by polyacrylamide.

Chapter III

SELECTION OF SIMULATOR

Based on the assumptions made in previous chapter, the black oil simulator is suitable for our purpose if we artificially reduce the permeability in some grids at a certain time during the simulation. Two black oil simulators, the Intercomp BETA II and the DOE BOAST are available in the Department of Petroleum Engineering. Both are suitable for our needs and will be briefly introduced here. For detailed description, reader can refer to the user's manual of Intercomp BETA II [25] and BOAST[26].

3.1 Description of the Simulators Available

Intercomp BETA II block oil model is designed to simulate numerically two or three-phase compressible fluid flow in heterogeneous reservoir. Gas is assumed to be soluble in oil only. Numerical solutions may be obtained in one, two, or three spatial dimension, using either rectangular or cylindrical coordinates.

With the finite difference formulations, the program decouples the equations and solves either pressure equations implicitly and saturation equations explicitly (so-called IMPES) or both pressure and saturation equations implicitly (fully implicit).

To solve the large system of linear algebraic equations, several choices are available in BETA II. Either direct or iteration methods can be used. In the direct method, the Gaussian elimination method is applied to solve a small system of equations. For large systems (for example, three-dimensional problem), an iteration method is used, in which both the successive overrelaxtion method (SOR) and the strongly implicit procedure (SIP) are applied.

Another simulator available in this Department is the DOE BOAST simulator. BOAST is also designed to model isothermal, three phase compressible fluid flow of reservoir in up to three dimensions . It can be used in rectangular coordinates only.

With IMPES formulation, BOAST solves the pressure implicitly and the saturation equation explicitly.

For the solution scheme, a band solver is used for small systems like the one dimensional problem, the D4 order scheme is used in intermediate systems such as two dimensional system, and an iteration solution method (LSOR) is used for large two dimensional or three dimensional systems.

Since both simulators are IMPES formulation simulators, the stability problem is commonly encountered when the transmissibility is estimated by an explicit method. In such a case, the mobility terms in system equations are treated at the old time level but the actual computation of pressure equations uses the new time level. Conditional instability occurs if the product of the time step size and the flow velocity is greater than a grid block size[31]. Therefore, to ensure the stability and accuracy of solution in the IMPES simulator, the maximum time step size used must be tested and selected cautiously to ensure the stability of solution. However, sometimes the well rate changes drastically between each time step, and use of manual selection of the time step size will jeopardize the results of simulation. Accordingly, to avoid the possible instability, the time step size may be adjusted through an automatic time step control. Both simulators have incorporated automatic time step control, where the users are able to choose either a maximum saturation or a maximum pressure change as the control parameter for adjusting the time step size. This option enables the automatic time step control to choose small time step sizes whenever conditions change drastically and large time step sizes in the case of condition where the changes in conditions are minimal, allowing the user to control either stability or computation time.

3.2 Selection of Simulator

BETA II and BOAST simulators have many similar features and both are suitable for our uses. According to the factors concerned such as (1)accessibility, (2)accuracy, and (3) computation time, BOAST simulator is chosen to use in our study.

(1) Accessibility

The BETA II is a commercialized simulator, it is designed for users to easily use, but the source code is not accessible publicly. However, BOAST is a simulator publicly available, and its source code is easy to modify.

(2) Accuracy

Two cases extracted from the sample problem of BOAST's users manual were run to compare the simulation results between these two existing simulators, and when possible, with analytical solutions.

(A) One dimensional waterflooding problem

The one dimensional waterflood problem is often chosen as a test problem used to validate a simulator, because its results are easily compared with analytical solutions from the Buckley-Leverett theory. In one dimensional water displacement, the water front velocity calculated from Buckley-Leverett equation is

$$(dx/dt)_{S_w} = (u_t / \phi)(df_w/dS_w)$$

which implies that the water front velocity is proportional to the first derivative of fractional flow with respect to the saturation of water front. Therefore, we can calculate the velocity analytically and then compare the results from both simulators. In the testing example 1, a one dimensional linear grid system is constructed as a model of a homogeneous, horizontal reservoir. Oil production is under a rate constraint of 600 STB per day from one grid block. The oil production is balanced by water injection under the rate constraint of 900 STB per day at the opposite end of the grid block system. The thickness of a grid block is 20 feet. The grid size in y direction is 1320 feet. The porosity is 0.25 and the df/dsw calculated from the fractional flow curve is 1.91. Thus, with a total flow rate of 900 STB/day, the velocity of the water front is 1.5 ft/day. By the 120th day and by the 360th day, the water front should have advanced 180 ft (the ninth grid) and 540 ft (the 27th grid), respectively.

The results at two different times for both simulators are shown in Fig. 3 and Fig. 4 where the water saturation profiles are plotted with some smearing against the analytical solution. There is not much difference between two profiles in each plot, but the smearing for Beta II simulator is a little larger. The smearing, due to numerical dispersion, which is attributed to the truncation errors, exists in all finite difference simulators. A higher order approximation, a moving point method, or a finite element method is helpful to minimize the smearing, but it is beyond the scope of this research.

FIG.3 WATER SATURATION PROFILE AT TIME= 120 DAYS
FOR TEST PROBLEM 1

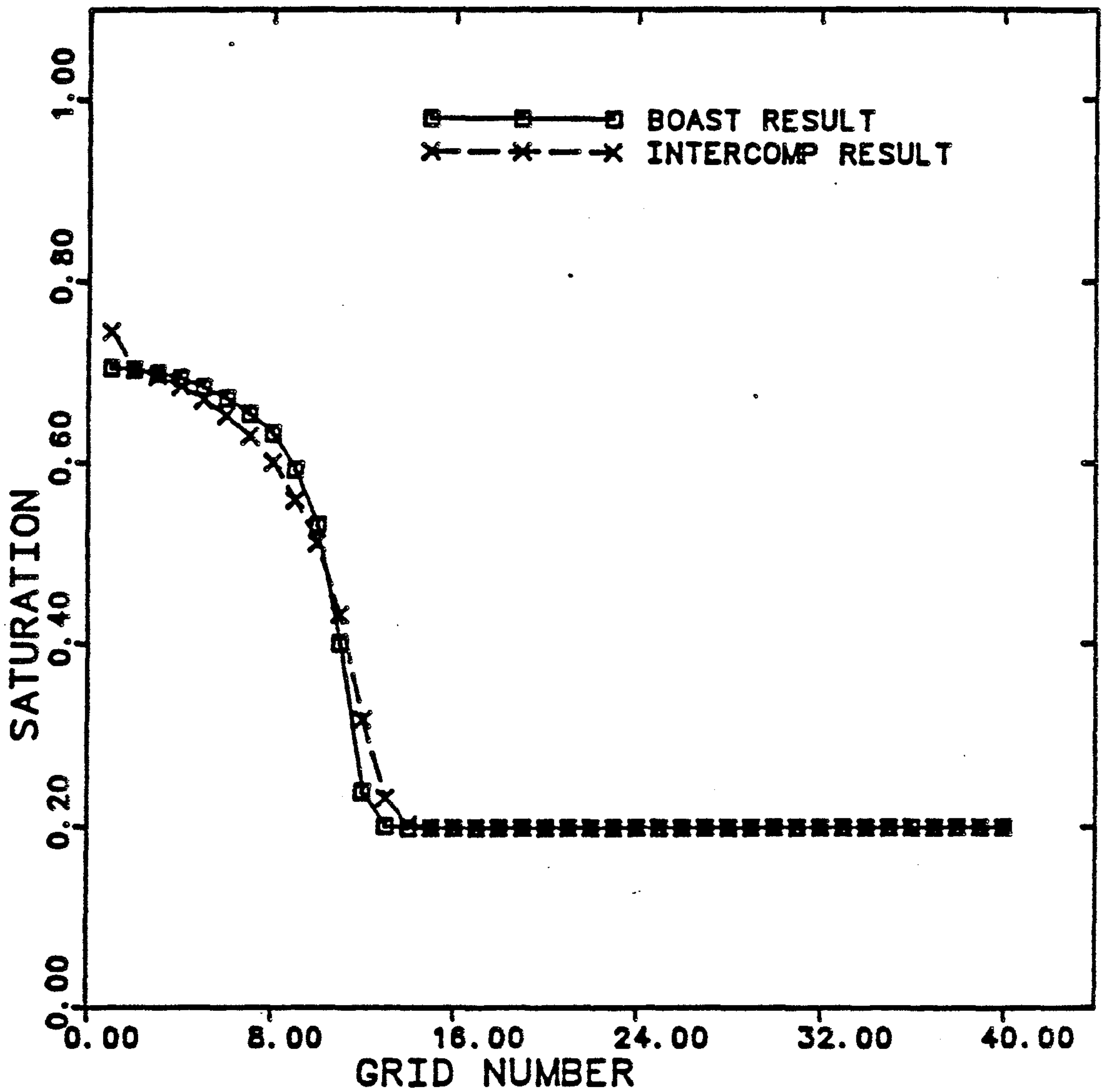

FIG. 4 WATER SATURATION PROFILE AT TIME = 360 DAYS
FOR TEST PROBLEM 1

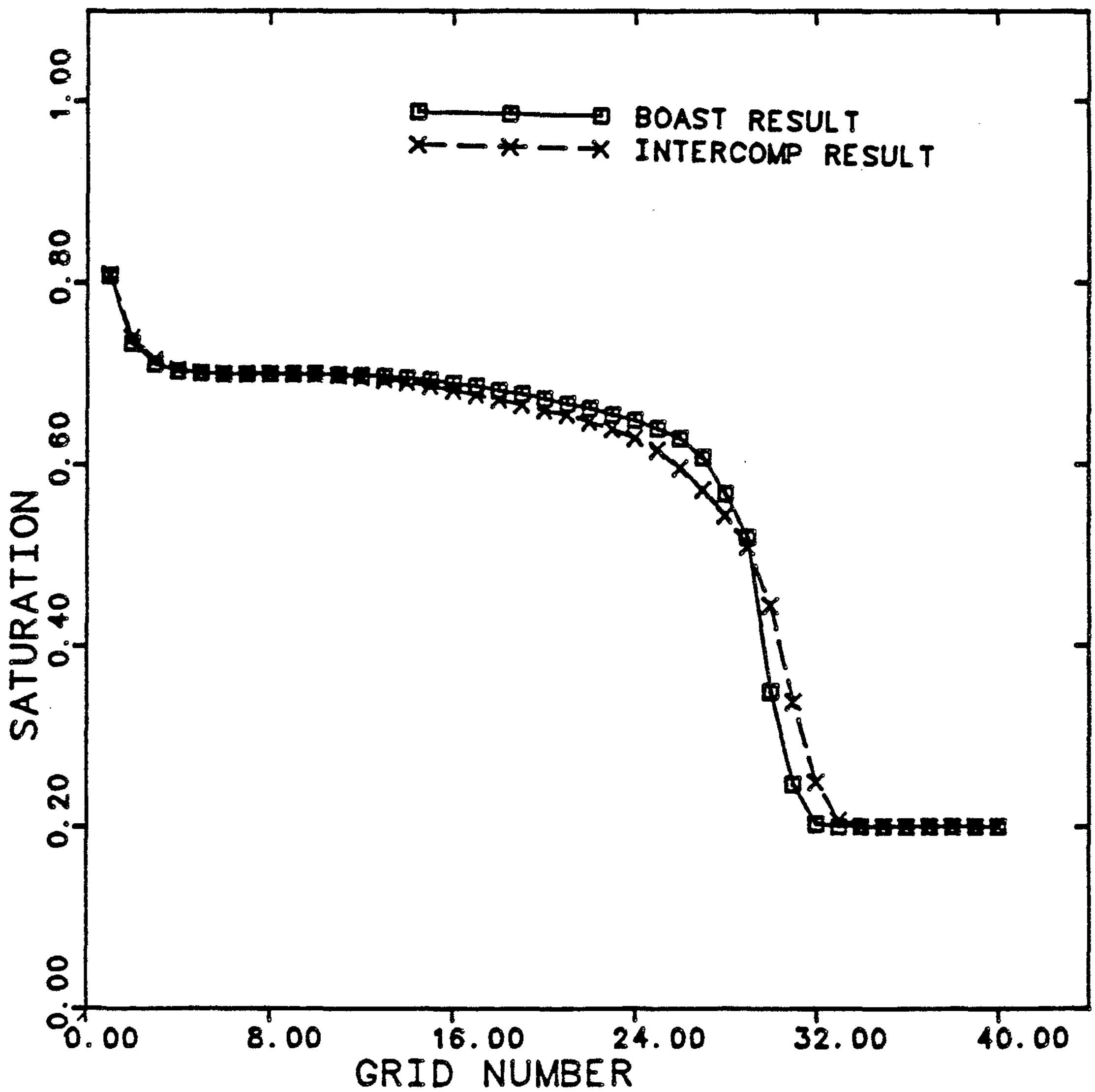

(B)Cross-sectional model showing line-drive waterflooding of an undersaturated reservoir

For practical reason, the cross-sectional problem is chosen to single out the effects of flow in vertical direction. A linear grid with 20 blocks in x direction, 5 grid blocks in z direction was constructed. Each end grid block contains one well, and a vertical to horizontal permeability ratio of 0.1 was used. The performance of the production well is shown in Fig. 5. The average pressure of the reservoir, production rate and water oil ratio are shown in Fig. 6, 7, 8, respectively. Although there is no analytical solution to be compared to, both simulators yield essentially identical results for a five layer cross-sectional system.

(3) Computation time

In the two examples where direct methods were used, the simulators showed different computation times. The BETA II which was on CDC computer had a computation time of 10 micro second for each time step per grid block, while BOAST which was run on VAX computer had a computation time of 12 micro second for each time step per grid block. This difference is small enough to be ignored.

From the comparisons mentioned earlier, the accuracy and computation time do not differ much for the two simulators. The BOAST was chosen simply because it was felt that there might be a need to modify the simulator in order to model vertical conformance treatment.

FIG. 5 PRODUCTION HISTORY FOR TEST PROBLEM 2

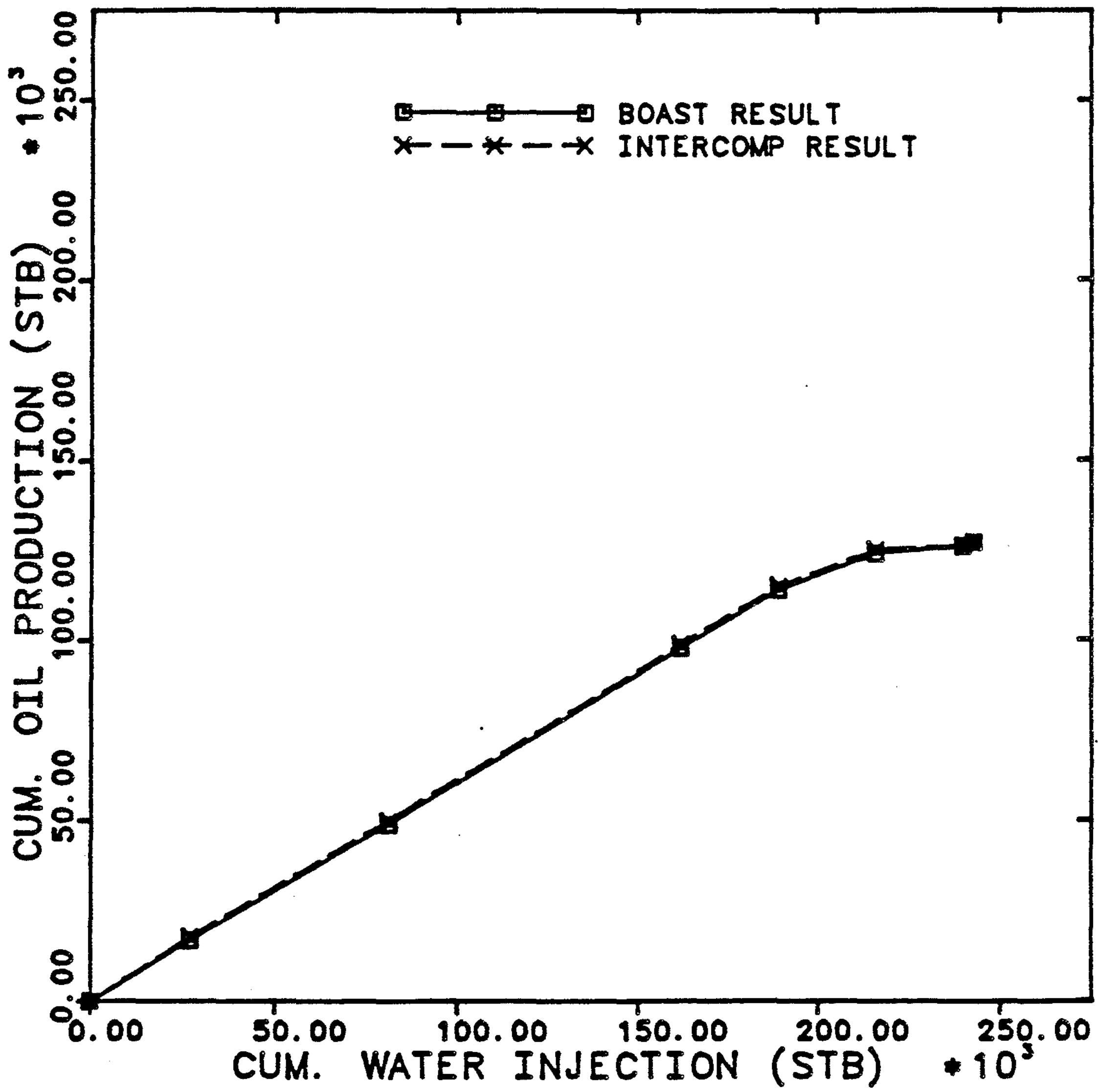

FIG. 6 RESERVOIR AVERAGE PRESSURE OF TEST PROBLEM 2

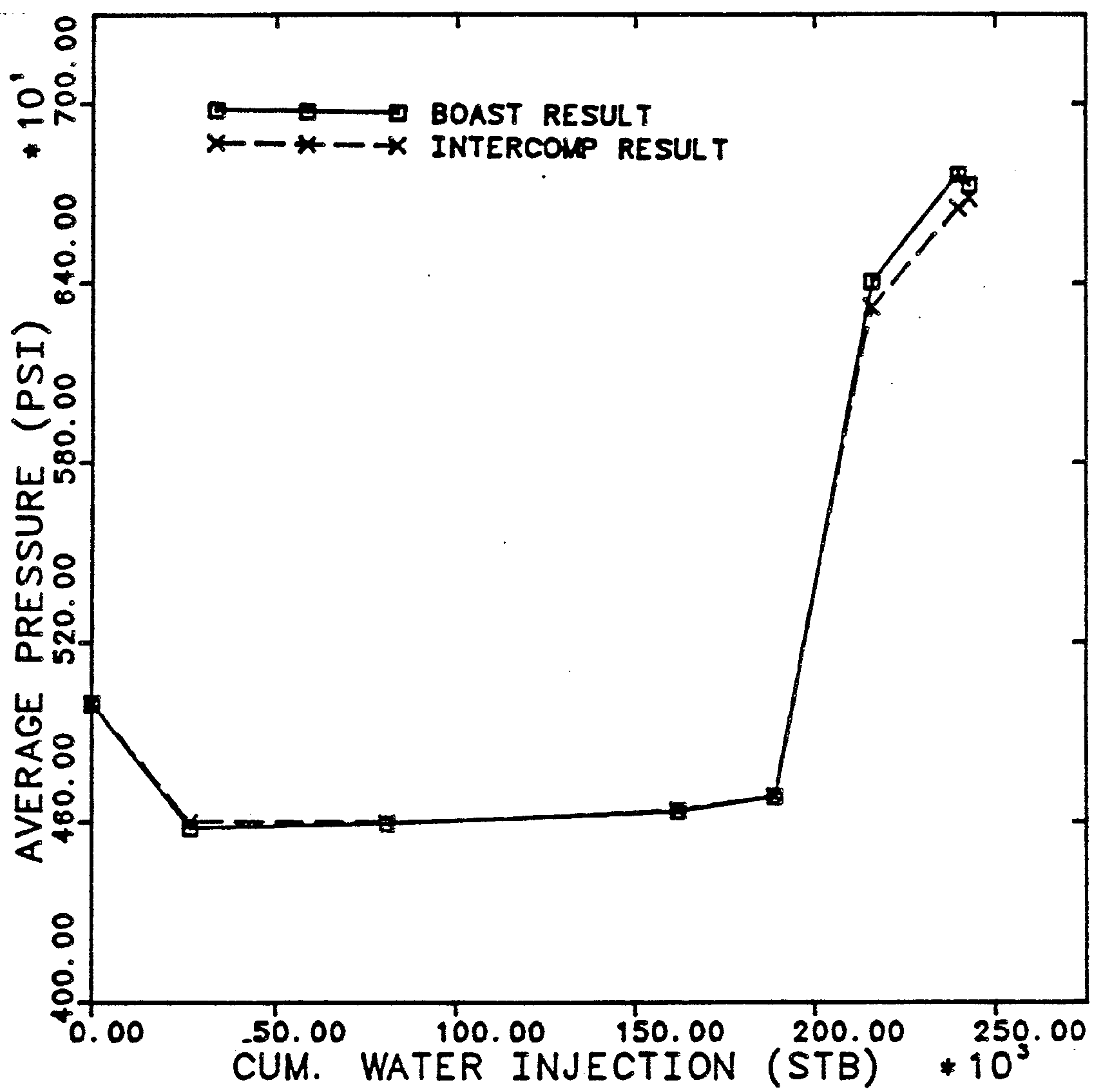

FIG. 7 OIL PRODUCTION RATE FOR TEST PROBLEM 2

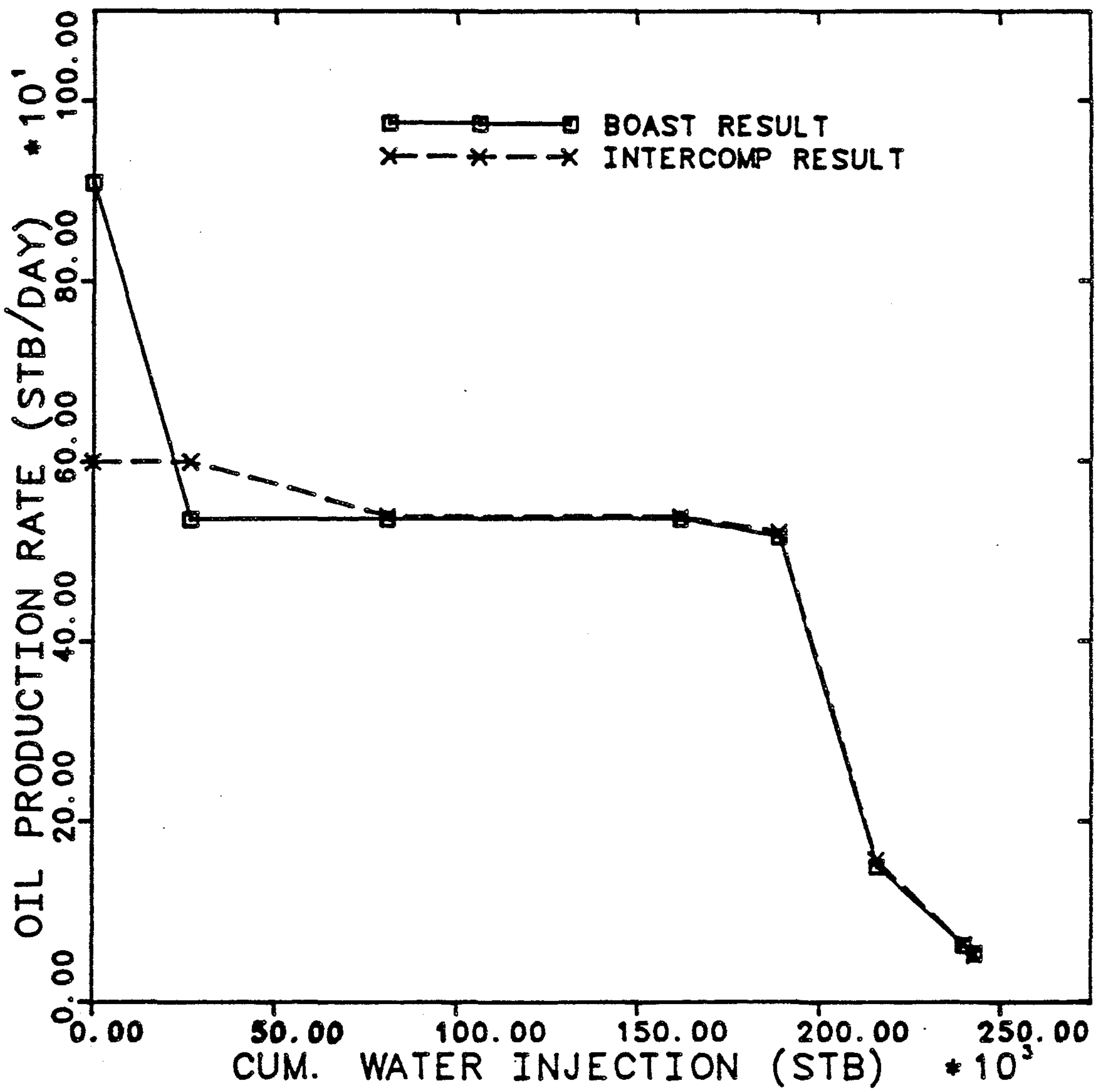

FIG. 8 WATER OIL RATIO FOR TEST PROBLEM 2

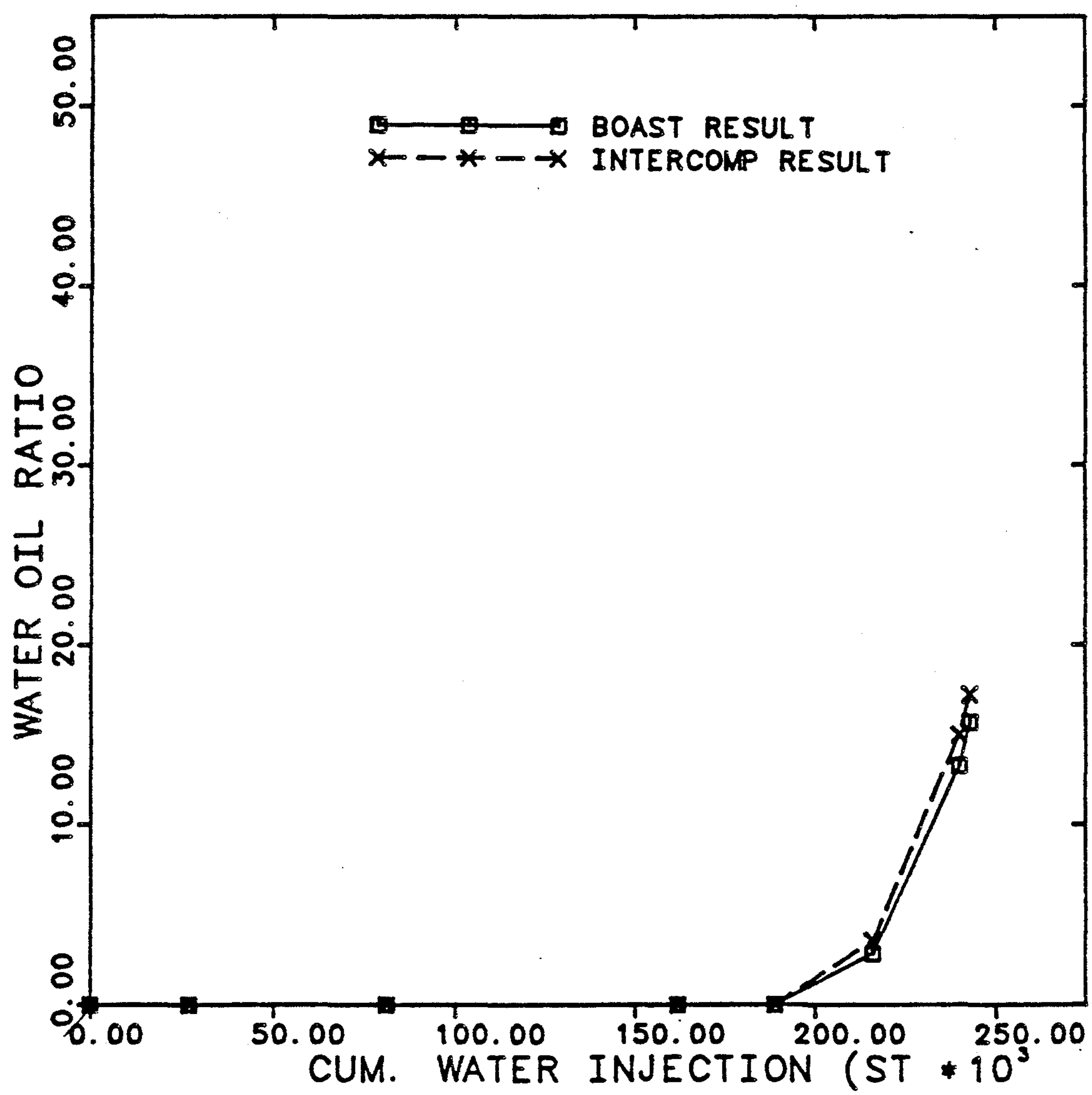

CHAPTER IV

MODIFICATION OF BOAST

Although many commonly encountered black oil reservoir simulation problems can be done by using BOAST, several modifications are needed to model a vertical conformance treatment. They are discussed in the following sections. First, a restart procedure was added to enable the program to change reservoir properties. Second, the rate allocation scheme was changed from a mobility method to a potential method to more realistically model well conditions. Third, the well constraint was modified to consider the injection well performance in the process. Fourth, a method to calculate the relative permeability of oil in a three-phase system was added to meet the requirement of input and interpretation of relative permeability data. Finally, a modification of source terms was incorporated to enable us to improve the stability of the pressure solution. As for their implementations, the first three modifications were used in the case studies discussed in Chapter V ; the last two modifications were specifically used in the field case study discussed in Chapter VI.

4.1 Restart Option

To simulate a polymer conformance treatment with a black oil model, the permeability of the formation in the grid block near the wellbore must be artificially modified at a certain time according to criteria concerning the waterflood. Thus, interruption in the simulation is needed. As a consequence, a restart option was added to BOAST to enable us to stop the simulation, change reservoir properties, and then continue the waterflooding. The criteria most often used in waterflooding are (1) cumulative injected water, (2) elapsed time, and (3) water oil ratio were included in the program to initiate the restart procedure.

In order to enable the restart option to work, the sequence of input data was changed and a subroutine REREAD was added in the program for retrieving the data . The sequence of input data was rearranged as two sections: Non-recurrent and Recurrent sections. Non-recurrent section includes (1) rock properties, (2) initial conditions, (3) PVT table of fluid, (4) reservoir dimensions, size, grid number. Recurrent section includes (1) well information, (2) time step size.

For the convenience of implementation of the restart, all the data needed were separated into several files in sequence. Rock properties were stored in a file called " KPHI.DAT " initially, but were changed once the treatment started. The changed rock properties were created in the file " MODKPHI.DAT " . The file " MODKPHI.DAT " was in place of " KPHI.DAT " after the treatment was assumed to take place. Besides, a specific file called " RESTART.DAT " was obtained as a result of the interruption simulation and applied in the continuation of simulation with the " MODKPHI.DAT ". The initial reservoir conditions set in " INITIAL.DAT " with all the other data necessary were involved in " REBOAST.DAT ". When waterflood proceeded before the treatment, the data files used were KPHI.DAT, INITIAL.DAT, and

REBOAST.DAT; but when treatment started, the files used were MODKPHI.DAT, RESTART.DAT, and REBOAST.DAT.

Several output files were also arranged to plot the saturation distribution, pressure distribution, production rate curve and production history, respectively. A brief description of the relationship between these files is incorporated in the flow chart of the simulation work in the appendix.

4.2 Modification of Rate Allocation Scheme

A well model is always incorporated in the simulation to represent the source or sink terms. In an areal model problem, the well model is interpreted as a point source or sink term, but in a cross-section model problem, the well model is interpreted as a line source or sink term. Distributing different flow into different layer is necessary in the cross-section model. There are two different rate allocation methods in the literature[27,28], the mobility allocation method and the potential allocation method.

(1) Mobility allocation method

The BOAST simulator uses the mobility allocation method which assures that the difference of potential between the wellbore and a grid block is the same for all blocks communicating with a given well. The rate is therefore allocated to each zone according to the ratio of mobility in each zone. Under this assumption, the flow rate into each layer was distributed as

$$Q_{\ell K} = \frac{F_K \sum_{\ell}^{M} (\lambda_\ell/B_\ell)_K}{\sum_{K}^{L}\sum_{\ell}^{M} F_K (\lambda_\ell/B_\ell)_K} Q_T \tag{4.1}$$

where

$$F_K = \frac{0.00708\, kh}{\ln(0.121\sqrt{\Delta x \Delta y}/r_w) + s}$$

(2)Potential allocation method

The potential method accounts for the fact that the potential difference between the well and a grid block containing the well may differ in each layer so that the potential difference is taken into account and the flow rate entering into each layer is

$$Q_{\ell K} = \frac{F_K \sum_{\ell}^{M} (\lambda_\ell/B_\ell)_K \Delta\Phi_{\ell K}}{\sum_{K}^{L}\sum_{\ell}^{M} F_K (\lambda_\ell/B_\ell)_K \Delta\Phi_{\ell K}} Q_T \tag{4.2}$$

where $\Delta\Phi$ is the potential difference between wellbore and grid block containing the well .

These two equations will be the same if we crossed out the potential difference in eq.(4.2), which implies that the potential difference in each layer is the same for all layers. Intuitively, eq.(4.1) seems to be a special case of eq. (4.2). In fact, we may derive eq.(4.2) as a general equation used in dealing with the rate distribution.

The basic equation describing the rate is

$$Q_{\ell K} = F_K (p_K^w - p_{\ell K}) (\lambda_\ell/B_\ell)_K \tag{4.3}$$

in terms of potential $\Phi_K = p_K + \rho gh$

eq.(4.3) becomes

$$Q_{\ell K} = F_K (\Phi_K^W - \Phi_{\ell K}) (\lambda_\ell/B_\ell)_K \tag{4.4}$$

By definition, the total rate is equal to the sum of rate in each layer, so

$$Q_T = \sum_K^L \sum_\ell^M Q_{\ell K} \tag{4.5}$$

Substituting eq(4.4) to (4.5)

$$Q_{\ell K} = \sum_K^L \sum_\ell^M F_K (\Phi_K^W - \Phi_{\ell K}) (\lambda_\ell/B_\ell)_K \tag{4.6}$$

and after combining and rearranging eq (4.4) and (4.6)

the general equation

$$Q_{\ell K} = \frac{F_K \sum_\ell^M (\lambda_\ell/B_\ell)_K \Delta\Phi_{\ell K}}{\sum_K^L \sum_\ell^M F_K (\lambda_\ell/B_\ell)_K \Delta\Phi_{\ell K}} Q_T$$

is obtained.

In a layered reservoir, the fluid flowing in vertical direction depends on the degree of communication with adjacent layers. If the adjacent layers are well-communicating, the fluid flows vertically easily; the resistance of fluid flow is low and as a result , the pressure difference in between will be small. Conversely, if the adjacent layers have poor communication or a lateral extent of shale in between, the fluid will hardly flow vertically; the resistance to flow is high and so is the pressure difference. To illustrate the different results of the pressure distribution, figures (9 to 16) were plotted. We can see that the pressure difference between two adjacent layers could range from hundreds psi to a few psi, with the largest differences existing in the non-communicating cases. However, a well incorporated in the reservoir is always assumed to be communicating. The

FIG.9 PRESSURE DISTRIBUTION OF LAYERED RESERVOIR
WITH EQUAL THICKNESS AT WATER BREAKTHROUGH
TOP LAYER = 200 MD ; BOTTOM LAYER = 20 MD
VERTICAL PERMEABILITY = 0.000001 MD

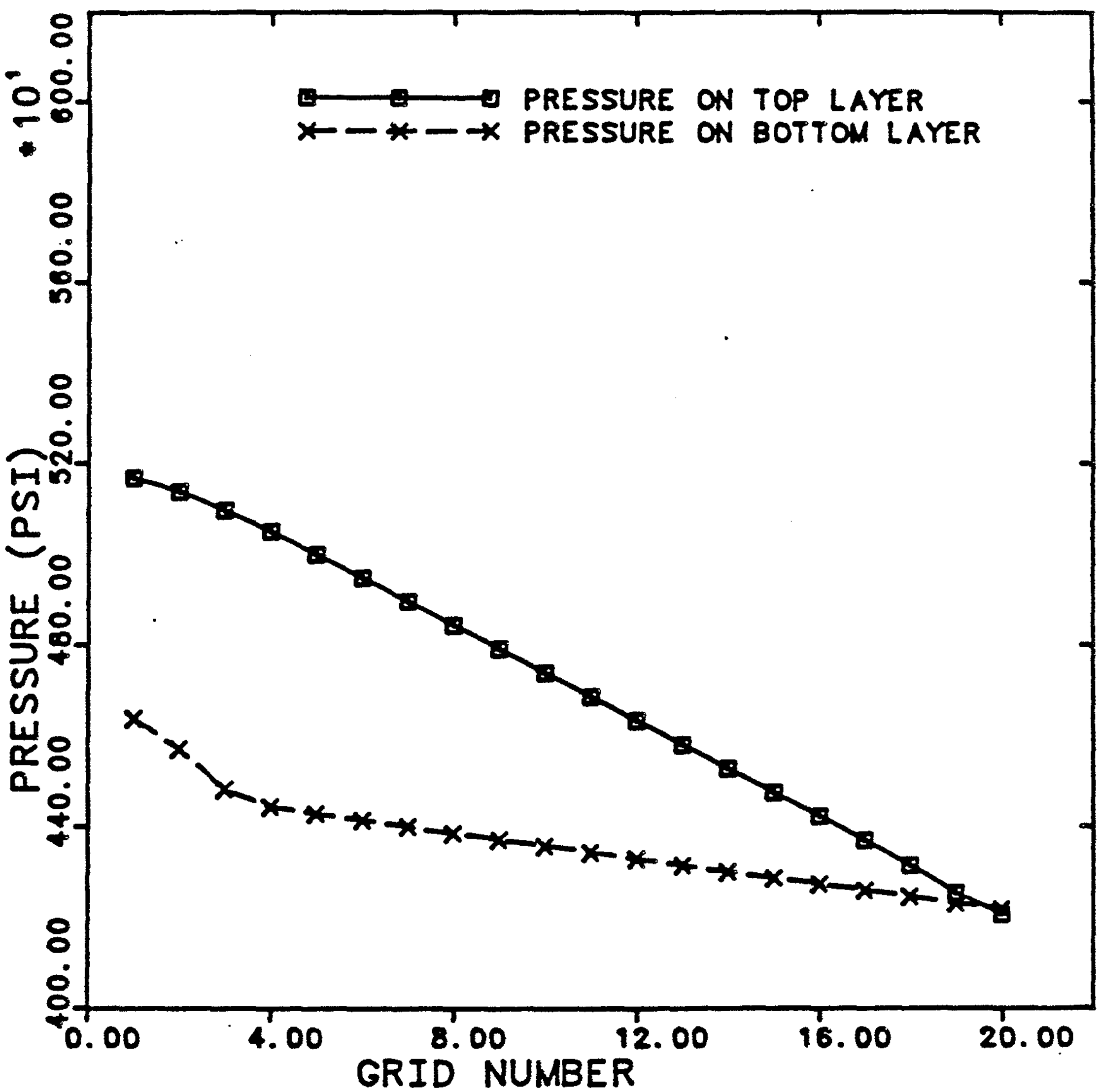

FIG. 10 PRESSURE DISTRIBUTION OF LAYERED RESERVOIR WITH EQUAL THICKNESS AT WATER BREAKTHROUGH TOP LAYER = 200 MD : BOTTOM LAYER = 20 MD VERTICAL PERMEABILITY = 0.02 MD

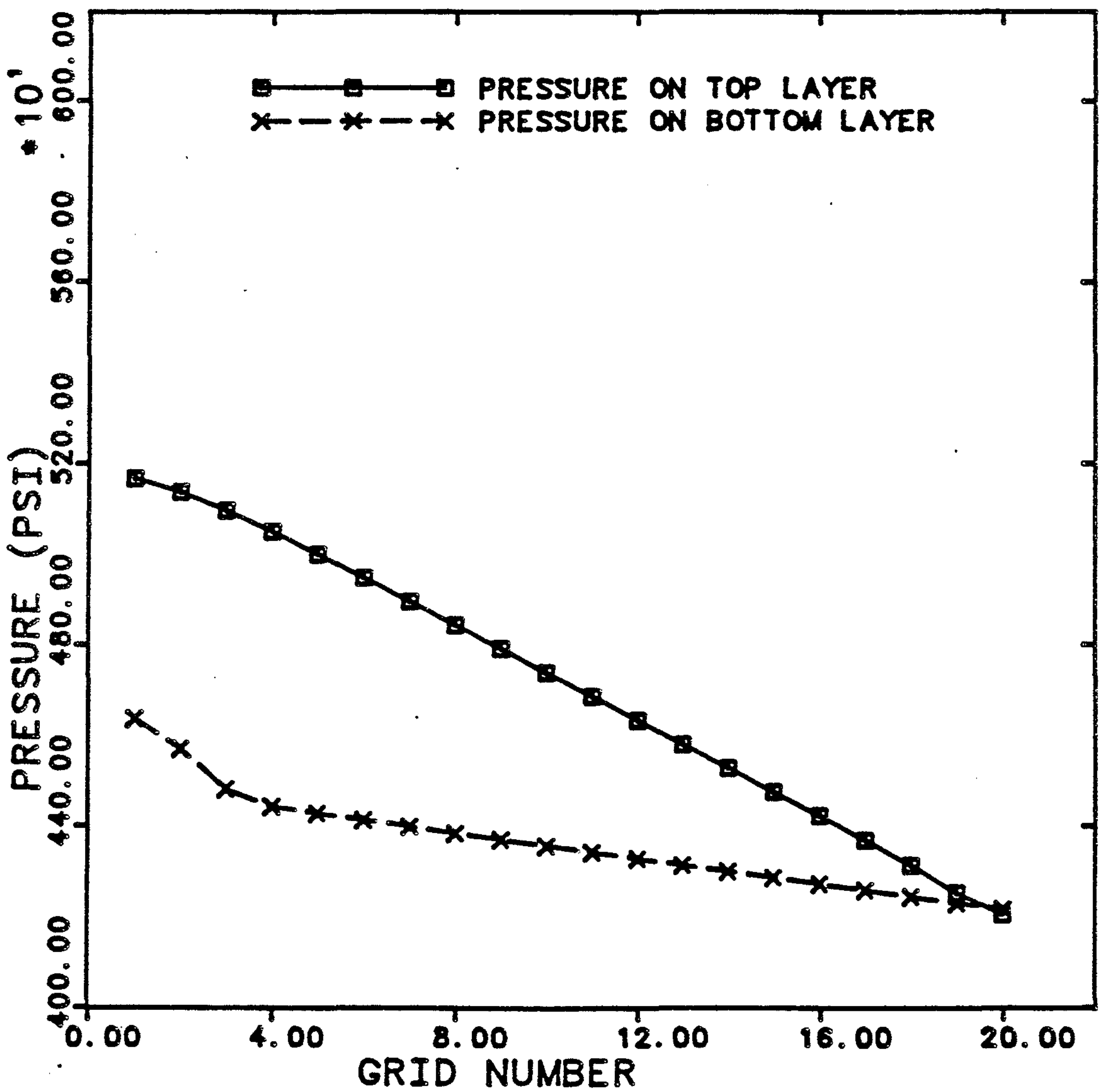

FIG. 11 PRESSURE DISTRIBUTION OF LAYERED RESERVOIR WITH EQUAL THICKNESS AT WATER BREAKTHROUGH TOP LAYER = 200 MD : BOTTOM LAYER = 20 MD VERTICAL PERMEABILITY = 2.0 MD

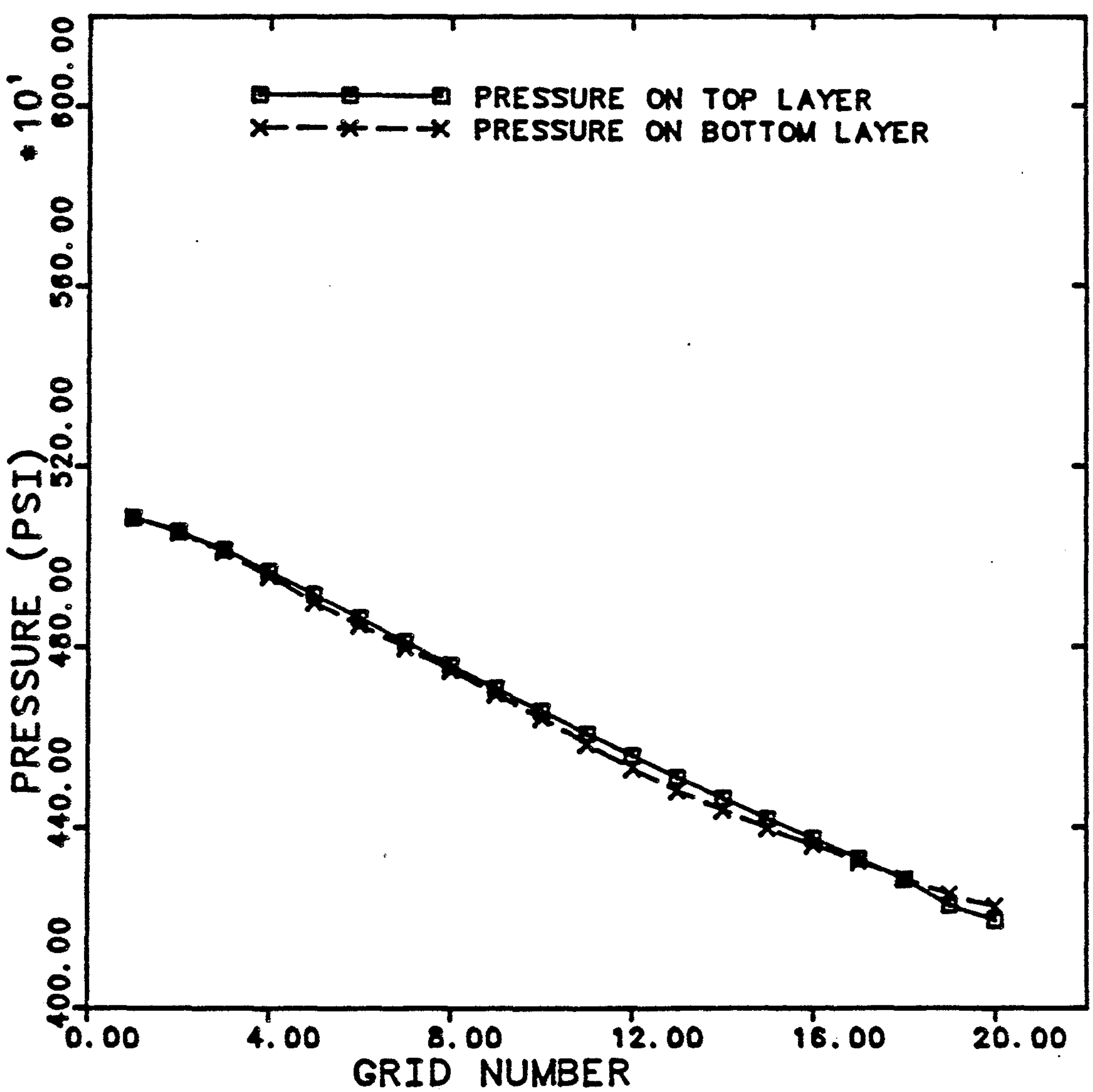

FIG. 12 PRESSURE DISTRIBUTION OF LAYERED RESERVOIR WITH EQUAL THICKNESS AT WATER BREAKTHROUGH TOP LAYER = 200 MD : BOTTOM LAYER = 20 MD VERTICAL PERMEABILITY = 20.0 MD

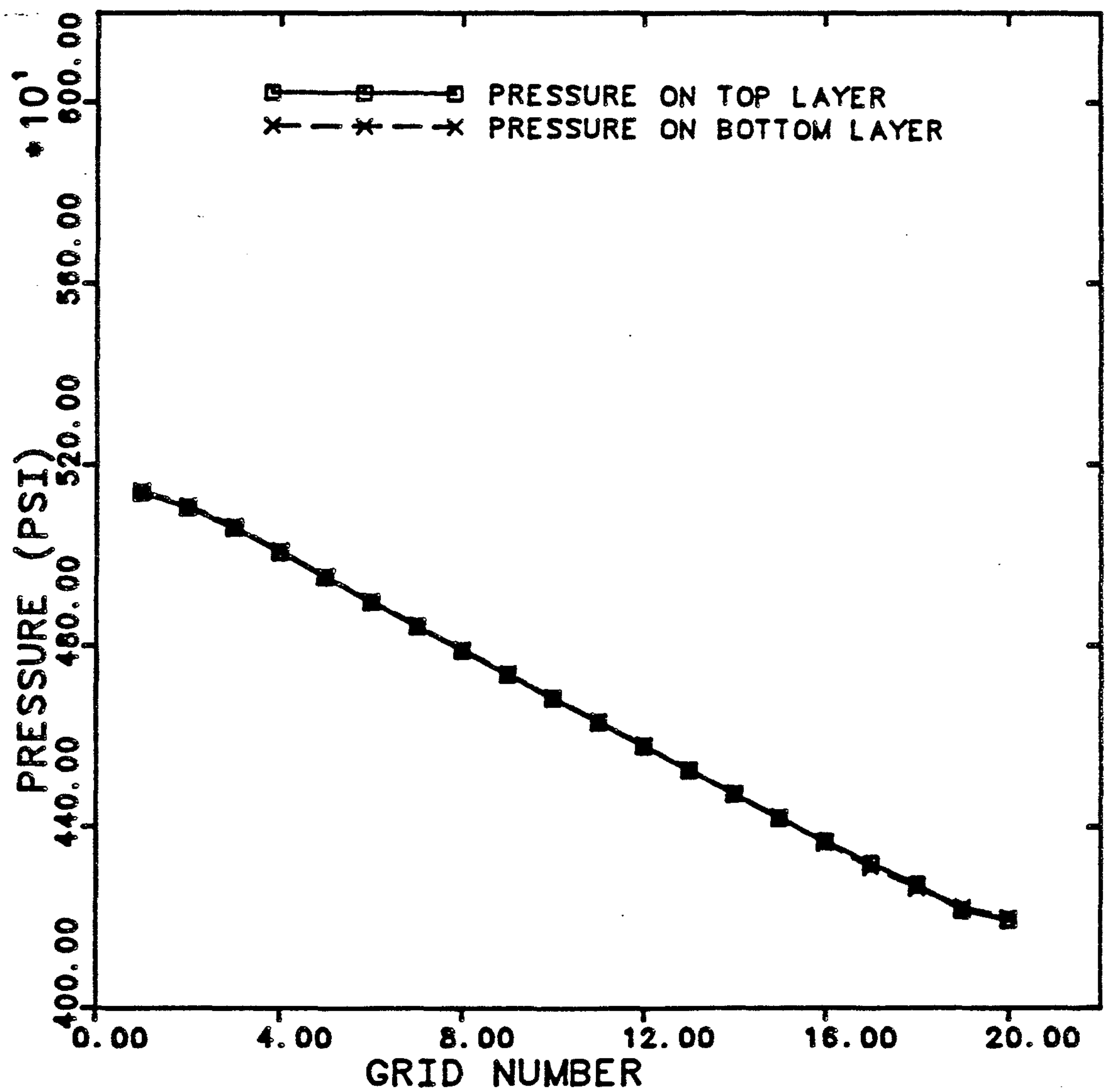

FIG. 13 PRESSURE DISTRIBUTION OF LAYERED RESERVOIR
WITH EQUAL THICKNESS AT WOR = 10
TOP LAYER = 200 MD ; BOTTOM LAYER = 20 MD
VERTICAL PERMEABILITY = 0.000001 MD

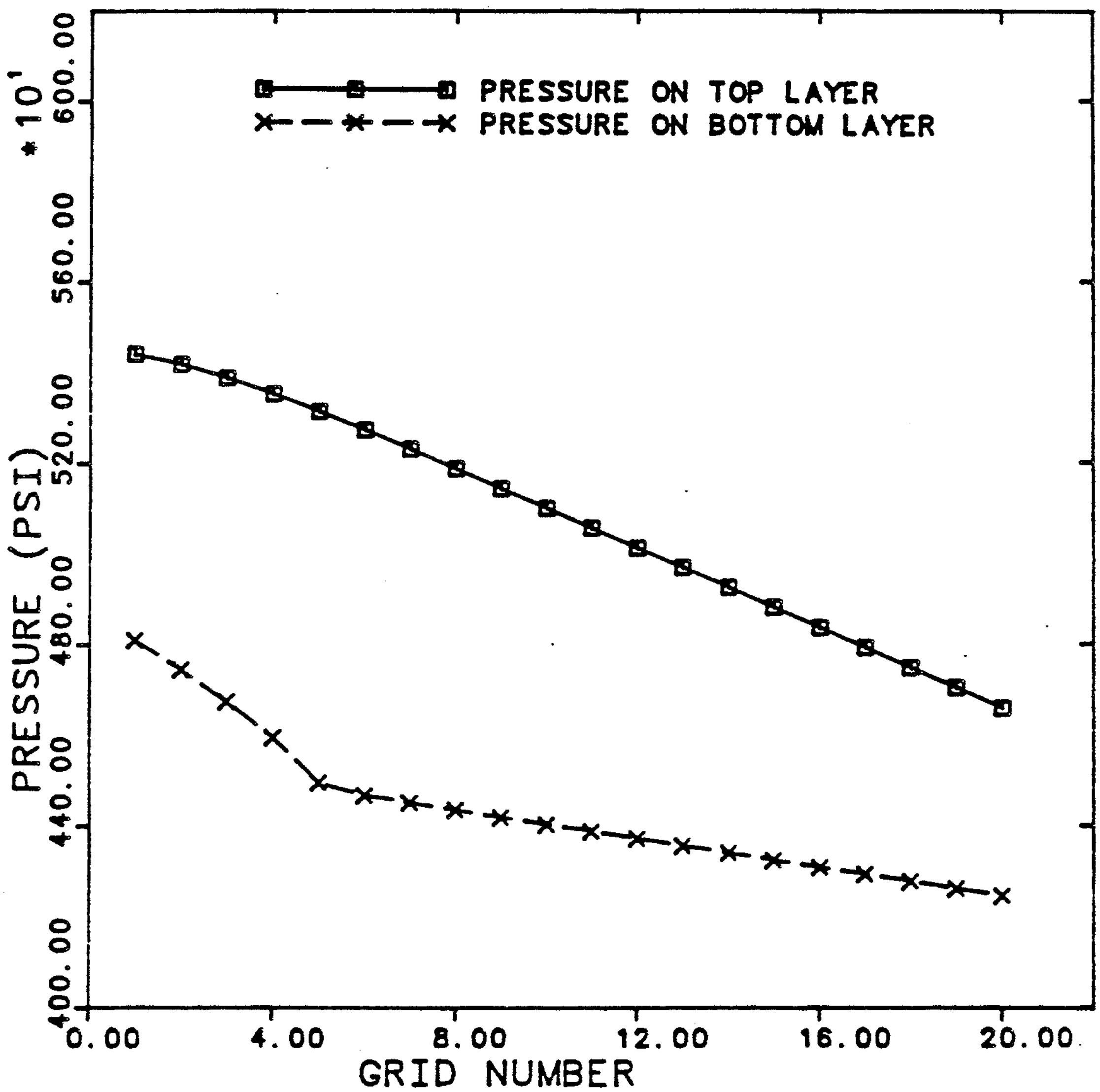

FIG. 14 PRESSURE DISTRIBUTION OF LAYERED RESERVOIR
WITH EQUAL THICKNESS AT WOR = 10
TOP LAYER = 200 MD ; BOTTOM LAYER = 20 MD
VERTICAL PERMEABILITY = 0.02 MD

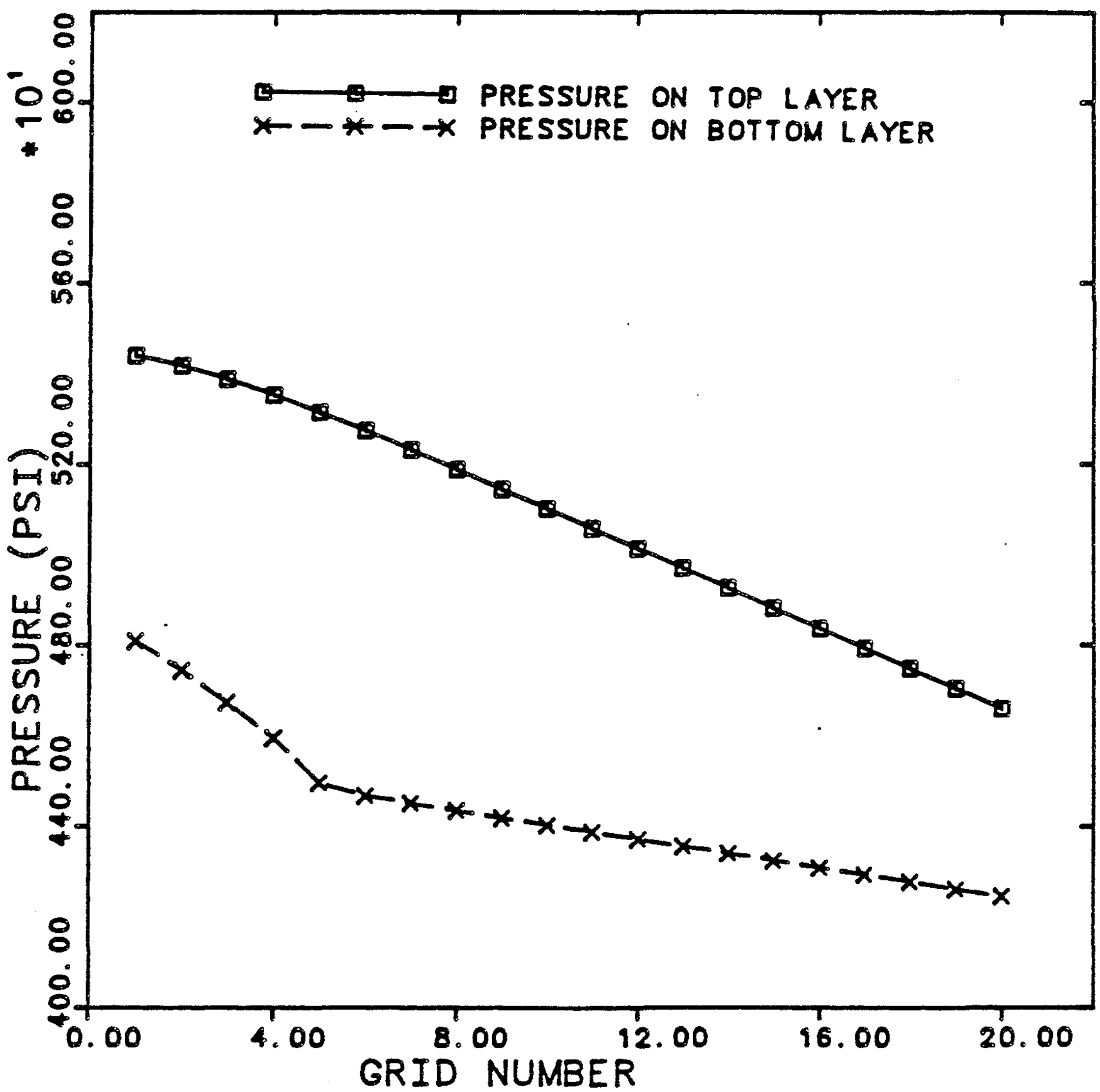

FIG. 15 PRESSURE DISTRIBUTION OF LAYERED RESERVOIR
WITH EQUAL THICKNESS AT WOR = 10
TOP LAYER = 200 MD : BOTTOM LAYER = 20 MD
VERTICAL PERMEABILITY = 2.00 MD

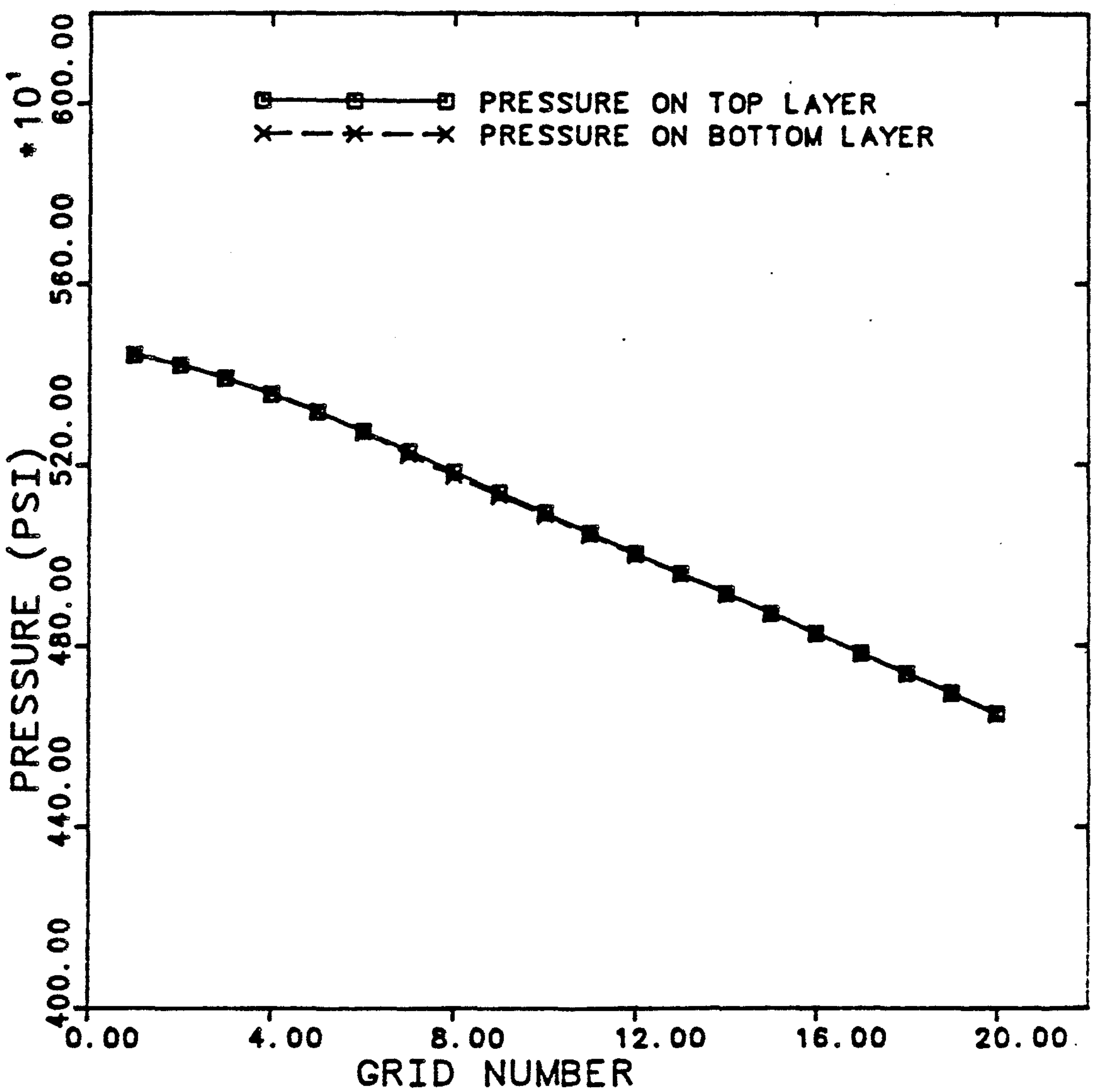

FIG. 16 PRESSURE DISTRIBUTION OF LAYERED RESERVOIR
WITH EQUAL THICKNESS AT WOR = 10
TOP LAYER = 200 MD ; BOTTOM LAYER = 20 MD
VERTICAL PERMEABILITY = 20.0 MD

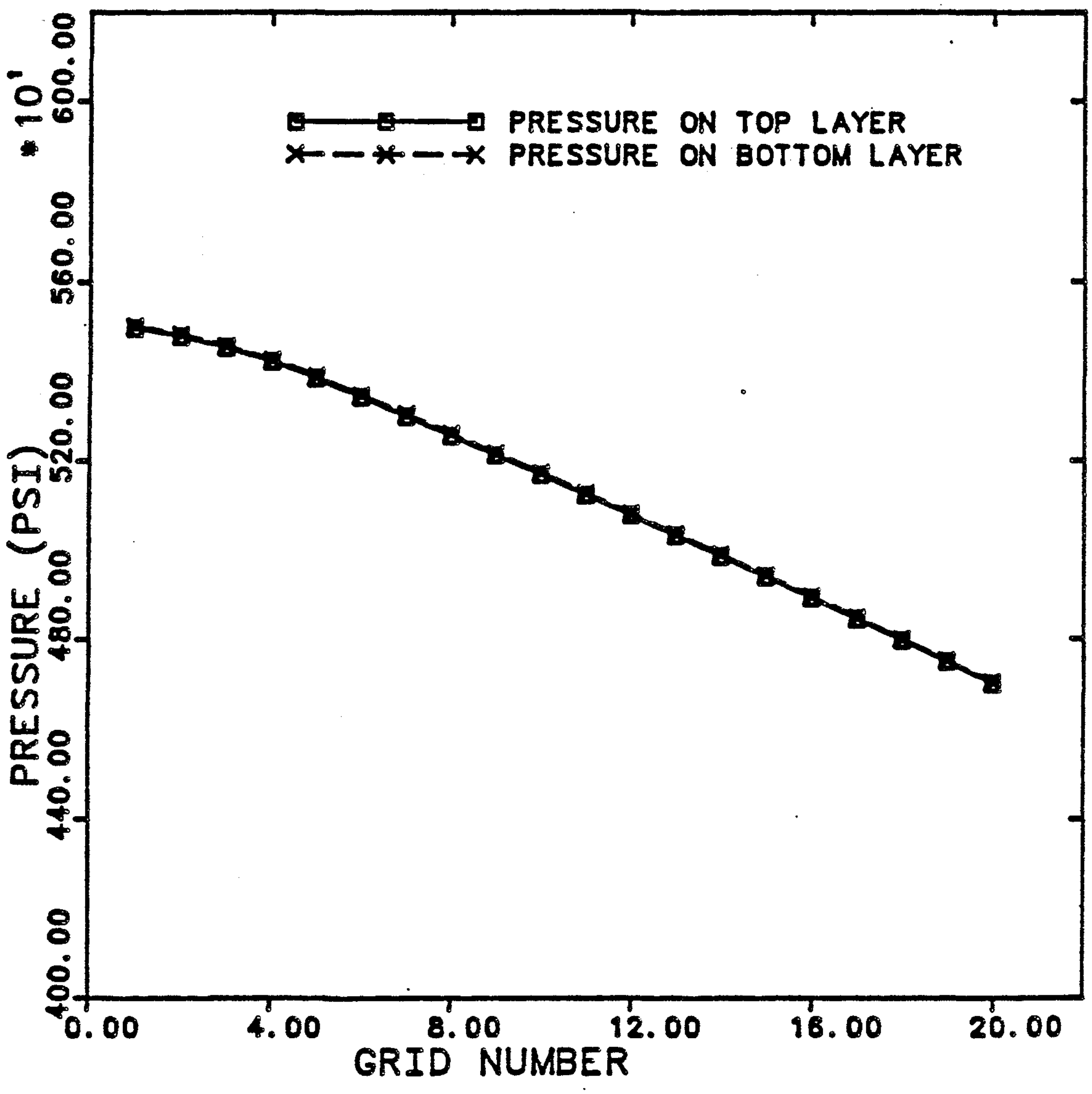

pressure difference in a interval should be approximated to a fluid density head when the fluid flows in the wellbore, if the viscous loss is neglected and the fluid density is constant. Therefore, in a layered reservoir with wells intersecting, the pressure differences between a certain point at the well and reservoir corresponding to the same depth as defined in eq.(4.2) will be quite different in each layer unless the reservoir has communication to the same degree as the well.

Accordingly, the potential difference defined in eq.(4.2) is not always constant, and the mobility allocation method is not always suitable for cross-sectional model unless the reservoir is " well communicating ". This observation has been reported by Nolen et al.[28] in his water coning model. We also found that it was true for our simulation that the results can be different for the two rate allocation methods. Four cases were run where the vertical permeability was varied from case to case to single out the effect of the rate allocation method. The results shown in figures 17 to 19 indicate that the difference between two methods is easily seen when vertical permeability is essentially zero, but the performance prediction is almost the same when vertical permeability equal to 20 md. In addition, the water oil ratio curve with vertical permeability equal to 10^{-6} md shown in Fig.20 rises rather fast when mobility allocation method is used. It indicates that an early economic life of a production well is possible.

In fact, in this study, vertical permeability is varied from case to case , and the horizontal permeability near the wellbore is also varied. All these changes will affect the pressure variation. Accordingly, the following changes were made to make rate allocation method suitable for our use in the cross-sectional model.

FIG. 17 COMPARISION OF RATE ALLOCATION SCHEME IN PRODUCTION HISTORY
VERTICAL PERMEABILITY = 0.000001 MD

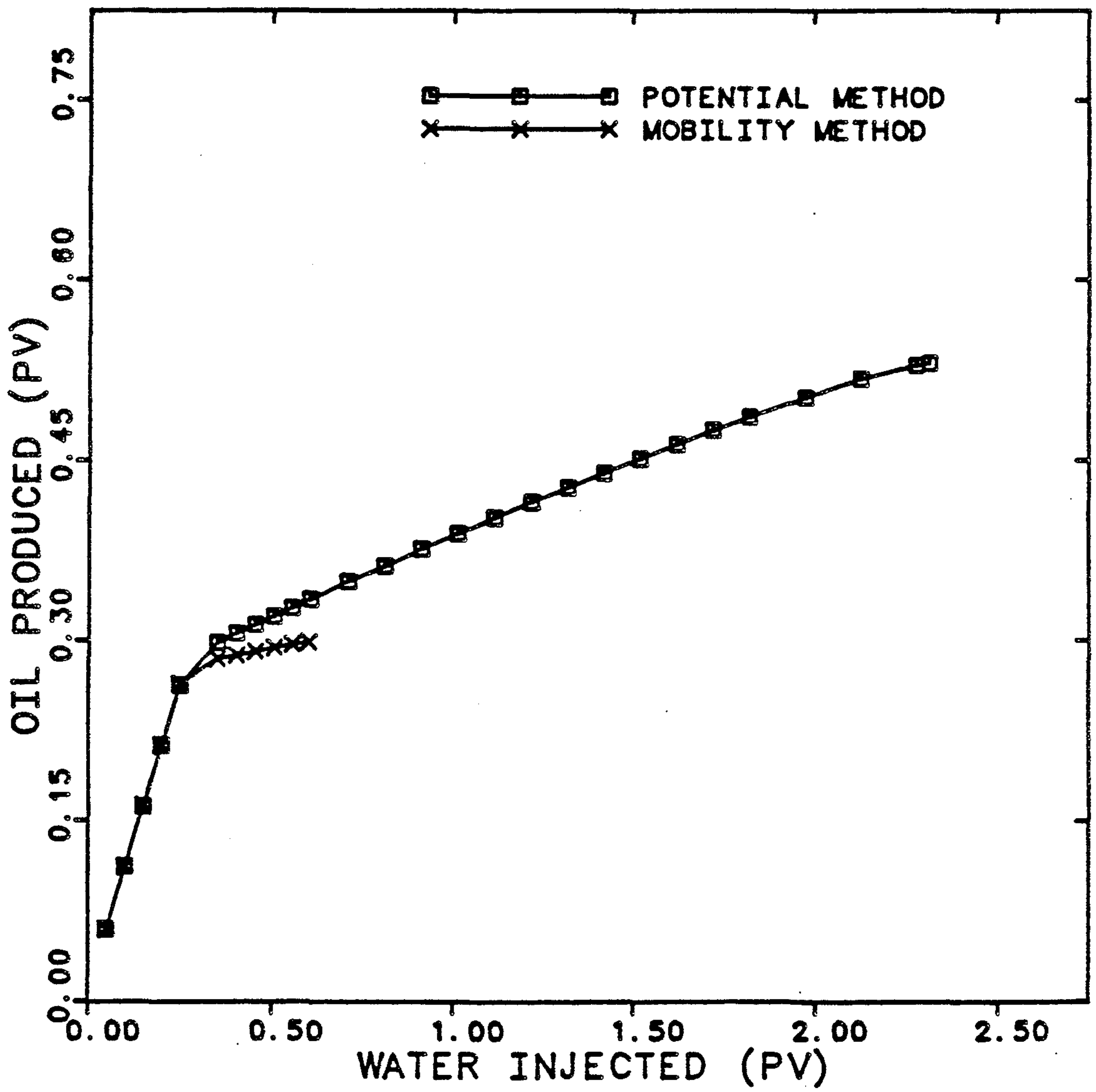

FIG. 18 COMPARISION OF RATE ALLOCATION SCHEME IN PRODUCTION HISTORY
VERTICAL PERMEABILITY = 0.02 MD

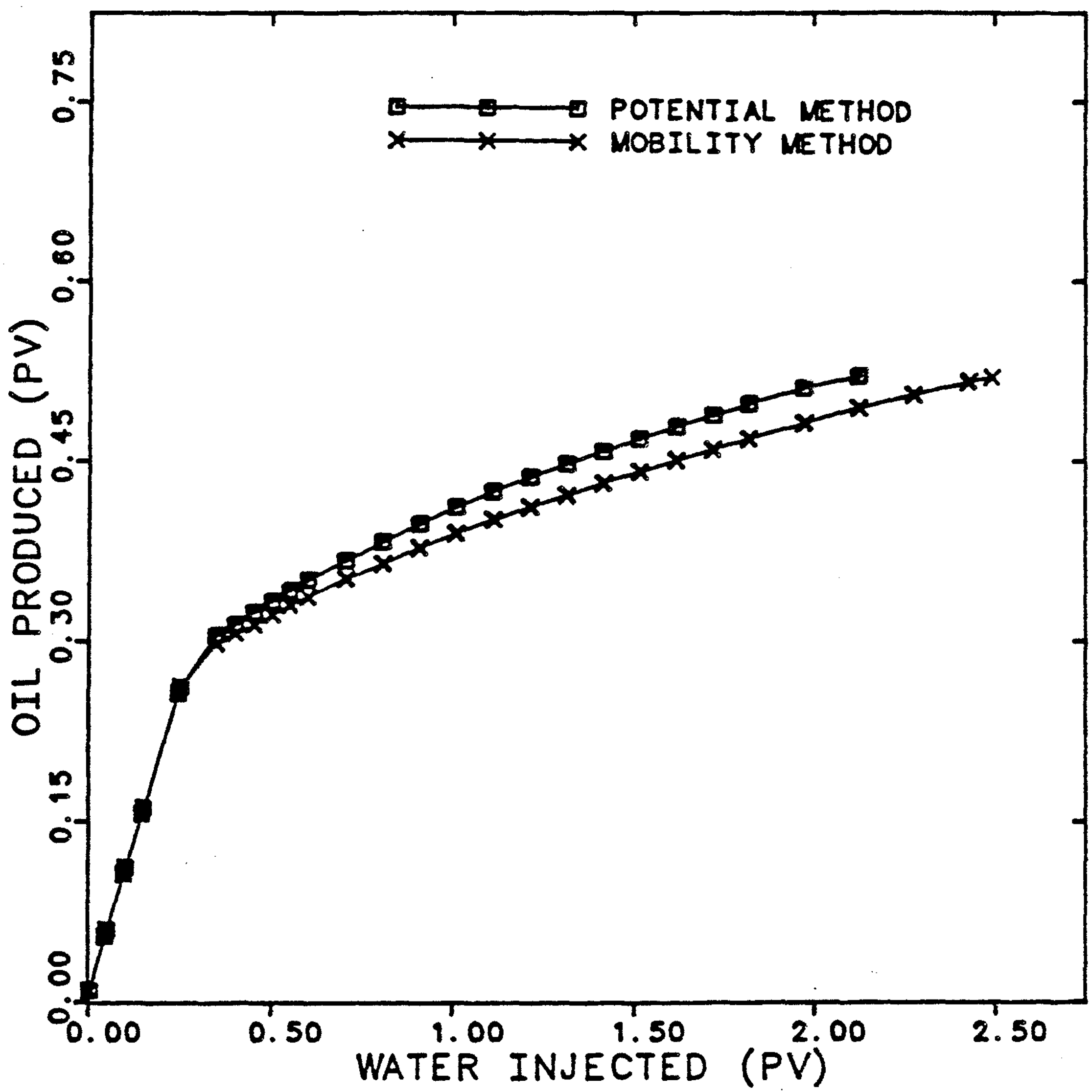

FIG. 19 COMPARISION OF RATE ALLOCATION SCHEME IN PRODUCTION HISTORY
VERTICAL PERMEABILITY = 20.0 MD

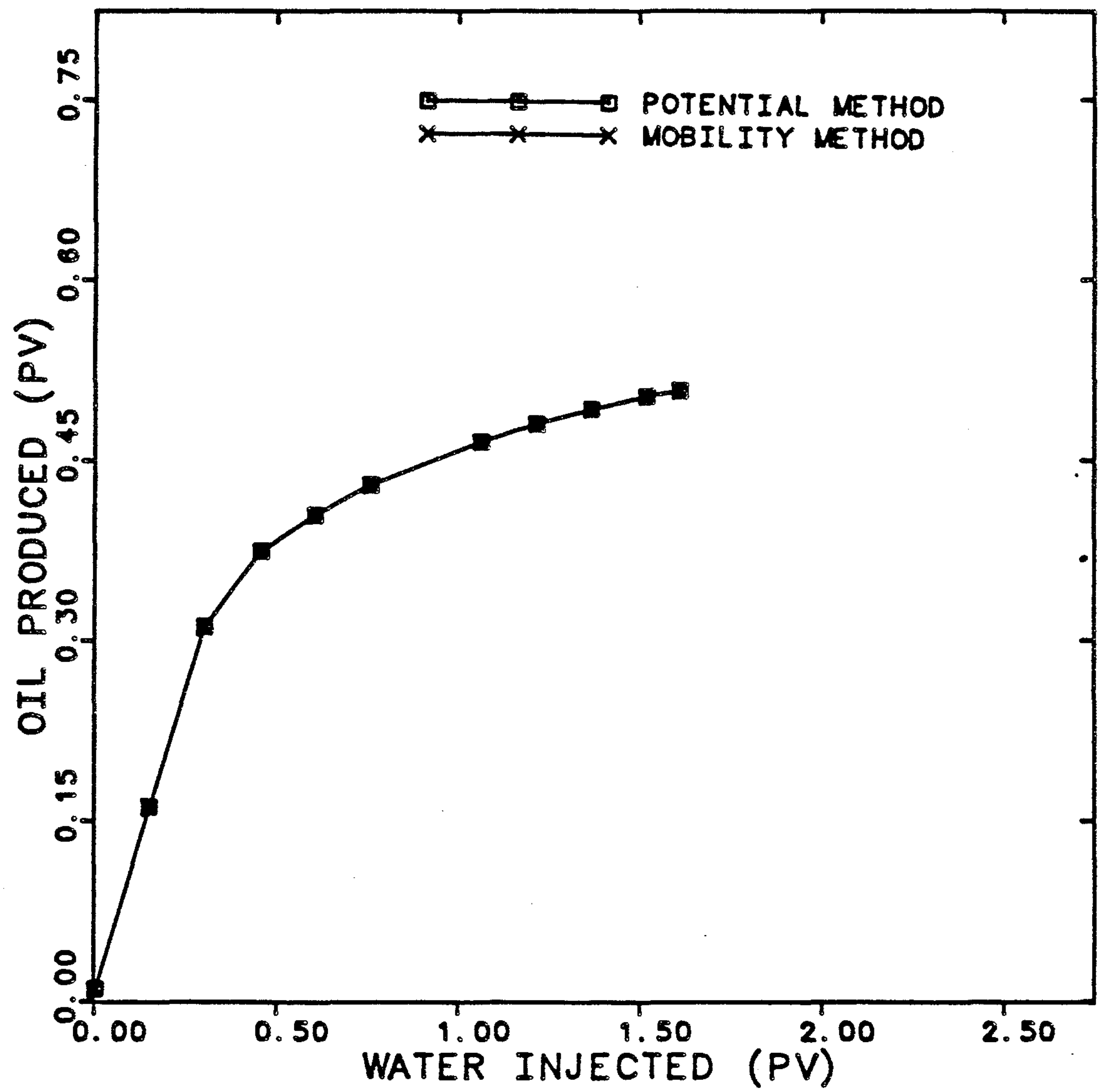

FIG. 20 COMPARISION OF RATE ALLOCATION SCHEME IN
WATER OIL RATIO CURVE
VERTICAL PERMEABILITY = 0.000001 MD

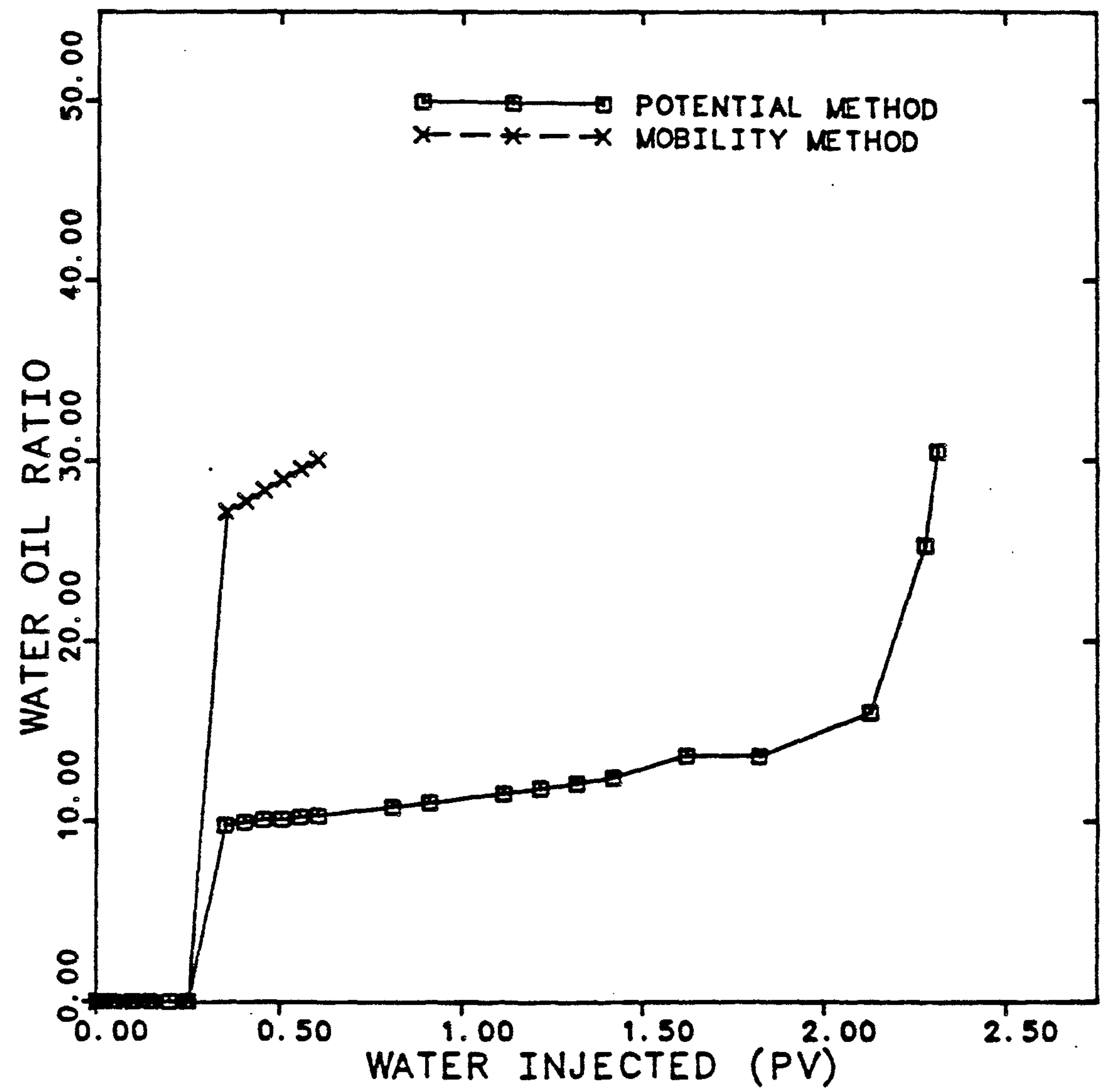

FIG. 21 COMPARISION OF RATE ALLOCATION SCHEME IN
WATER OIL RATIO CURVE
VERTICAL PERMEABILITY = 0.02 MD

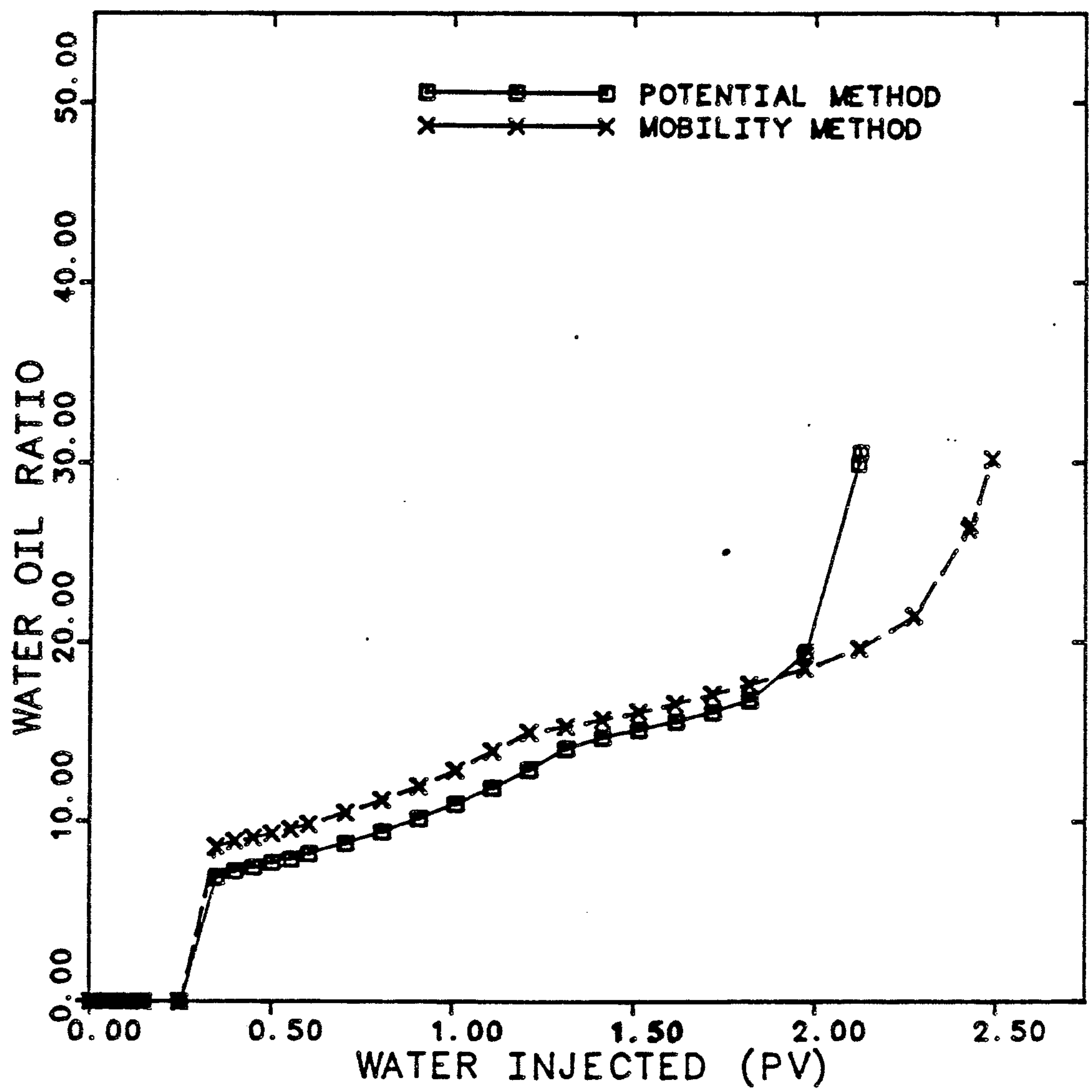

FIG. 22 COMPARISION OF RATE ALLOCATION SCHEME IN
WATER OIL RATIO CURVE
VERTICAL PERMEABILITY = 20.0 MD

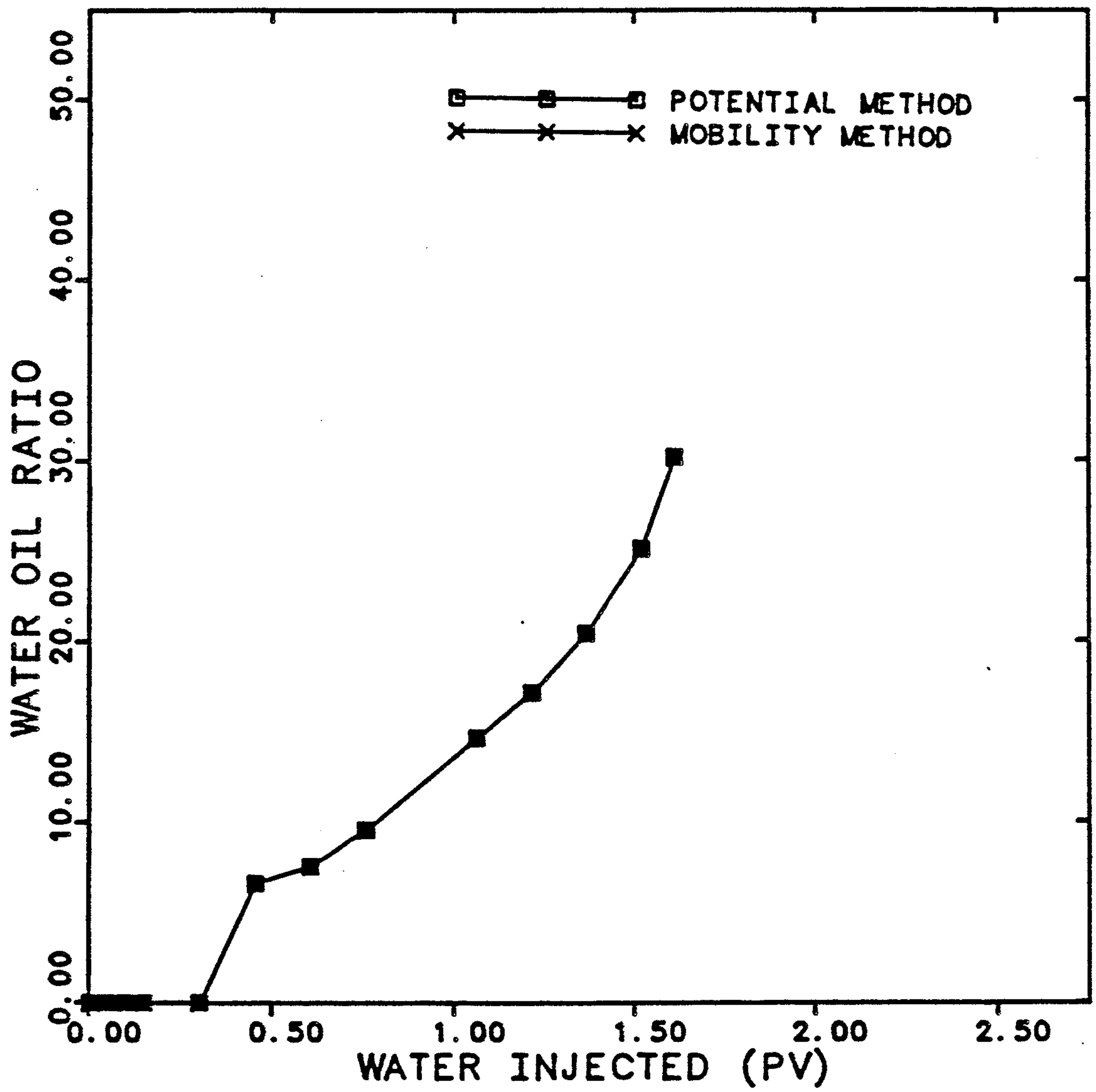

As mentioned before, the basic equation describing rate is

$$Q_{\ell K} = F_K\,(p_K^W - p_{\ell K})\,(\lambda_\ell/B_\ell)_K \tag{4.3}$$

and the sum of flow rate in each layer is

$$Q_T = \Sigma_K^L\, \Sigma_\ell^M\, Q_{\ell K} \tag{4.5}$$

Whereas, the pressure in the wellbore is constrained by the well head density, so

$$p_K^W = p_U^W + \Sigma_{m=U}^N (\rho\Delta z)_{m+1/2} \tag{4.7}$$

where p_U^W is the uppermost wellbore pressure, $N = k-1$.

Substituting (4.7) to (4.3), we get

$$Q_{\ell K} = F_K[\, p_U^W + \Sigma_{m=U}^N (\rho\Delta z)_{m+1/2} - p_{\ell K}\,]\,(\lambda_\ell/B_\ell)_K \tag{4.8}$$

With the total rate constraint eq(4.5), substituting eq(4.8) to (4.5), the total rate can be expressed in terms of p_U^W as

$$Q_T = \Sigma_K^L\, \Sigma_\ell^M\, F_K[\, p_U^W + \Sigma_{m=U}^N (\rho\Delta z)_{m+1/2} - p_{\ell K}\,]\,(\lambda_\ell/B_\ell)_K \tag{4.9}$$

And then p_U^W can be solved as

$$p_U^W = [Q_T + \Sigma_K^L\, \Sigma_\ell^M\, F_K(\lambda_\ell/B_\ell)_K p_{\ell K} - \Sigma_K^L \Sigma_{m=U}^N (\rho\Delta z)_{m+1/2}\,] \;/\; [\,\Sigma_K^L\, \Sigma_\ell^M\, F_K(\lambda_\ell/B_\ell)_K\,] \tag{4.10}$$

Finally the rate in each layer can be calculated from

$$Q_{\ell K} = F_K\,(p_K^W - p_{\ell K})\,(\lambda_\ell/B_\ell)_K \tag{4.3}$$

or essentially represented as the form of potential allocation method

$$Q_{\ell K} = \frac{F_K\, \Sigma_\ell^M\, (\lambda_\ell/B_\ell)_K\, \Delta\Phi_{\ell K}}{\Sigma_K^L \Sigma_\ell^M\, F_K\, (\lambda_\ell/B_\ell)_K\, \Delta\Phi_{\ell K}}\, Q_T \tag{4.2}$$

There is a possibility that the injection well could be placed at a block where the relative permeability to injected fluid is zero such that the fluid is prohibited from flowing into the reservoir. The mobility term of eq(4.3) and in the numerator of eq(4.2) are kept in a form of total mobility rather than single phase mobility so that even though the water injection well is placed at the block where the relative permeability of water is zero, water still can flow into the reservoir. This technique, somewhat, will affect the rate distribution initially; however, the impact will fade away as soon as the grid block containing the well is saturated with the injected fluid.

4.3 Modification of Well Constraint

Another feature added in BOAST is the ability to control injection rate based on a critical pressure. It is possible that the bottomhole flowing pressure for an injection well is beyond the formation fracturing pressure. In particular, after a simulated treatment has taken place, it is very often the case that injection pressure will become quite high if a constant rate scheme is used. Thus, the program was modified so that when the critical pressure in the injection well (usually the fracturing pressure) is reached, the rate is reduced to maintain injection at a pressure lower than that critical pressure.

In an injection well, to prevent the injection pressure from exceeding the fracturing pressure, the uppermost pressure of injection well p is always compared with the fracturing pressure corresponding to that depth, that is

Allowable bottomhole pressure = Fracture gradient *Depth

where fracture gradient is chosen depending on the particular problem.

If the injection pressure is under the allowable bottom pressure, the injection well performs with a constant rate injection, otherwise , the rate will be reduced to satisfy the pressure constraint.

4.4 Calculation of Relative Permeability

To simulate a two or three-phase fluid flow in a reservoir, the interpretation of permeability of each phase is important in terms of their effects in the simulation results. Previous studies [29,30,31] have shown that the relative permeability of water (gas) can be interpreted as a single function of water saturation (gas saturation). For the oil relative permeability , it should be interpreted as a function of the oil saturation associated with other concurrent phases. In the original BOAST program , the way of inputing the relative permeability treats the oil relative permeability as a function of oil phase saturation only. Intuitively, this is true only for a two-phase system (either oil-water or gas- oil) . For a three-phase flow system, a more accurate method to interpret the oil relative permeability is needed.

A method using two sets of two-phase data (water-oil and gas-oil) to predict the relative permeability is presented by Stone [31] . In his probability model, the relative permeability of oil is treated as a function of oil, water and gas saturation, while relative permeability of water is a function of water saturation alone, and relative permeability of gas is a function of gas saturation alone. To obtain the oil relative permeability , the fluid saturations were first normalized as

$$S_o^* = (S_o - S_{or}) / (1 - S_{wc} - S_{or}) \quad (4.11)$$

$$S_w^* = (S_w - S_{wc}) / (1 - S_{wc} - S_{or}) \quad (4.12)$$

$$S_g^* = S_g / (1 - S_{wc} - S_{or}) \quad (4.13)$$

where $S_o^* + S_w^* + S_g^* = 1$

The oil relative permeability in a three-phase system can be written as

$$k_{ro} = S_o^* \beta_w \beta_g \quad (4.14)$$

where β_w is determined from the equation (4.14) in a extreme case of $Sg = S_g^* = 0$, namely from a water-oil system data set.

$$\beta_w = k_{row} / (1 - S_w^*) \quad (4.15)$$

Likewise, in case of $Sw = Swc$

$$\beta_g = k_{rog} / (1 - S_g^*) \quad (4.16)$$

With eqs. (4.11) to (4.16), the oil relative permeability in three phase system can be calculated as

$$k_{ro} = (k_{row})(k_{rog}) \times \frac{(S_o - S_{or})(1 - S_{wc} - S_{or})}{(1 - S_{or} - S_w)(1 - S_{wc} - S_{or} - S_g)} \quad (4.17)$$

where k_{row} is a function of water saturation alone and is determined by a two phase experiment, while k_{rog} is a function of gas saturation only.

According to eq. (4.17), knowing each phase saturation, the residual oil saturation and the connate water saturation, we can easily calculate oil relative permeability. Consequently, a subroutine FORKRO is coded. With an interpolation scheme, the calculation of k_{ro} was allowed in the simulator internally . Table 1 is an example illustrating the collection of k_{ro} where $S_o = 0.5$ and various values of S_w and S_g are used.

TABLE 1
EXAMPLE OF OIL RELATIVE PERMEABILITY
at So= 0.5 with different values of Sw
and Sg

So	Sw	Sg	Kro	Krw	Krg
0.50	0.50	0.0	0.0157	0.250	0.0
0.50	0.49	0.01	0.0164	0.2367	0.0
0.50	0.48	0.02	0.0162	0.2233	0.0
0.50	0.47	0.03	0.0153	0.2100	0.0
0.50	0.46	0.04	0.0141	0.1955	0.0
0.50	0.45	0.05	0.0121	0.1810	0.0
0.50	0.43	0.07	0.0161	0.1550	0.006
0.50	0.42	0.08	0.0187	0.1440	0.009
0.50	0.41	0.09	0.0211	0.1330	0.012
0.50	0.40	0.10	0.0233	0.1220	0.015
0.50	0.39	0.11	0.0266	0.1120	0.0215
0.50	0.38	0.12	0.0296	0.1020	0.0280
0.50	0.37	0.13	0.0323	0.0920	0.0345
0.50	0.36	0.14	0.0350	0.0820	0.0410
0.50	0.35	0.15	0.0374	0.0720	0.0475
0.50	0.34	0.16	0.0406	0.0460	0.0540
0.50	0.33	0.17	0.0496	0.0561	0.0605
0.50	0.32	0.18	0.0640	0.0484	0.0670
0.50	0.31	0.19	0.0777	0.0407	0.0735
0.50	0.30	0.20	0.0910	0.0330	0.0800
0.50	0.29	0.21	0.1081	0.0264	0.0895
0.50	0.28	0.22	0.1264	0.0198	0.0990
0.50	0.27	0.23	0.1464	0.0132	0.1085
0.50	0.26	0.24	0.1686	0.0066	0.1180
0.50	0.25	0.25	0.1939	0.0	0.1275

It is worthmentioning that this approach will reduce exactly to two-phase data only if the relative permeability at the end points is equal to 1, that is,

$$k_{row}(S_{wc}) = k_{rog}(S_g = 0) = 1$$

Otherwise, k_{ro} will only approximate to a two-phase data. For instance, each value of the new generated relative permeability k_{ro}, shown in Table 2, is only equal to 0.982 of the two-phase value (k_{row} or k_{rog}) shown in Table 3. Nevertheless, since this slight difference will not significantly affect the simulation run, we ignore this deviation.

4.5 Modification of the Source Terms

When an IMPES formulation simulator like BOAST was used, one can control the stability of solution by adjusting the time step size. But, in the field case study (discussed in Chapter VI), the instability of pressure solution still occurred in the grid blocks near the well location, even when a very small time step size (less than 0.01 day) was used. By investigating the equation (4.9), we found that by handling the source terms implicitly, we were able to improve the stability of pressure solution and use a larger time step size. The last modification was then added to treat the source terms implicitly.

Back to eq.(4.9), in order to calculate the bottomhole pressure, the pressure at a known time level n needs to be used. Pressure instability might occur if the rate calculation is coupled with pressure explicitly. To solve this problem, an implicit method for calculating the rate was investigated. The approach being used approximates the rate change over a time step size as :

TABLE 2
EXAMPLE OF OIL RELATIVE PERMEABILITY
in two extreme cases where Sg=0 or Sw=Swc

******* Sg = 0 *******

So	Sw	Sg	Kro	Krw	Krg
0.75	0.25	0.0	0.9643	0.0	0.0
0.70	0.30	0.0	0.5224	0.033	0.0
0.665	0.335	0.0	0.2209	0.06	0.0
0.65	0.35	0.0	0.1676	0.072	0.0
0.60	0.40	0.0	0.0962	0.122	0.0
0.57	0.43	0.0	0.0579	0.155	0.0
0.55	0.45	0.0	0.0393	0.181	0.0
0.53	0.47	0.0	0.0285	0.21	0.0
0.50	0.50	0.0	0.0157	0.25	0.0
0.45	0.55	0.0	0.0069	0.313	0.0
0.392	0.608	0.0	0.0	0.386	0.0

******* Sw = Swc *******

So	Sw	Sg	Kro	Krw	Krg
0.75	0.25	0.0	0.9643	0.0	0.0
0.70	0.25	0.05	0.383	0.0	0.0
0.65	0.25	0.10	0.3339	0.0	0.015
0.55	0.25	0.20	0.216	0.0	0.08
0.45	0.25	0.30	0.1718	0.0	0.175
0.35	0.25	0.40	0.1227	0.0	0.295
0.25	0.25	0.50	0.0756	0.0	0.41
0.15	0.25	0.60	0.0471	0.0	0.53
0.05	0.25	0.70	0.0245	0.0	0.645
0.006	0.25	0.744	0.147	0.0	0.70

TABLE 3
RELATIVE PERMEABILITY DATA

****** WATER-OIL TABLE ******

Sw	Krw	Krow	Pcow
0.250	0.000	0.982	0.0
0.300	0.0330	0.532	0.0
0.335	0.06	0.225	0.0
0.400	0.122	0.098	0.0
0.430	0.155	0.059	0.0
0.450	0.181	0.04	0.0
0.470	0.210	0.029	0.0
0.500	0.250	0.016	0.0
0.550	0.313	0.007	0.0
0.608	0.386	0.0	0.0
1.000	1.000	0.0	0.0

****** GAS-OIL TABLE ******

Sg	Krg	Krog	Pcog
0.0	0.0	0.982	0.0
0.05	0.0	0.390	0.0
0.10	0.015	0.340	0.0
0.20	0.08	0.220	0.0
0.30	0.175	0.175	0.0
0.40	0.295	0.125	0.0
0.50	0.410	0.077	0.0
0.60	0.530	0.048	0.0
0.70	0.645	0.025	0.0
0.744	0.700	0.015	0.0
0.800	0.760	0.005	0.0
0.850	0.825	0.0	0.0
1.00	1.000	0.0	0.0

$$\partial q_\ell/\partial t \approx (q_\ell^{n+1} - q_\ell^n)/\Delta t \tag{4.18}$$

Since

$$\partial q_\ell/\partial t = (\partial q_\ell/\partial p) (\partial p/\partial t) \approx (\partial q_\ell/\partial p) (p^{n+1} - p^n)/\Delta t \tag{4.19}$$

and

$$q_{\ell K} = F_K (\lambda_\ell/B_\ell)_K (p_{\ell K} - p_K^w) \tag{4.20}$$

where the sign convention is the same as in the BOAST .

Thus,

$$(\partial q_\ell/\partial p)_K = F_K (\lambda_\ell/B_\ell)_K \tag{4.21}$$

Combining eqs.(4.18),(4.19),(4.21) and rearranging then , we obtain

$$q_{\ell K}^{n+1} - q_{\ell K}^n = F_K (\lambda_\ell/B_\ell)_K^n (p_{\ell K}^{n+1} - p_{\ell K}^n)$$

or

$$q_{\ell K}^{n+1} = q_{\ell K}^n + F_K (\lambda_\ell/B_\ell)_K^n (p_{\ell K}^{n+1} - p_{\ell K}^n) \tag{4.22}$$

Now, if we return to the finite difference eq. (2.22) and rearrange it in the form as presented in the BOAST manual, it becomes

$$\begin{aligned}
&(B_o - B_g^n R_{so}^n)_{ijK} \; [\Delta A_o^n \Delta p^{n+1} + GOWT^n - QVO]_{ijK} \\
&+ (B_w^n)_{ijK} \; [\Delta A_w^n \Delta p^{n+1} + GWWT^n - QVW]_{ijK} \\
&+ (B_g^n)_{ijK} \; [\Delta A_g^n \Delta p^{n+1} + \Delta R_{so}^n A_o^n \Delta p^{n+1} + \Delta R_{sw}^n A_w^n \Delta p^{n+1} \\
&+ GGWT^n - QVG]_{ijK} \\
&= (V_p C_t/\Delta t)_{ijK}^n (p^{n+1} - p^n)_{ijK}
\end{aligned} \tag{4.23}$$

where QVO, QVW, and QVG are terms of source-oil rate,water rate, and gas rate for each well, respectively. The definition of others is the same as in BOAST manual.

According to eq.(4.22), we may treat three source(rate) terms implicitly as follows:

$$QVO_K^{n+1} = QVO_K^n + F_K (\lambda_o/B_o)_K^n (p_K^{n+1} - p_K^n) \tag{4.24}$$

$$QVW_K^{n+1} = QVW_K^n + F_K (\lambda_w/B_w)_K^n \, (p_K^{n+1} - p_K^n) \tag{4.25}$$

$$QVG_K^{n+1} = QVG_K^n + F_K (\lambda_g/B_g)_K^n \, (p_K^{n+1} - p_K^n) \tag{4.26}$$

After substituting eqs. (4.24), (4.25), and (4.26) to eq. (4.23) and rearranging it, we can move the unknown pressure p^{n+1} to the lefthand side of the equation, and move those known terms to the righthand side of the equation. The matrix form of the pressure system equation

$$AT_K p_{K-1}^{n+1} + AS_j p_{j-1}^{n+1} + AW_i p_{i-1}^{n+1} + AB_K p_{K-1}^{n+1} + AN_j p_{j-1}^{n+1} + AZ_i p_{i-1}^{n+1} + E p_{ijK}^{n+1} = B_{ijK} \tag{4.27}$$

will become

$$AT_K p_{K-1}^{n+1} + AS_j p_{j-1}^{n+1} + AW_i p_{i-1}^{n+1} + AB_K p_{K-1}^{n+1} + AN_j p_{j-1}^{n+1} + AZ_i p_{i-1}^{n+1} + (E - FCOEF)\, p_{ijK}^{n+1} = B_{ijK} - FCOEF\, p_{ijK}^n \tag{4.28}$$

where

$$FCOEF = F_K \times (\lambda_o/B_o + \lambda_w/B_w + \lambda_g/B_g)_K$$

Accordingly, we redefine the coefficients of the pressure equation as following:

$$E^{n+1} = E^n - FCOEF$$

$$B^{n+1} = B^n - FCOEF \times p^n$$

where n+1 indicates the new coefficient, whereas n indicates old coefficient. Within the program, these modified coefficients are calculated before the solver subroutine is called. And when the new pressure is calculated, the new rate q^{n+1} is computed from eq.(4.22). However, observing from eq.(4.22) , the rate calculated might deviate from the prescribed one, and its deviation is proportional to the pressure change that takes place over a time step. To obtain an accurate rate, an iteration method is needed. Without incorporating an iteration method to calculate the rate, we alternatively minimize the rate deviation by setting the pressure changes over one time step in a reasonable range. Later on, we shall see this scheme works fine in the field case study-with the pressure stability being improved and the rate quite undeviated.

4.6 Summary of Changes to BOAST

As discussed in this chapter, a restart option was adopted in the program with a subroutine REREAD to initiate a treatment study. A rate allocation method was modified in the subroutine QRATE for the purpose of obtaining more reasonable rates when high permeability contrast exists between zones. A method to calculate relative permeability of oil in a three-phase fluid flow system was added in the subroutine FORKRO to enable us to simulate more practical problems. Finally, a modification of source terms was incorporated to enable us to improve the stability of solution. Several additional input and output files were created to make the BOAST simulator more flexible and accessible.

CHAPTER V

SIMULATION RESULTS OF CASE STUDIES

After modifying the BOAST program, a comprehensive model for polymer treatment was set to test the sensitivity of vertical conformance treatment results on various reservoir parameters. Based on a series of runs, it was found that many factors influence the outcome of a vertical conformance treatment. Some of the factors were vertical permeability, permeability contrast, permeability thickness product contrast between layers, and the level of permeability reduction in the treated region.

5.1 Model Used in Case Studies

Studies have been made with a two-dimension cross-sectional model which is 400 ft horizontally and 20 ft thick with zero dip. A 20 by 2 grid system was used to model a two-layer reservoir with an injection well at one end, and a production well at the opposite end of the system, as shown in (Fig. 2). A constant injection rate of 900 STB/day was employed initially at the injection well while the production well was at a constant bottom hole pressure of 4015 psi (the bubble point pressure).

The reservoir was assumed to be under both capillary and gravity equilibrium initially. Fluid and rock properties used in this model were taken from the BOAST user's manual (see Tables 4 to 7) where the properties of the fluid are functions of pressure only.

TABLE 4

RESERVOIR AND FLUID PROPERTIES

Initial reservoir pressure, psia at 8330 ft.	4990
Injection well, rate constraint, STB/DAY	900
Production well, pressure constraint, psia	4015
Rock compressibility, psi^{-1}	3×10^{-6}
Wellbore radius, feet	0.33
Capillary pressure, psi	0
Water density, lbm/cu ft	62.238
Oil density, lbm/cu ft	46.244
Runs are terminated at WOR at 10	

TABLE 5

PVT PROPERTIES OF WATER

Reservoir pressure (psia)	Formation Volume Factor (RB/STB)	Viscosity (cp)
14.7	1.019	0.500
1014.7	1.016	0.501
2014.7	1.013	0.502
3014.7	1.010	0.503
4014.7	1.007	0.505
6014.7	1.001	0.510
9014.7	0.992	0.520

TABLE 6

PVT PROPERTIES OF OIL

Reservoir pressure (psia)	Formation Volume Factor (RB/STB)	Viscosity (cp)
14.7	1.062	1.040
1014.7	1.295	0.830
2014.7	1.435	0.695
3014.7	1.565	0.594
4014.7	1.695	0.510
6014.7	1.648	0.620
9014.7	0.579	0.740

TABLE 7

RELATIVE PERMEABILITY DATA

Sw	Krw	Kro
1.0	0.5	0.0
0.9	0.4704	0.0
0.8	0.2688	0.00147
0.7	0.1344	0.00228
0.6	0.0672	0.0370
0.5	0.0336	0.0571
0.4	0.0244	0.134
0.3	0.0122	0.207
0.2	0.0	0.604
0.1	0.0	1.000
0.0	0.0	1.000

To study the effect of permeability contrast, the high permeability zone which has a permeability of either 200 md or 1000 md was always at the top layer in the system, while the permeability of the bottom layer was 20 md.

To study the effect of vertical permeability, a range of 10^{-6} md to 20 md was used, but for each run the vertical permeability was constant throughout the whole reservoir.

To study the permeability thickness product contrast, the total thickness of the reservoir was maintained at 20 feet, while the thickness of the high permeable zone was varied. The values of the high permeable zone thickness that were studied included 10, 9, 7, 5, and 3 feet.

The vertical conformance treatment was assumed to have taken place when the top layer is at water breakthrough. As we can see from Tables 8 to 9, there is a large quantity of oil remaining in the bottom layer. Choosing water breakthrough arbitrarily as a restart criterion will help us observe the results of the treatment easily. The incremental oil recovery due to the treatment is defined as the difference between the oil recovery in a treatment case and a case where no treatment occurred at the restart. The permeability in the first grid block of the top zone is changed from the original one to simulate the treatment in the vicinity of the injection well.

5.2 Simulation Result and Discussions

The effectiveness of a simulated treatment was determined by comparing the oil recovery in reservoir pore volumes at a WOR limit of 10. Also, the recovery for the base case was at this same water oil ratio limit. The base case is defined to be where there is no permeability modification occurring during a complete simulation run. In the other cases the permeability of the

TABLE 8
OIL REMAINING IN THE RESERVOIR WHEN
WATER BREAKTHROUGH AT TOP LAYER
(Permeability Contrast is 10:1)

Vertical	Thickness		Oil saturation		
permeability	Top layer	Bottom layer	Top layer	Bottom layer	Average
10^{-6}	10	10	0.329	0.752	0.540
0.02	10	10	0.334	0.744	0.539
2.00	10	10	0.335	0.662	0.498
20.0	10	10	0.449	0.628	0.488
10^{-6}	7	13	0.329	0.752	0.604
0.02	7	13	0.328	0.745	0.599
2.00	7	13	0.335	0.667	0.550
20.0	7	13	0.345	0.629	0.530
10^{-6}	5	15	0.329	0.752	0.646
0.02	5	15	0.330	0.746	0.642
2.00	5	15	0.335	0.666	0.583
20.0	5	15	0.346	0.627	0.556
10^{-6}	3	17	0.329	0.752	0.688
0.02	3	17	0.329	0.746	0.683
2.00	3	17	0.341	0.683	0.616
20.0	3	17	0.362	0.621	0.582

TABLE 9
OIL REMAINING IN THE RESERVOIR WHEN WATER BREAKTHROUGH AT TOP LAYER
(Permeability Contrast is 50 :1)

Vertical	Thickness		Oil saturation		
permeability	Top layer	Bottom layer	Top layer	Bottom layer	Average
10^{-6}	10	10	0.348	0.787	0.567
0.02	10	10	0.342	0.785	0.558
2.00	10	10	0.348	0.766	0.557
20.0	10	10	0.350	0.727	0.538
10^{-6}	7	13	0.348	0.788	0.634
0.02	7	13	0.348	0.785	0.632
2.00	7	13	0.346	0.766	0.619
20.0	7	13	0.360	0.712	0.588
10^{-6}	5	15	0.348	0.788	0.678
0.02	5	15	0.346	0.785	0.675
2.00	5	15	0.345	0.766	0.660
20.0	5	15	0.331	0.714	0.618
10^{-6}	3	17	0.348	0.788	0.722
0.02	3	17	0.346	0.786	0.717
2.00	3	17	0.349	0.767	0.704
20.0	3	17	0.355	0.755	0.695

high permeable zone in the injection grid block was reduced to 1/10th, 1/100th, and 1/1000th of the original permeability.

All the results are presented in tables 10 to 18. Several factors that were considered to affect the treatment outcome are discussed below:

(1) Vertical Permeability

Four different vertical permeabilities were used in this study where a vertical permeability of 10^{-6} md was defined to be a non-communicating stratified reservoir; and with the increase in vertical permeability, the degree of communication of adjacent layers increases. A vertical permeability of 20 md was defined to be a communicating reservoir.

A low vertical permeability was found conducive to high incremental recovery from a water shut-off treatment (where the permeability in the treated zone is reduced to 1/1000th of original one). For a reservoir with layers of equal thickness which is also non-communicating, the incremental oil recovery in the treatment case was 0.195 pore volume (Table 10). However, as the reservoir becomes more communicating (vertical permeability increasing to 20 md), the incremental oil decreases to 0.049 pore volume of incremental oil recovered after treatment. Table 15 shows a similar trend as the above case, but where the permeability contrast between layers was 50 to 1 instead of 10 to 1 as in the above case (Table 10).

Fig. 23 shows the decrease in incremental oil recovery observed as vertical permeability increases for the cases of initial permeability contrasts between layers of ten to one and fifty to one. In both cases, incremental recoveries were high when vertical permeability were essentially zero (10^{-6} md) and decreased continuously as vertical permeability increased. This illustrates that the increase of vertical permeability results in the increased oil recovery

TABLE 10
SIMULATION TREATMENT RESULTS FOR CASE
T_{high} = 10 feet ; T_{low} = 10 feet
K_{high} = 200 md ; K_{low} = 20 md.

Kz	Cases	Water injected (PV)	Oil produced (PV)	Incremental oil (PV)
10^{-6}	Base	0.424	0.303	
	Run 1	1.127	0.507	0.204
	Run 2	0.582	0.505	0.202
	Run 3	0.516	0.498	0.195
0.02	Base	0.889	0.392	
	Run 1	1.143	0.500	0.108
	Run 2	0.686	0.504	0.112
	Run 3	0.639	0.503	0.111
2.0	Base	0.498	0.370	
	Run 1	0.731	0.406	0.036
	Run 2	0.770	0.423	0.053
	Run 3	0.767	0.426	0.056
20.0	Base	0.808	0.442	
	Run 1	0.848	0.480	0.038
	Run 2	0.772	0.490	0.048
	Run 3	0.760	0.491	0.049

TABLE 11
SIMULATION TREATMENT RESULTS FOR CASE
T_{high} = 9 feet ; T_{low} = 11 feet
K_{high} = 200 md ; K_{low} = 20 md.

Kz	Cases	Water injected (PV)	Oil produced (PV)	Incremental oil (PV)
10^{-6}	Base	1.158	0.402	
	Run 1	1.078	0.508	0.106
	Run 2	0.576	0.506	0.104
	Run 3	0.518	0.499	0.097
0.02	Base	1.080	0.417	
	Run 1	1.109	0.504	0.087
	Run 2	0.681	0.505	0.088
	Run 3	0.639	0.504	0.087
2.0	Base	0.742	0.398	
	Run 1	0.915	0.431	0.036
	Run 2	0.896	0.438	0.040
	Run 3	0.888	0.441	0.043
20.0	Base	0.858	0.447	
	Run 1	0.863	0.482	0.034
	Run 2	0.791	0.489	0.042
	Run 3	0.781	0.490	0.043

TABLE 12
SIMULATION TREATMENT RESULTS FOR CASE
T_{high} = 7 feet ; T_{low} = 13 feet
K_{high} = 200 md ; K_{low} = 20 md.

Kz	Cases	Water injected (PV)	Oil produced (PV)	Incremental oil (PV)
10^{-6}	Base	1.646	0.502	
	Run 1	0.966	0.507	0.005
	Run 2	0.568	0.507	0.005
	Run 3	0.521	0.500	-0.002
0.02	Base	1.460	0.488	
	Run 1	0.996	0.503	0.015
	Run 2	0.670	0.505	0.017
	Run 3	0.631	0.504	0.016
2.0	Base	0.931	0.431	
	Run 1	1.108	0.456	0.025
	Run 2	1.102	0.465	0.034
	Run 3	1.004	0.466	0.035
20.0	Base	0.952	0.466	
	Run 1	0.873	0.485	0.019
	Run 2	0.817	0.490	0.024
	Run 3	0.811	0.490	0.024

TABLE 13
SIMULATION TREATMENT RESULTS FOR CASE
T_{high} = 5 feet ; T_{low} = 15 feet
K_{high} = 200 md ; K_{low} = 20 md.

Kz	Cases	Water injected (PV)	Oil produced (PV)	Incremental oil (PV)
10^{-6}	Base	1.385	0.507	
	Run 1	0.857	0.507	0.000
	Run 2	0.559	0.505	-0.002
	Run 3	0.525	0.505	-0.002
0.02	Base	1.268	0.499	
	Run 1	0.879	0.504	0.005
	Run 2	0.653	0.505	0.006
	Run 3	0.624	0.504	0.005
2.0	Base	0.920	0.444	
	Run 1	0.989	0.473	0.029
	Run 2	0.980	0.479	0.035
	Run 3	0.976	0.480	0.036
20.0	Base	0.949	0.485	
	Run 1	0.844	0.492	0.007
	Run 2	0.810	0.492	0.009
	Run 3	0.806	0.494	0.009

TABLE 14
SIMULATION TREATMENT RESULTS FOR CASE
T_{high} = 3 feet ; T_{low} = 17 feet
K_{high} = 200 md ; K_{low} = 20 md.

Kz	Cases	Water injected (PV)	Oil produced (PV)	Incremental oil (PV)
10^{-6}	Base	1.063	0.506	
	Run 1	0.733	0.507	0.001
	Run 2	0.551	0.505	-0.001
	Run 3	0.530	0.503	-0.002
0.02	Base	0.991	0.500	
	Run 1	0.760	0.504	0.004
	Run 2	0.632	0.505	0.005
	Run 3	0.614	0.504	0.004
2.0	Base	0.977	0.490	
	Run 1	0.908	0.496	0.006
	Run 2	0.891	0.498	0.008
	Run 3	0.887	0.499	0.009
20.0	Base	0.804	0.496	
	Run 1	0.745	0.498	0.002
	Run 2	0.734	0.499	0.003
	Run 3	0.732	0.499	0.003

TABLE 15
SIMULATION TREATMENT RESULTS FOR CASE
T_{high} = 10 feet ; T_{low} = 10 feet
K_{high} = 1000 md ; K_{low} = 20 md.

Kz	Cases	Water injected (PV)	Oil produced (PV)	Incremental oil (PV)
10^{-6}	Base	0.273	0.261	
	Run 1	0.283	0.265	0.004
	Run 2	0.985	0.500	0.239
	Run 3	0.550	0.506	0.245
0.02	Base	0.275	0.264	
	Run 1	0.280	0.265	0.001
	Run 2	1.073	0.499	0.235
	Run 3	0.683	0.504	0.240
2.0	Base	0.299	0.272	
	Run 1	0.299	0.284	0.002
	Run 2	0.302	0.337	0.070
	Run 3	0.601	0.362	0.085
20.0	Base	0.834	0.390	
	Run 1	0.859	0.392	0.002
	Run 2	0.857	0.455	0.065
	Run 3	0.850	0.470	0.080

TABLE 16
SIMULATION TREATMENT RESULTS FOR CASE
T_{high} = 7 feet ; T_{low} = 13 feet
K_{high} = 1000 md ; K_{low} = 20 md.

Kz	Cases	Water injected (PV)	Oil produced (PV)	Incremental oil (PV)
10^{-6}	Base	0.201	0.188	
	Run 1	0.223	0.199	0.011
	Run 2	0.845	0.504	0.316
	Run 3	0.537	0.504	0.316
0.02	Base	0.207	0.191	
	Run 1	0.234	0.202	0.011
	Run 2	0.945	0.499	0.308
	Run 3	0.665	0.504	0.313
2.0	Base	0.341	0.276	
	Run 1	0.380	0.286	0.010
	Run 2	0.644	0.308	0.082
	Run 3	0.646	0.321	0.095
20.0	Base	0.968	0.361	
	Run 1	0.931	0.371	0.010
	Run 2	0.904	0.434	0.073
	Run 3	0.907	0.443	0.083

TABLE 17
SIMULATION TREATMENT RESULTS FOR CASE
T_{high} = 5 feet ; T_{low} = 15 feet
K_{high} = 1000 md ; K_{low} = 20 md.

Kz	Cases	Water injected (PV)	Oil produced (PV)	Incremental oil (PV)
10^{-6}	Base	0.152	0.140	
	Run 1	1.409	0.362	0.223
	Run 2	0.763	0.507	0.366
	Run 3	0.536	0.504	0.364
0.02	Base	0.159	0.143	
	Run 1	1.351	0.355	0.212
	Run 2	0.855	0.502	0.359
	Run 3	0.664	0.503	0.360
2.0	Base	0.640	0.257	
	Run 1	0.785	0.280	0.033
	Run 2	0.835	0.336	0.089
	Run 3	0.831	0.336	0.089
20.0	Base	1.077	0.353	
	Run 1	0.968	0.369	0.016
	Run 2	0.963	0.427	0.074
	Run 3	0.962	0.434	0.081

TABLE 18
SIMULATION TREATMENT RESULTS FOR CASE
T_{high} = 3 feet ; T_{low} = 17 feet
K_{high} = 1000 md ; K_{low} = 20 md.

Kz	Cases	Water injected (PV)	Oil produced (PV)	Incremental oil (PV)
10^{-6}	Base	0.089	0.088	
	Run 1	1.776	0.502	0.414
	Run 2	0.676	0.506	0.418
	Run 3	0.536	0.504	0.416
0.02	Base	0.098	0.094	
	Run 1	1.765	0.349	0.245
	Run 2	0.773	0.466	0.362
	Run 3	0.660	0.469	0.365
2.0	Base	0.682	0.256	
	Run 1	1.069	0.346	0.090
	Run 2	1.137	0.387	0.131
	Run 3	1.135	0.395	0.139
20.0	Base	0.677	0.324	
	Run 1	1.050	0.409	0.085
	Run 2	1.028	0.443	0.019
	Run 3	1.023	0.446	0.122

The notation used in tables from Table 8 to 18 are defined as :

Base	: Case without treatment
Run 1	: Well treated by reducing permeability to 1/10th.
Run 2	: Well treated by reducing permeability to 1/100th.
Run 3	: Well treated by reducing permeability to 1/1000th.
T_{high}	: Thickness of top layer .
T_{low}	: Thickness of bottom layer .
K_{high}	: Horizontal permeability of top layer .
K_{low}	: Horizontal permeability of bottom layer .
K_Z	: Vertical permeability.
PV	: Pore Volume.

FIG. 23 DEPENDENCE OF OIL INCREMENTAL RECOVERY ON VERTIVAL PERMEABILITY

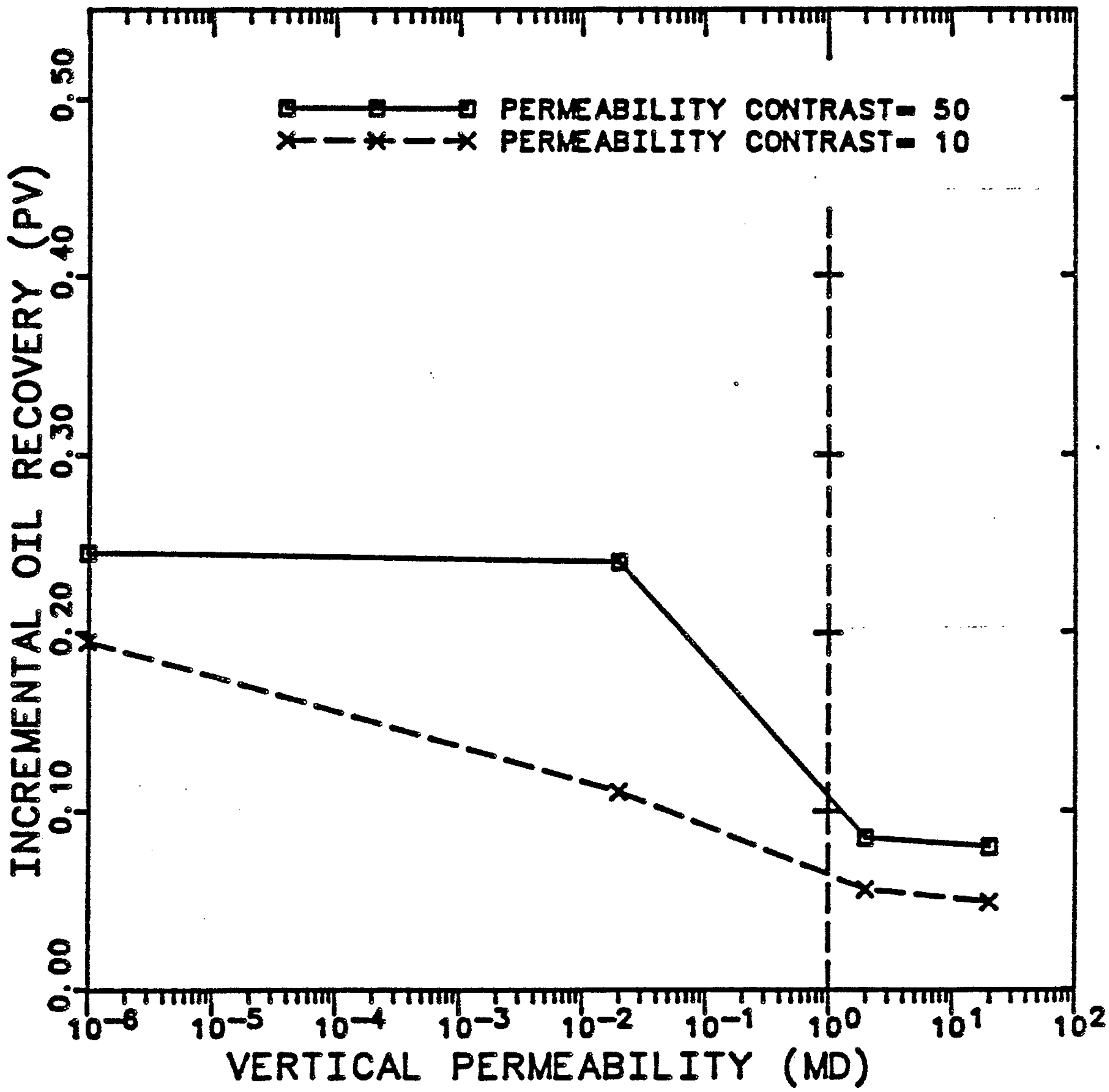

in the base cases where the vertical sweep efficiency was improved by the crossflow and, therefore, less benefit was obtained from vertical conformance treatment (Fig. 24, 25).

(2) Permeability thickness Product Contrast

The permeability thickness product also known as fluid conductivity plays a very important role on the allocation of the fluid between layers. In the case of water injection, the more contrast in permeability thickness product, the more irregular the distribution of water will be, and thus the injection profile is totally controlled by kh contrast initially. However, as water goes deeper into the reservoir, other characteristics of the reservoir could alter the water movement path and thus affect the displacement of oil by water.

When significant crossflow could take place in a reservoir, the incremental oil recovery from a water shutoff treatment increased gradually and continuously as the ratio of the permeability thickness product of the high permeability zone to that of the low permeability zone increased. This result is illustrated in Fig. 26 for cases where the permeability of the zones were 200 md and 20 md, and the vertical permeability was 20 md.

For the same reservoir except the degree of communicating being decreased, a similar result was found when vertical permeability is equal to 0.02 md (see Fig. 27).

A quite different response to permeability-thickness contrast was seen when kz = 10^{-6} md which is an assumed non-communicating reservoir. There was very little incremental oil obtained when the ratio of the permeability-thickness product of the high permeability zone to that of the low permeability zone was less than 5.4 (see Fig. 28); for contrasts above this level, significant incremental recovery was obtained. This result is due in large part to the water

FIG. 24 PRODUCTION HISTORY FOR RESERVOIR WITHOUT CROSSFLOW
(VERTICAL PERMEABILITY = 0.000001 MD)

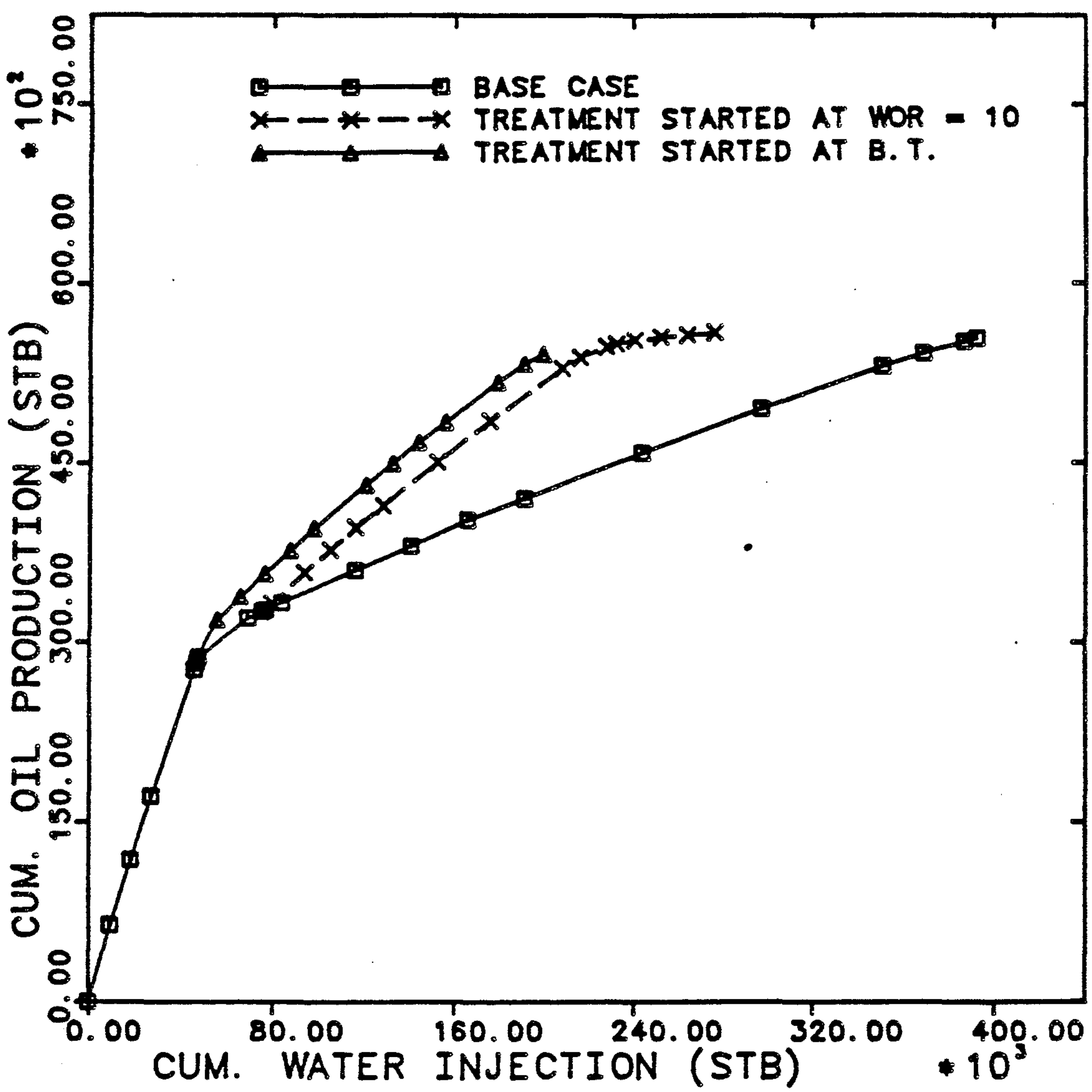

FIG. 24A WATER OIL RATIO CURVE FOR RESERVOIR WITHOUT CROSSFLOW (VERTICAL PERMEABILITY = 0.000001 MD)

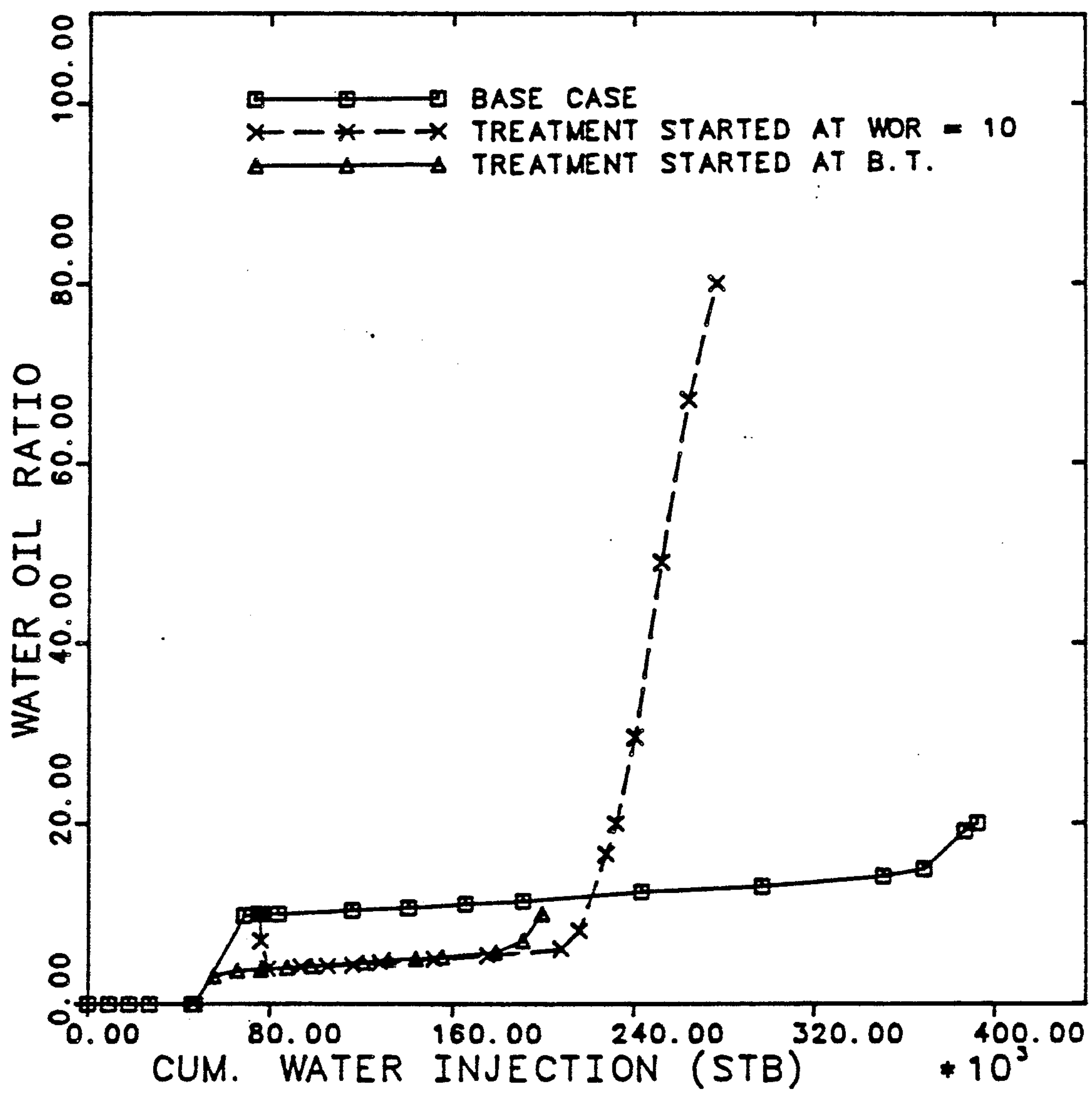

FIG. 25 PRODUCTION HISTORY FOR RESERVOIR WITH CROSSFLOW
(VERTICAL PERMEABILITY = 20.0 MD)

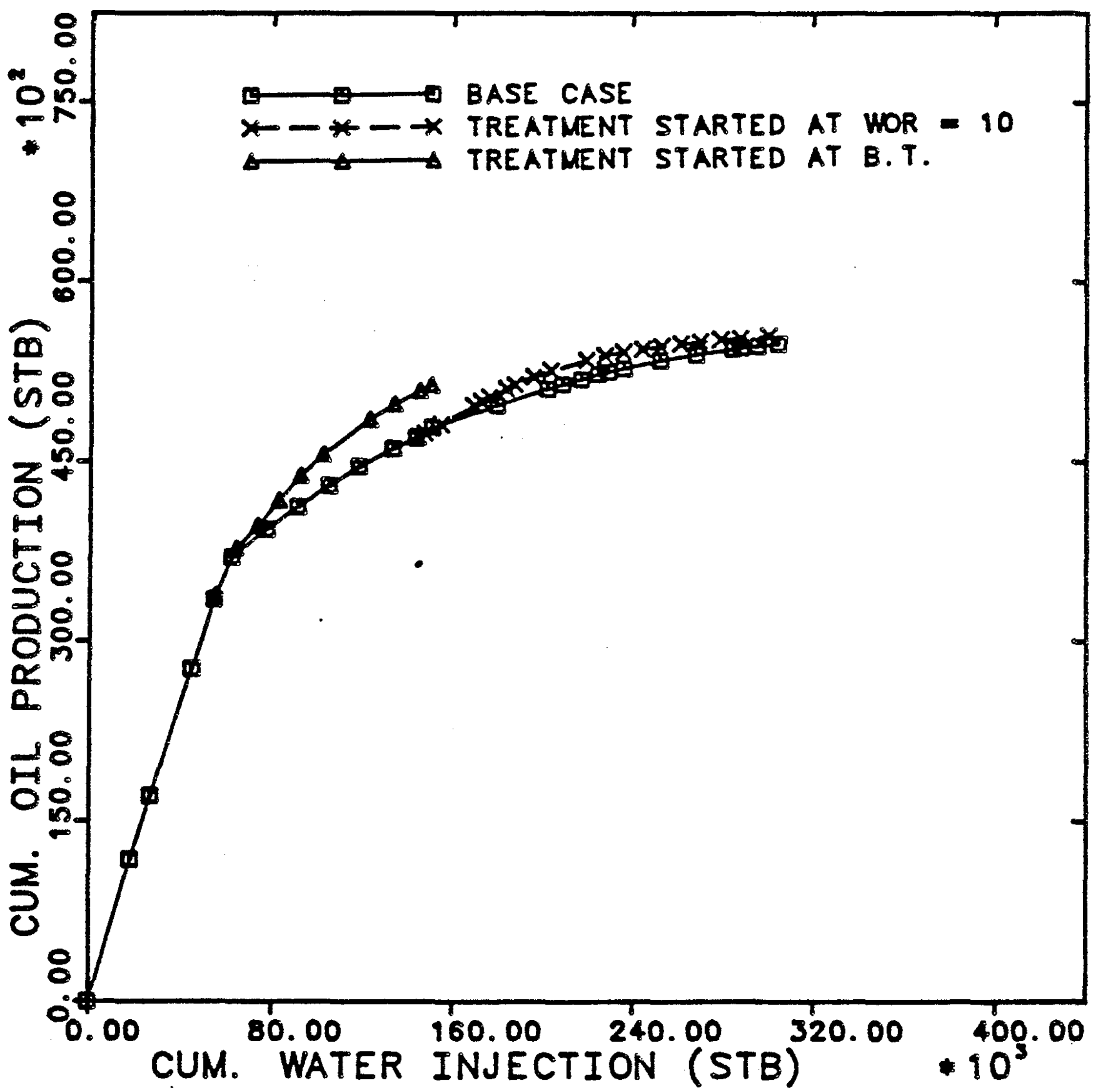

FIG. 25A WATER OIL RATIO CURVE FOR RESERVOIR
WITH CROSSFLOW
(VERTICAL PERMEABILITY = 20.0 MD)

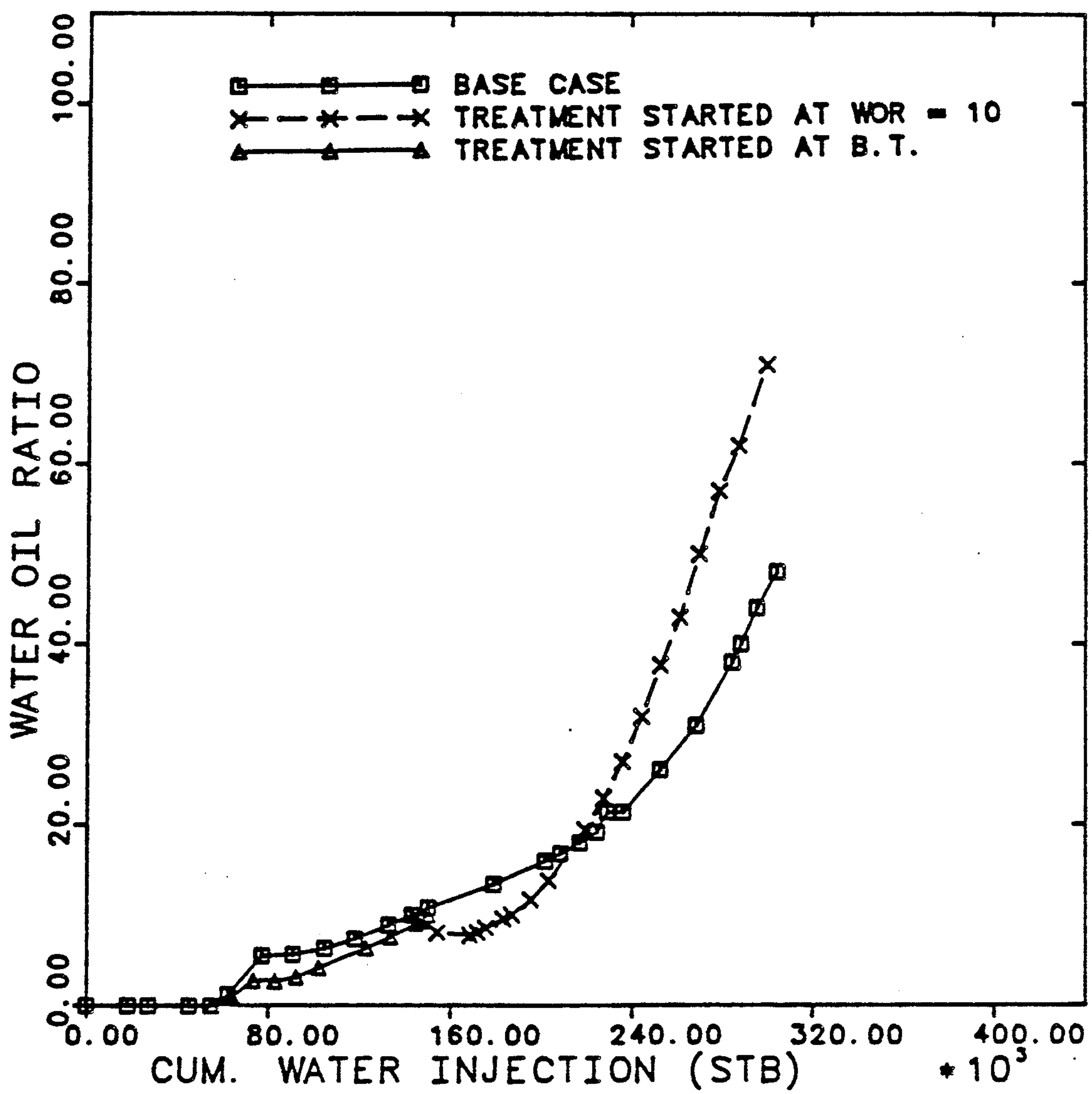

FIG. 26 DEPENDENCE OF INCREMENTAL RECOVERY ON KH CONTRAST- 10:1 PERMEABILITY RATIO WITH CROSSFLOW (VERTICAL PERMEABILITY = 20 MD)

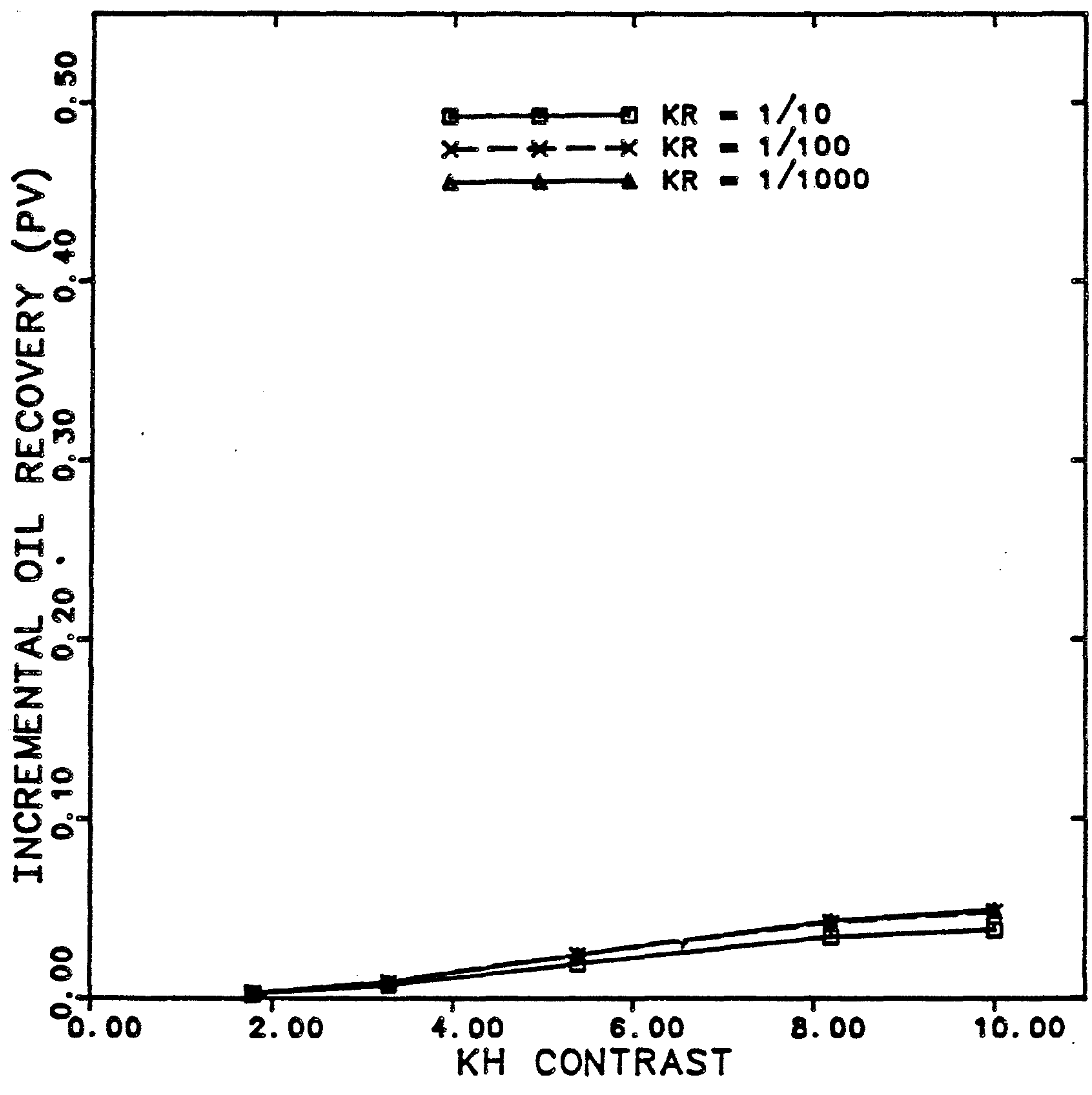

FIG. 27 DEPENDENCE OF INCREMENTAL RECOVERY ON KH CONTRAST- 10:1 PERMEABILITY RATIO WITH LITTLE CROSSFLOW (VERTICAL PERMEABILITY = 0.02 MD)

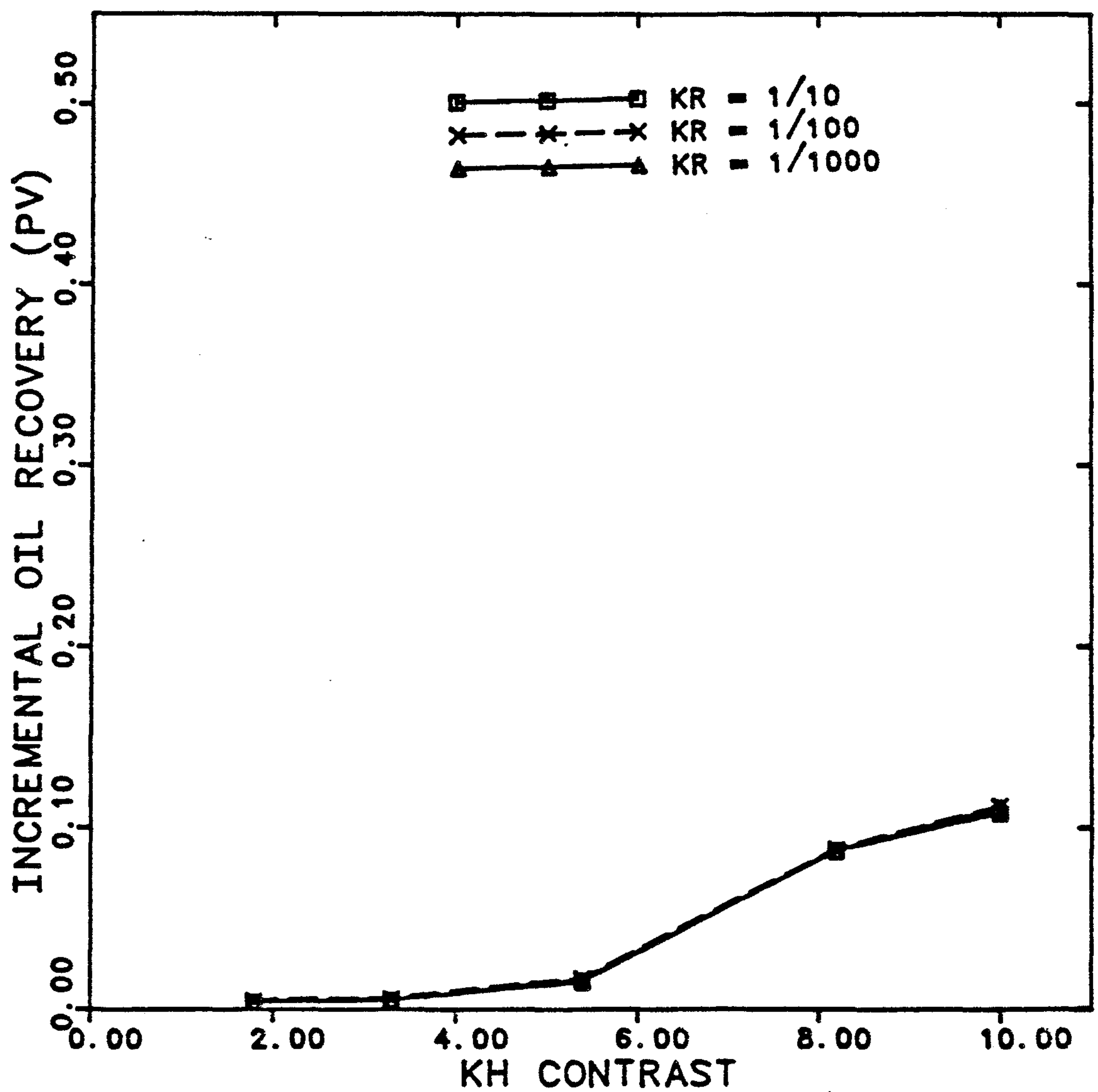

FIG. 28 DEPENDENCE OF INCREMENTAL RECOVERY ON KH CONTRAST– 10:1 PERMEABILITY RATIO WITHOUT CROSSFLOW (VERTICAL PERMAEBILITY = 0.000001 MD)

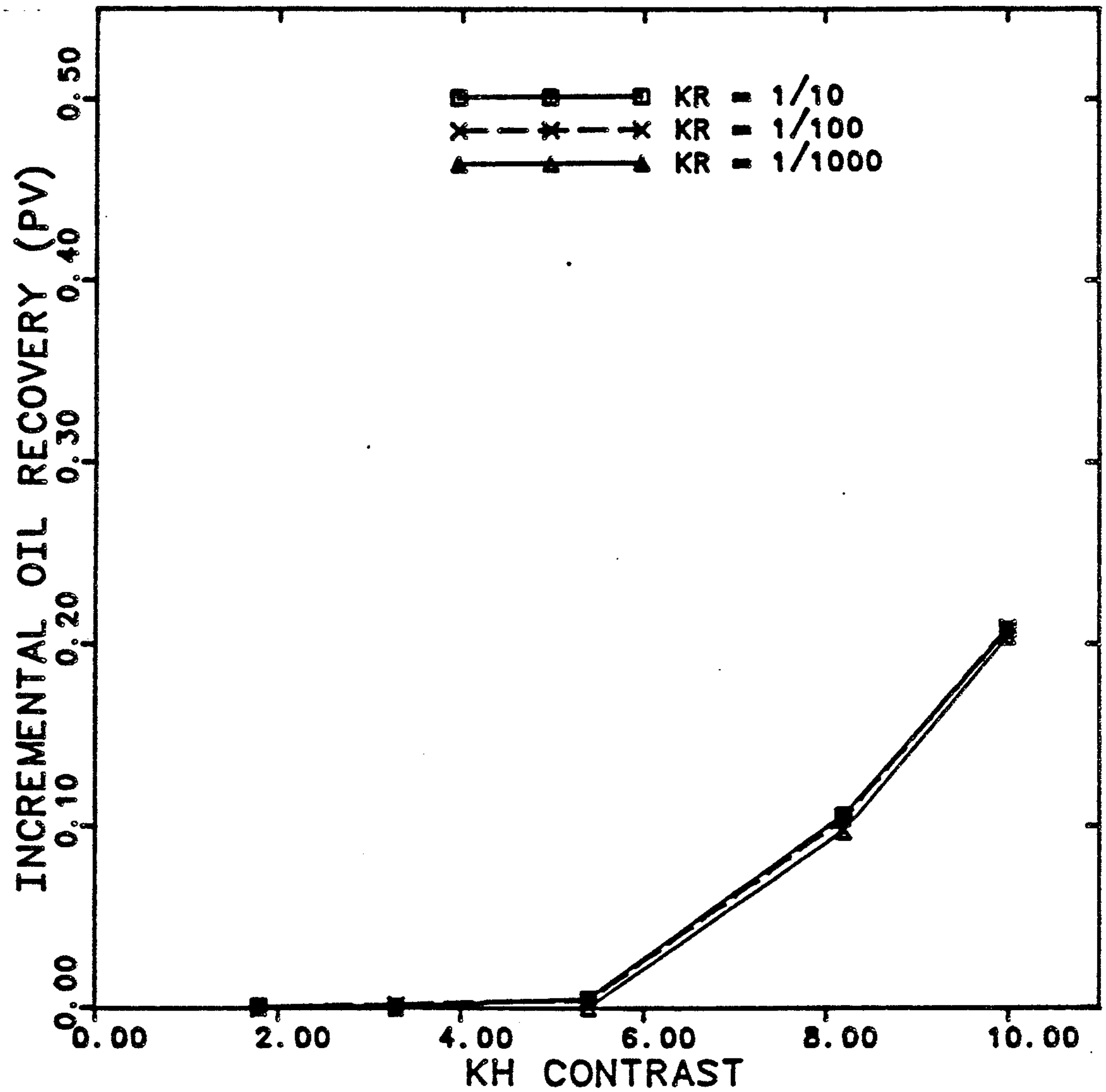

oil ratio limit used to determine ultimate recovery from the reservoir. With a WOR limit of 10, when the high permeability zone is relatively thin, waterflooding can continue long after the high permeability zone has been depleted without the WOR reaching the value of 10. Thus, the base case recovery will be high resulting in low incremental recovery from a conformance treatment. Fig. 29 and 30 illustrate the WOR curve variation during the waterflooding and treatment performance. With a thicker high permeability zone, as reflected in higher kh contrast, the water oil ratio reaches 10 shortly after breakthrough in the high permeability zone, leaving a large incremental oil target for a conformance treatment.

For cases with a permeability of 1000 md in the high permeability zone and 20 md in the low permeability zone, incremental oil recovery from a vertical conformance treatment decreases as the permeability-thickness contrast between layers increased. With no crossflow (Fig. 31), high incremental recoveries were obtained when the high k zone permeability was reduced to 1/100th or 1/1000th of its original value. The incremental recovery decreased with increasing kh contrast because of increasing base case (no treatment) recovery as the high permeability zone became thicker where there also existed a high permeability contrast between layers.

The same trend was observed (Fig. 32), for the same high k contrast reservoir with an increasing crossflow, but with lower incremental oil recovery. All incremental recoveries were lessened with the same reservoir, especially, for those cases exhibiting significant crossflow as shown in (Fig. 33). This is again due to higher recoveries from waterflooding without treatment.

FIG. 29 PRODUCTION HISTORY WITH WATER OIL RATIO CURVE FOR RESERVOIR PERMEABILITY CONTRAST BEING 10 TO 1
H1 = 10 FEET ; H2 = 10 FEET
VERTICAL PERMEABILITY = 0.000001 MD

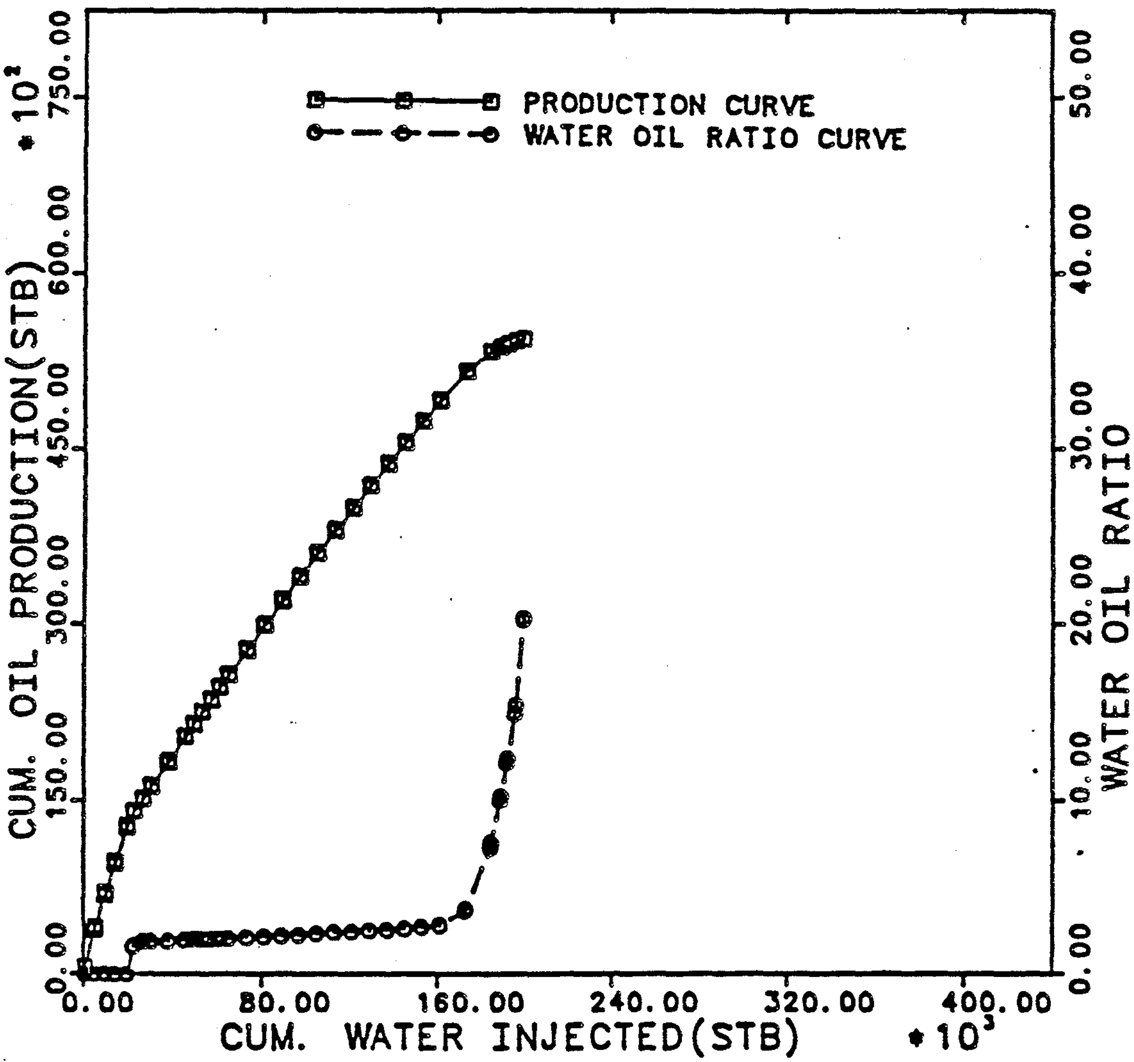

FIG. 30 PRODUCTION HISTORY WITH WATER OIL RATIO CURVE FOR RESERVOIR PERMEABILITY CONTRAST BEING 10 TO 1
H1 = 3 FEET : H2 = 17 FEET
VERTICAL PERMEABILITY = 0.000001 MD

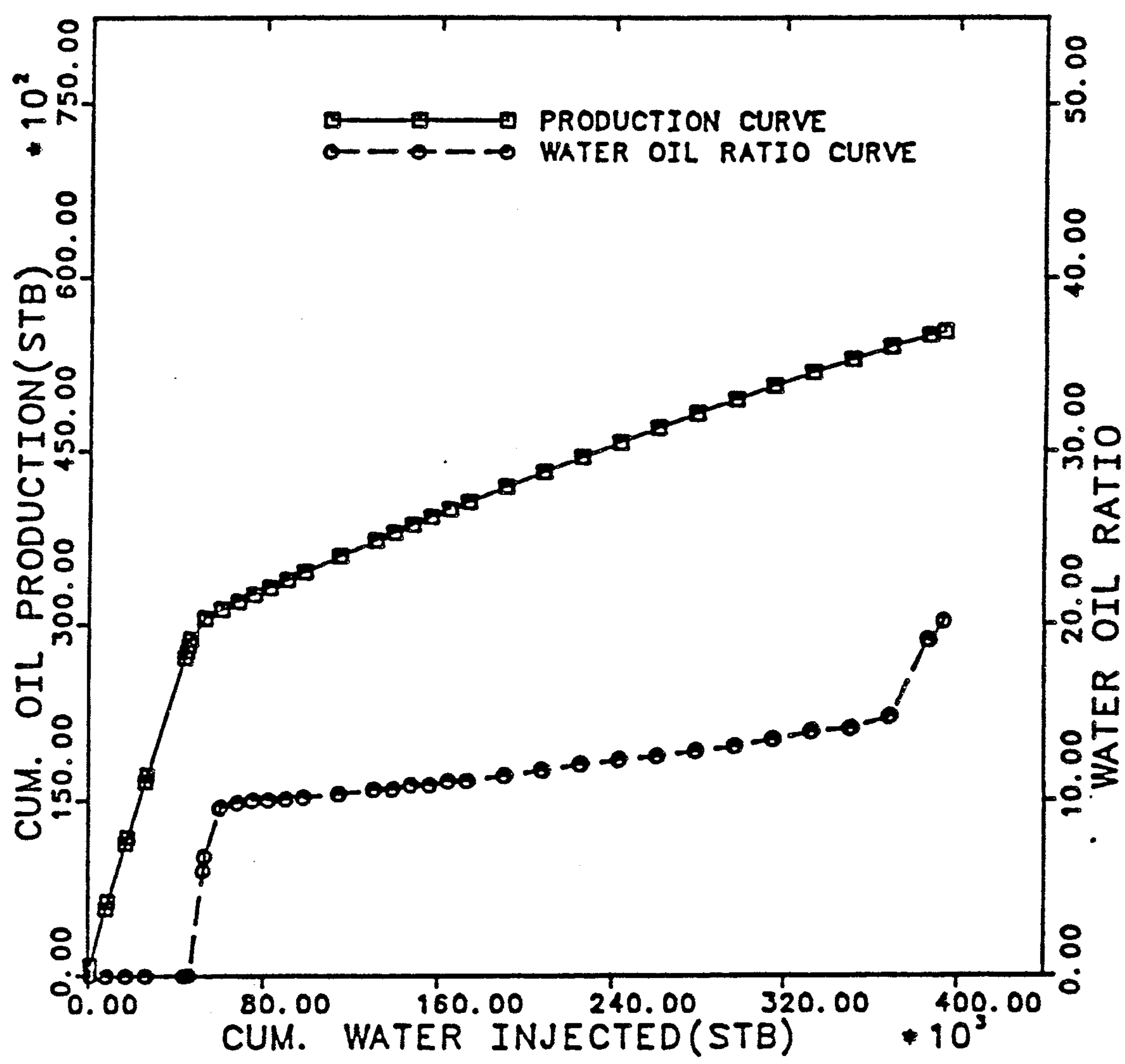

FIG. 31 DEPENDENCE OF INCREMENTAL RECOVERY ON KH CONTRAST– 50:1 PERMEABILITY RATIO WITHOUT CROSSFLOW
(VERTICAL PERMEABILITY = 0.000001 MD)

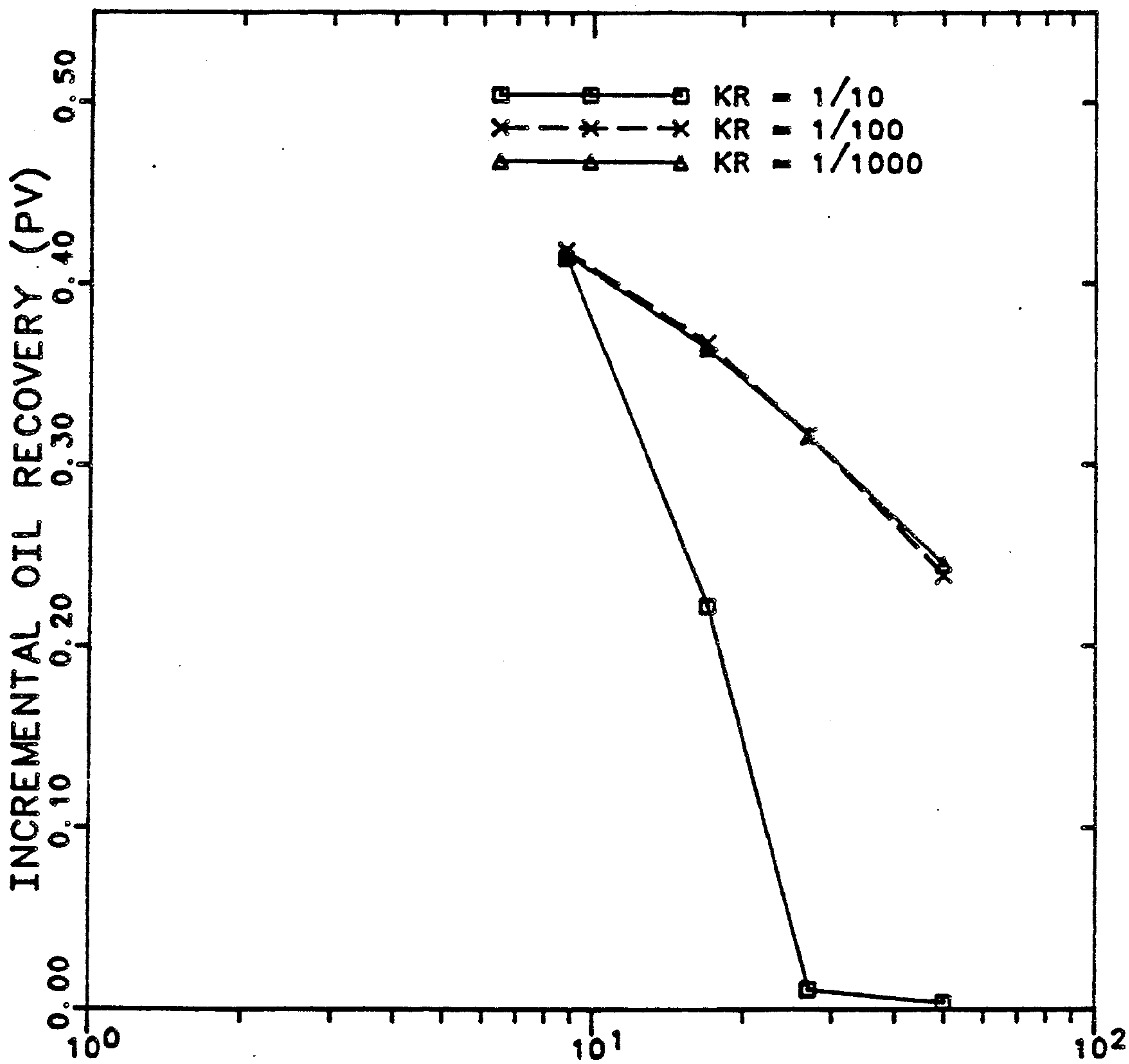

FIG. 32 DEPENDENCE OF INCREMENTAL RECOVERY ON KH CONTRAST- 50:1 PERMEABILITY RATIO WITH LITTLE CROSSFLOW (VERTICAL PERMEABILITY = 0.02 MD)

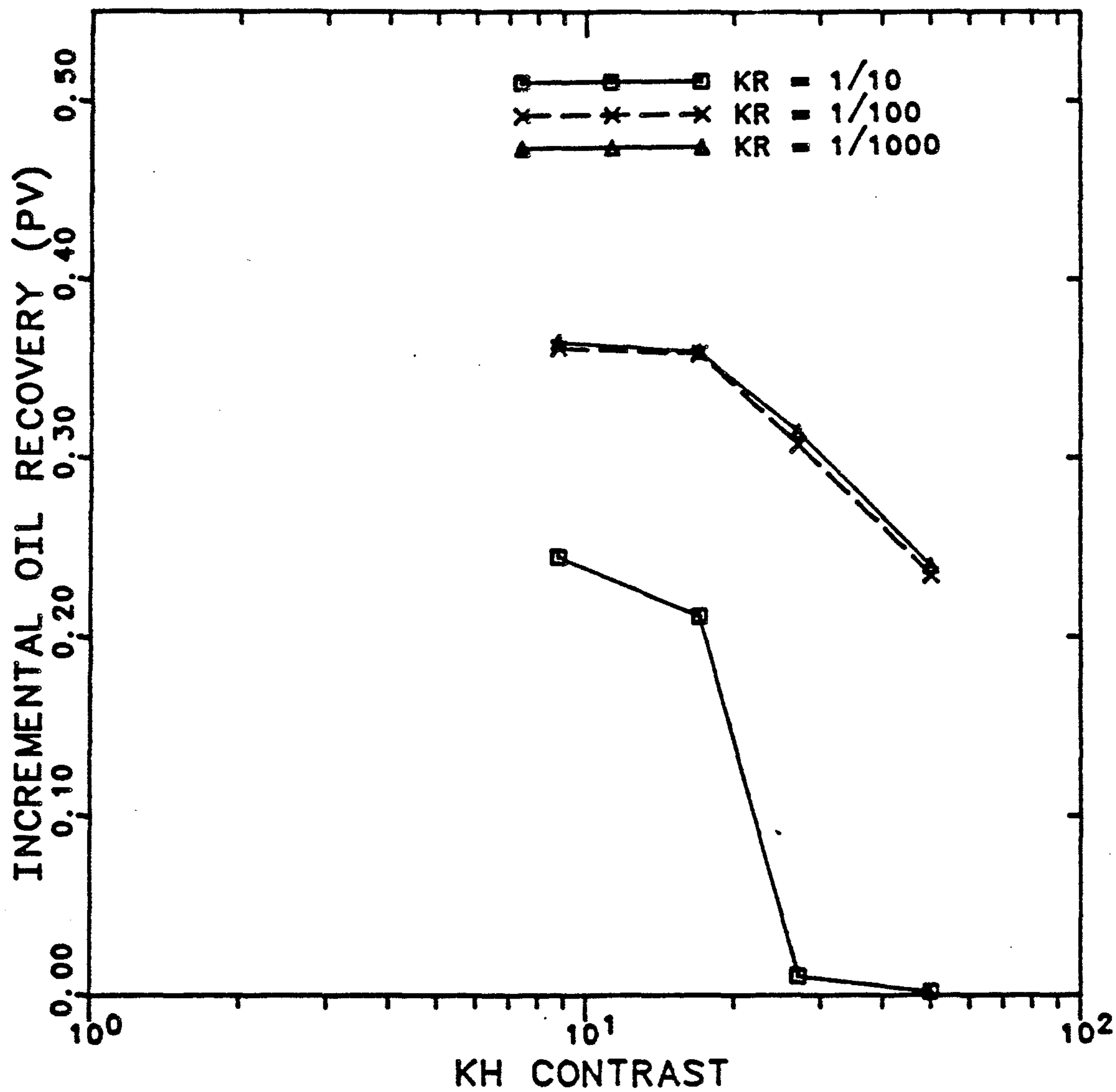

FIG. 33 DEPENDENCE OF INCREMENTAL RECOVERY ON KH CONTRAST- 50:1 PERMEABILITY RATIO WITH CROSSFLOW
(VERTICAL PERMEABILITY = 20.0 MD)

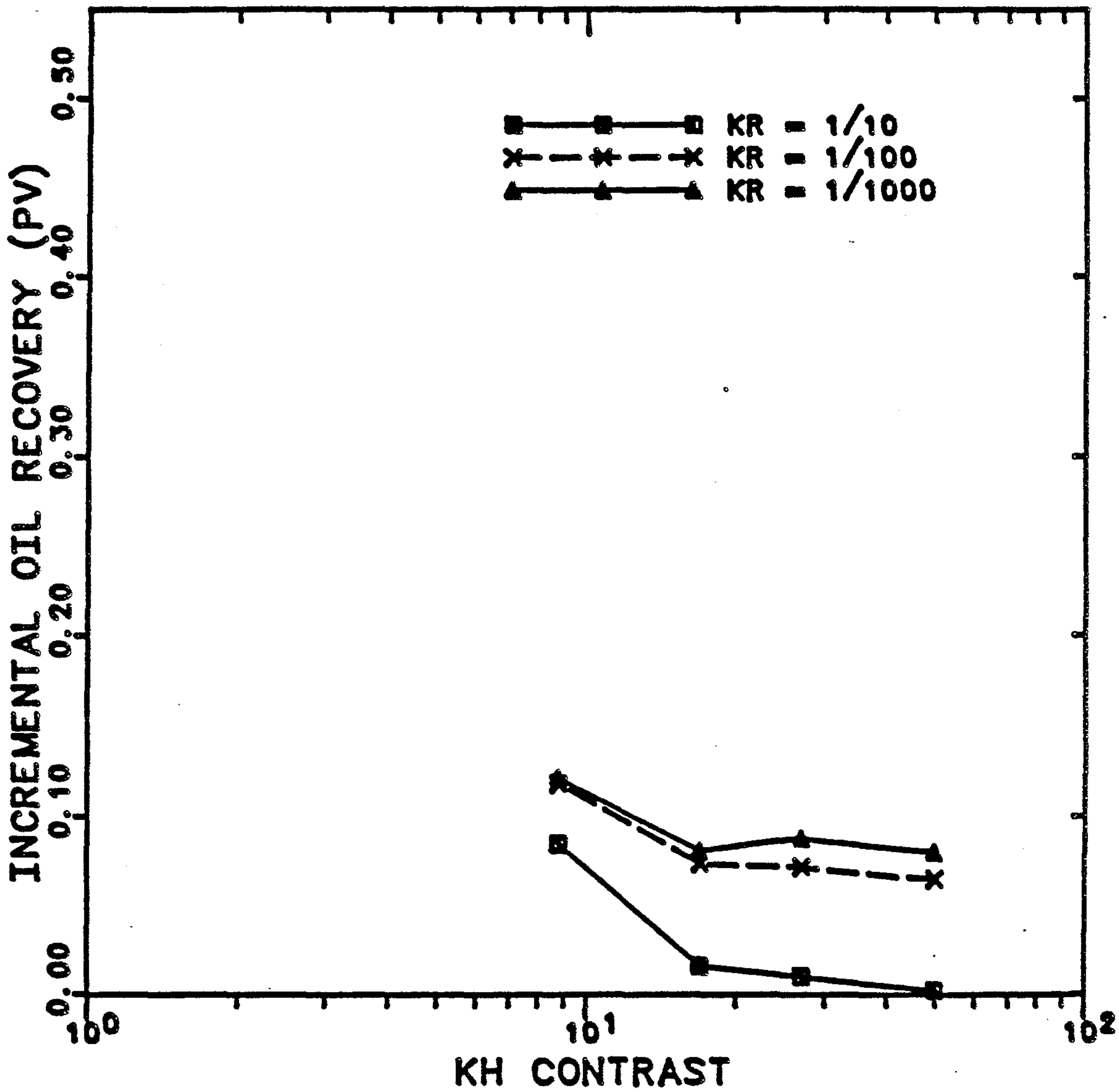

(3) Permeability Contrast

The layer permeability contrasts had a marked influence on the crossflow, the lower permeability contrast will induce more crossflow and thus improve the oil recovery at the water breakthrough and beyond. Fig. 23 is a plot showing that the high permeability contrast results in high incremental oil recovery when the thicknesses of layers are equal. The same situation happens in other cases that have unequal thickness ratio (Fig. 34 to 36). Although the incremental oil recovery decreases gradually in the case of permeability contrast being 50 and increases continuously in the case of permeability contrast being 10. With a certain thickness ratio, the high k contrast results in high incremental oil recovery (Fig. 34 to 36).

(4) Level of Reduced Permeability

Three levels of reduction are investigated through the whole study. For cases where the permeability contrast is 10, whether the reservoir is with or without crossflow, incremental oil recovery showed little sensitivity to the level of permeability reduction in the simulated treated region as the incremental recoveries were almost identical for permeability reduction of 1/10th to 1/100th of the original permeability (see Fig. 26 and Fig. 28). However, as seen in Fig. 31 to Fig. 33, with a higher permeability contrast 50, a treated case of permeability of 1/10th was insufficient to significantly improve oil recovery. This indicates that to guarantee a successful treatment job, a high level reduced permeability is necessary for a high k contrast reservoir. For a low k contrast reservoir, the permeability reduced in treatment does not have to be lower than the lowest one. Several low level reduced permeability cases were studied. Fig. 37 shows that a low level permeability reduction will increase the oil recovery in a low k contrast reservoir.

FIG. 34 DEPENDENCE OF INCREMENTAL RECOVERY ON THICKNESS RATIO WHERE RESERVOIR HAS NO CROSSFLOW (VERTICAL PERMEABILITY = 0.000001 MD)

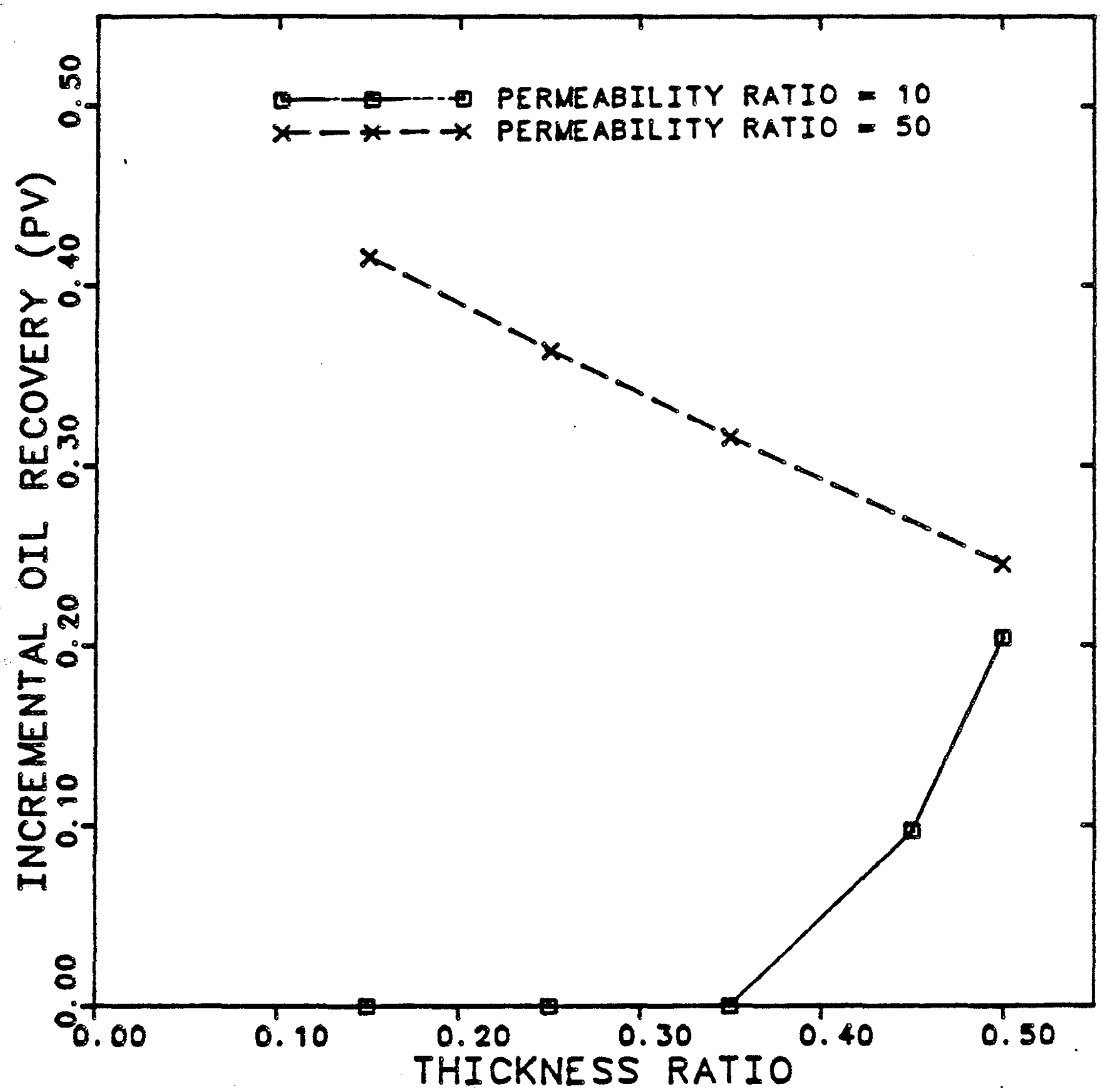

FIG. 35 DEPENDENCE OF INCREMENTAL RECOVERY ON THICKNESS RATIO WHERE RESERVOIR HAS LITTLE CROSSFLOW (VERTICAL PERMEABILITY = 0.02 MD)

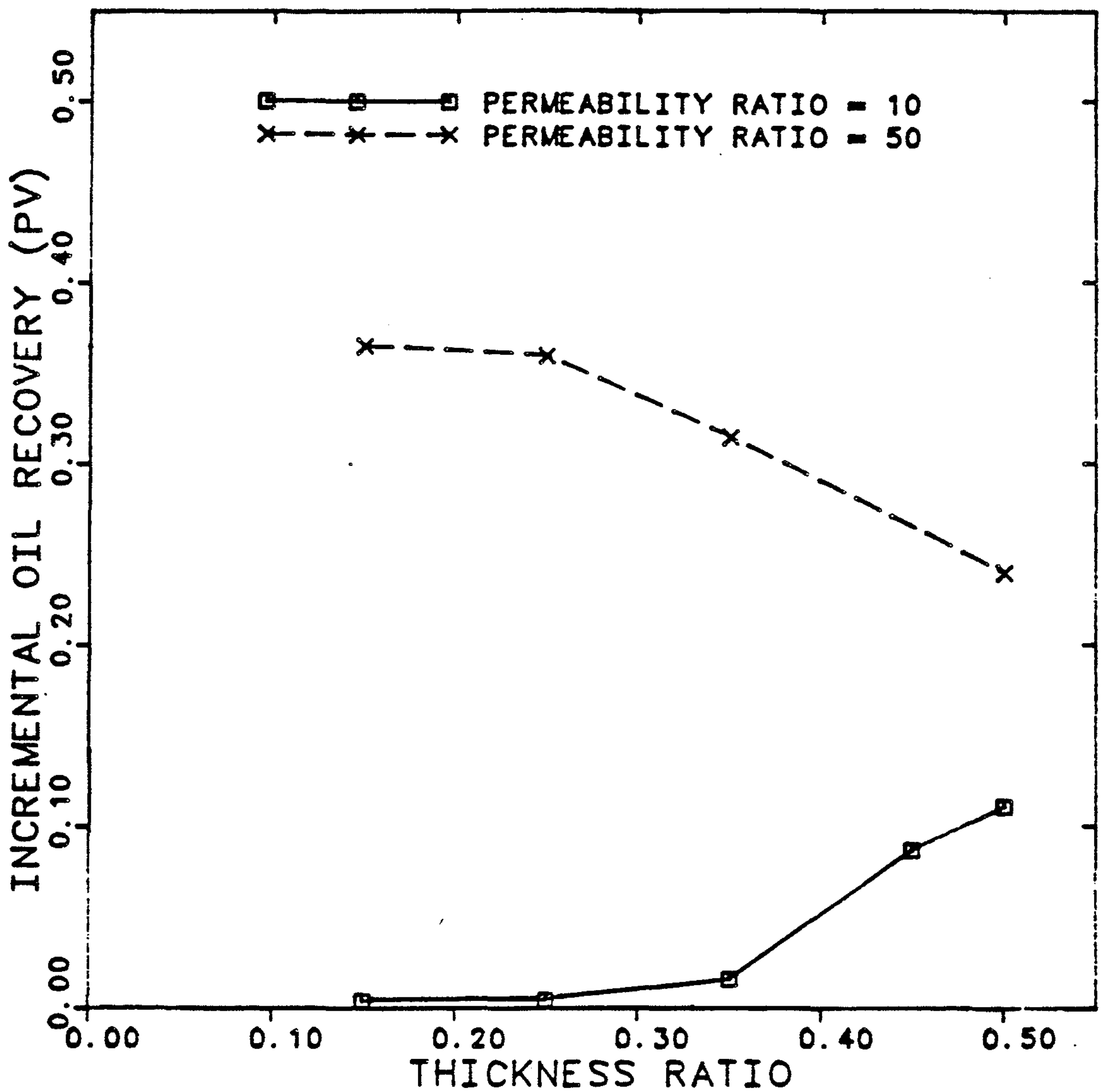

FIG. 36 DEPENDENCE OF INCREMENTAL RECOVERY ON THICKNESS RATIO WHERE RESERVOIR HAS CROSSFLOW (VERTICAL PERMEABILITY = 20.0 MD)

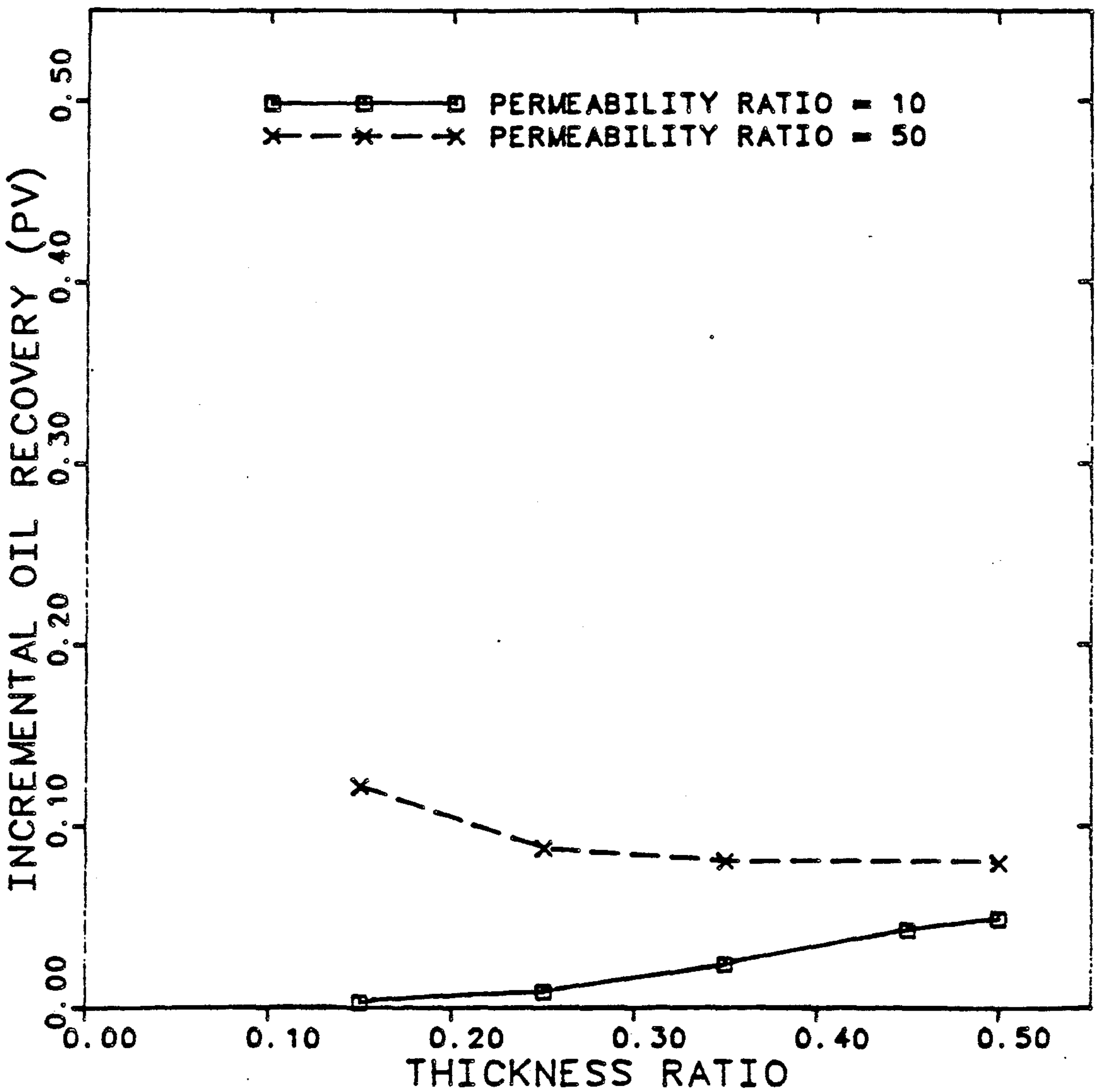

FIG. 37 DEPENDENCE OF INCREMENTAL OIL RECOVERY ON THE LEVEL OF REDUCED PERMEABILITY
Permeability of the top layer = 200.0 md
Permeability of the bottom layer = 20.0 md

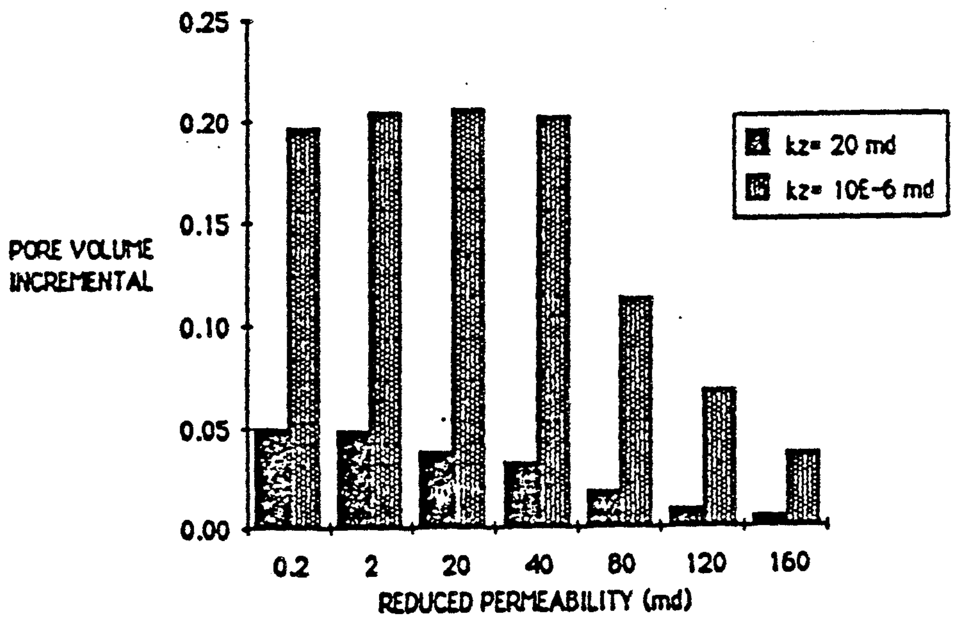

In several cases where the incremental recovery was found to be low, some possible benefits of a vertical conformance treatment were observed due to the fact that smaller volumes of injected water were needed to recover oil. Table 19 illustrates the injected water volume, oil recovery, and actual time needed to reach the water-oil ratio limit of 10 in cases where the incremental oil recovery due to treatment was less than 0.01 reservoir pore volume. In every case, the water volumes injected are decreasing as the level of reduced permeability increases and the simulated treatments result in decreased water volumes to reach the ultimate oil recovery. Due to the lower injectivity after treatment, however, the time required to reach the final oil recovery was longer for the treated reservoir than the untreated reservoir. Therefore, unless water treating and lifting costs were exceptionally high, it is not likely that vertical conformance treatments would be economically beneficial in these cases.

TABLE 19
CUMULATIVE PRODUCTION FOR LOW RECOVERY CASES

k_1 = 200 md

k_2 = 20 md

KH	KZ	Injected water (p.v.)				Produced oil (p.v.)				Time (day)			
		untreated	Permeability reduction 1/10	1/100	1/1000	untreated	Permeability reduction 1/10	1/100	1/1000	untreated	Permeability reduction 1/10	1/100	1/1000
5.4	10^{-6}	1.646	0.966	0.568	0.521	0.502	0.507	0.507	0.500	431	470	514	529
3.3	10^{-6}	1.385	0.857	0.559	0.525	0.507	0.507	0.507	0.505	455	486	491	526
1.8	10^{-6}	1.063	0.733	0.551	0.530	0.506	0.507	0.505	0.503	472	498	518	523
3.3	0.02	1.268	0.879	0.653	0.624	0.499	0.504	0.505	0.504	419	493	539	544
1.8	0.02	0.991	0.760	0.632	0.614	0.500	0.504	0.505	0.504	442	511	536	538
3.3	20	0.949	0.844	0.810	0.806	0.485	0.492	0.492	0.494	356	476	512	516
1.8	20	0.804	0.745	0.734	0.732	0.496	0.498	0.499	0.499	409	509	530	532

CHAPTER VI

Field Case Study

In this chapter we discuss a field case run in which actual reservoir properties were used. Unlike the two-layer oil-water system reservoir studied in previous chapter, a five-layer three-phase system reservoir is modeled in this chapter with three major stages, depletion, waterflooding, and vertical conformance treatment . In the depletion stage, the system was dominated by two-phase (gas-oil) flow. Before and after the conformance treatment, the flow region of waterflooding was either three-phase flow or two-phase (water-oil) flow. During the whole simulation run , since the fluid flow region may change , the interpretation of relative permeability of each phase is very important in terms of their effects on the simulation results. A scheme to interpret the relative permeability of each phase in a three-phase system (discussed in section 4.4) is applied here. Besides, due to the instability of solution in this case run, a scheme to implicitly treat source term is applied as well (discussed in section 4.5). Realizing these two additional modifications were applied , we are able to discuss the implementation of the field case in the next section , and then present the results and the discussions at the end.

6.1 Implementation of the Field Case

Studies were made with a two dimension cross-sectional model.

The reservoir was 800 feet horizontally and 32 feet thick with zero dip. A 10 by 5 grid system was used as shown in Fig.38. The grid size in x direction is 80 feet for each grid. The width in y direction was varied at 25, 88, 198, 342, 355, 355, 342, 198, 88, and 25 feet for each grid. The thickness in Z direction was varied at 6, 8, 8, 6, and 4 feet for each layer. The horizontal permeability of each layer was 26, 102, 160, 360, and 2.4 md from top to bottom, and the vertical permeability was approximately zero.

The reservoir was assumed to be in capillary and gravity equilibrium initially and then started to deplete. In the depletion stage, wells located at each end of the system started producing at a constant bottomhole pressure of 1300 psi and was followed by a stepwise decrease in bottomhole pressure until a pressure of 50 psi had been reached. In our simulation run, it was 300 days elapsed time from the very beginning. Then, one of the production wells was converted to an injection well with a constant rate of 60 STB/DAY, while the other well remained at the same producing bottomhole pressure of 50 psi. Treatment around the injection well took place at an elapsed time of 1609 days (1309 days since waterflooding) at which time the water oil ratio in the production well had reached 20. To study the effect of conformance treatment, three different ratios of permeability reduction in two candidate layers were investigated. Following the treatment, waterflooding was continued to WOR value up to 25. Finally, the result of oil recovery was compared with the case in which there is no treatment throughout the simulation run.

Fluid and rock properties used are listed in Tables 20 to 23 and Table 3 , where two different sets of relative permeability were used in input instead of only one being used in the original BOAST program.

Fig. 38 Reservoir grid system for field case

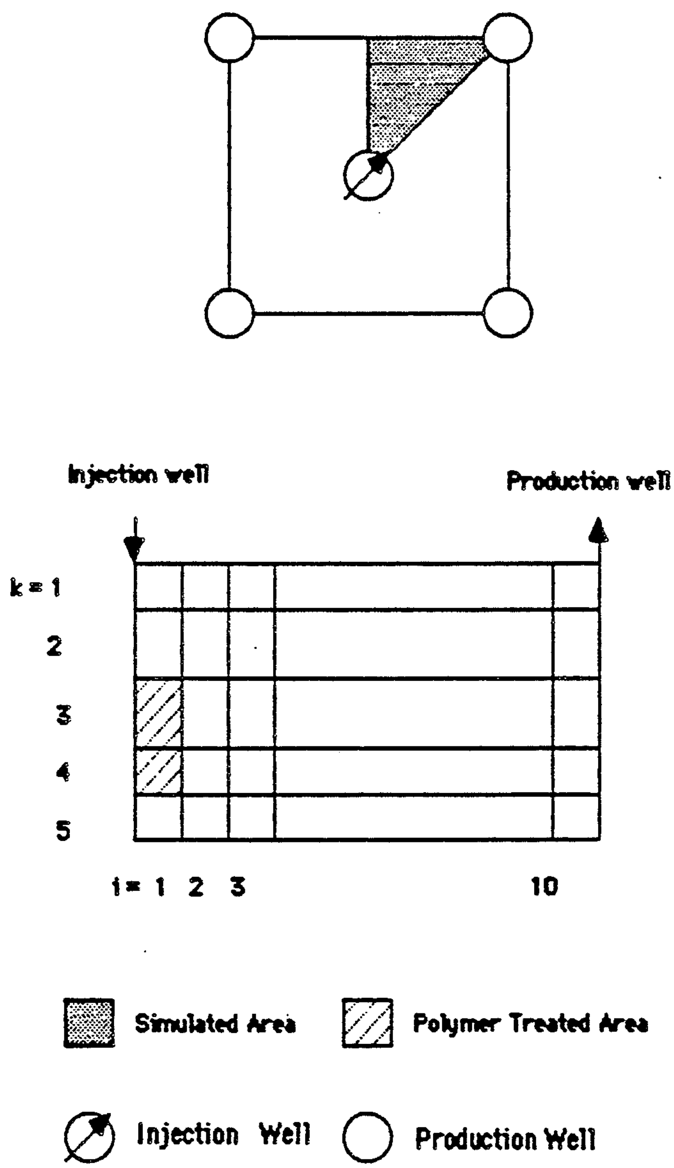

TABLE 20

RESERVOIR AND FLUID PROPERTIES

Initial reservoir pressure, psia at 3900 ft.	1405
Bubble point pressure, psia	1405
Injection well, rate constraint, STB/DAY	60
Production well, pressure constraint, psia	50
Rock compressibility, psi^{-1}	4×10^{-6}
Wellbore radius, feet	0.33
Capillary pressure, psi	0
Water density, lbm/cu ft	66.800
Oil density, lbm/cu ft	48.000
Gas specific gravity	0.0534

TABLE 21

PVT PROPERTIES OF OIL

Reservoir Pressure (psia)	Viscosity (cp)	Formation Volume Factor (RB/STB)	Solution Gas Ratio (cu ft/STB)
50.0	2.52	1.030	5.00
100.0	2.41	1.036	17.01
200.0	2.25	1.046	43.00
300.0	2.13	1.057	68.00
400.0	1.97	1.069	93.00
500.0	1.85	1.080	119.00
600.0	1.74	1.091	145.00
700.0	1.64	1.102	170.00
800.0	1.56	1.114	196.00
900.0	1.48	1.125	220.00
1000.0	1.41	1.136	247.00
1100.0	1.34	1.148	272.00
1200.0	1.28	1.158	298.00
1300.0	1.23	1.170	323.00
1405.0	1.182	1.182	350.00
1600.0	1.108	1.203	400.00
1795.0	1.045	1.225	450.00
1990.0	1.000	1.247	500.00

TABLE 22
PVT PROPERTIES OF WATER

Reservoir Pressure (psia)	Viscosity (cp)	Formation Volume Factor (RB/ STB)	Solution Gas Ratio (cu ft/STB)
50.0	0.64	1.017	0.00
1405.0	0.64	1.014	0.00
2000.0	0.64	1.012	0.00

TABLE 23
PVT PROPERTIES OF GAS

Reservoir Pressure (psia)	Viscosity (cp)	Formation Volume Factor (RB/STB)
50.0	0.0112	0.3302
127.0	0.0113	0.1291
254.0	0.0115	0.0629
382.0	0.0117	0.0410
510.0	0.0119	0.0301
638.0	0.0121	0.0236
766.0	0.0124	0.0191
894.0	0.0128	0.0163
1022.0	0.0132	0.0140
1150.0	0.0136	0.0124
1277.0	0.0140	0.0107
1405.0	0.0145	0.0095
2000.0	0.0168	0.0067

Seven runs were made in this field case. An auto timestep controller was applied in all these runs. To minimize the problem of rate convergence and assure the stability of solution, the maximum pressure change per time step was set to 40 psi, and maximum saturation change per time step to 0.05.

6.2 Results and Discussions

The effectiveness of treatment in this field case was determined by comparing the oil recovery in stock tank barrel at water oil ratio of 25 between treatment cases and base case. The base case is defined as no permeability modification occurs during a complete simulation. Whereas in the other cases, the injection grid block(blocks) of the candidate layer(layers) is (are) reduced to 1/10th , 1/100th, 1/1000th of the original permeability. The candidate layers here are two highest permeability zones of 360 and 160 md.

All the results are presented in Table 24, and several plots related to the comparison are discussed below.

Fig. 39 to 41 represent the production history comparison for each case. If we compare the result at a certain time after treatment, apparently, a two-layer treated case with a high level of permeability reduction increases the oil recovery but reaches the WOR limit sooner than a one-layer treated case.

Fig. 42 to 44 show the oil rate change due to treatment. Consequently, we conclude that high reduction of permeability increases the oil rate immediately.

TABLE 24

RESULTS OF CONFORMANCE TREATMENT IN THE FIELD CASE

	Total Time (DAY)	Water Injected (STB)	Oil Produced (STB)	Oil Increment (STB)	Average Injection Rate (STB/DAY)
case 1	2123.0	108500.0	20350.0		59.5
case 2	2321.0	120100.0	20990.0	640.0	59.4
case 3	2382.0	123700.0	21060.0	710.0	59.4
case 4	2495.0	130200.0	21640.0	1290.0	59.3
case 5	2419.0	125600.0	21490.0	1140.0	59.3
case 6	2480.0	129300.0	21680.0	1330.0	59.3
case 7	2368.0	122400.0	21510.0	1160.0	59.2

Note :

case 1 None Treatment (Base Case)

case 2 Factor of permeability reduction is 1/10th, 4th layer treated

case 3 Factor of permeability reduction is 1/10th, 3rd and 4th layers treated

case 4 Factor of permeability reduction is 1/100th, 4th layer treated

case 5 Factor of permeability reduction is 1/100th, 3rd and 4th layers treated

case 6 Factor of permeability reduction is 1/1000th, 4th layer treated

case 7 Factor of permeability reduction is 1/1000th, 3rd and 4th layers treated

FIG. 39 COMPARISON OF PRODUCTION HISTORY BETWEEN
TWO TREATMENT SCHEMES AND NONE TREATMENT CASE
WATERFLOODING START AT 300.0 DAYS
TREATMENT START AT 1609.0 DAYS (WOR=20.0)
PERMEABILITY REDUCTION IS FACTOR OF 10

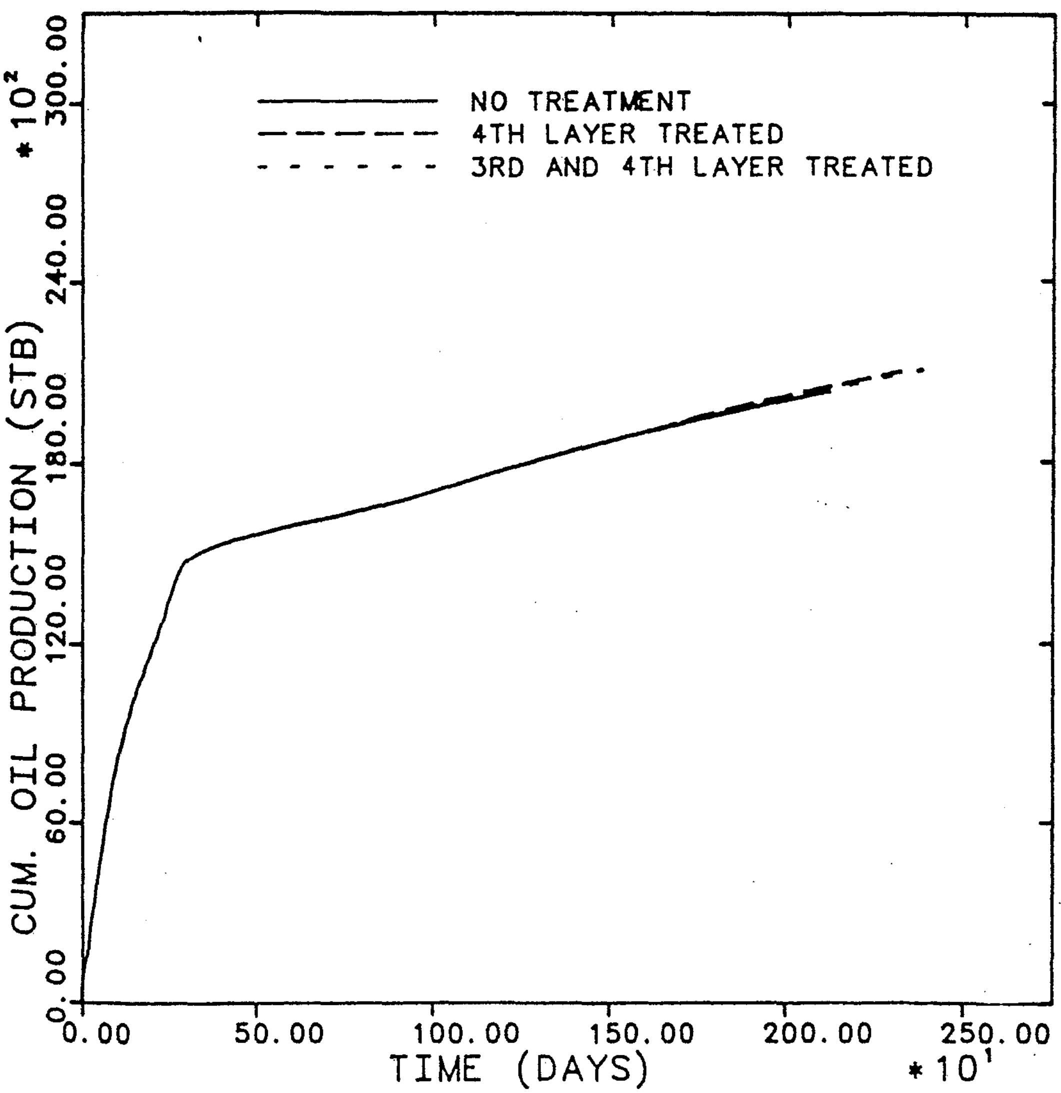

FIG. 40 COMPARISON OF PRODUCTION HISTORY BETWEEN
TWO TREATMENT SCHEMES AND NONE TREATMENT CASE
WATERFLOODING START AT 300.0 DAYS
TREATMENT START AT 1609.0 DAYS (WOR=20.0)
PERMEABILITY REDUCTION IS FACTOR OF 100

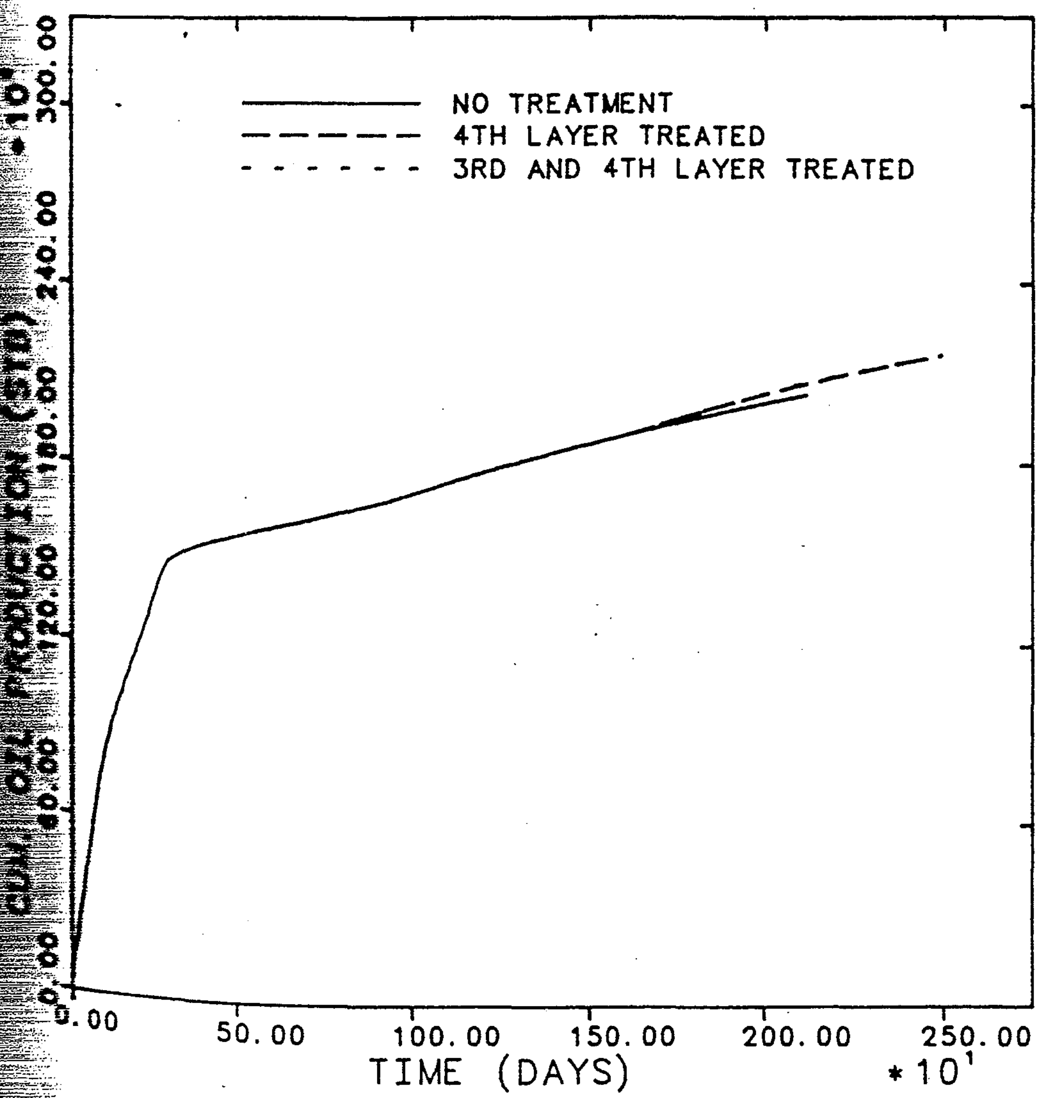

FIG. 41 COMPARISON OF PRODUCTION HISTORY BETWEEN
TWO TREATMENT SCHEMES AND NONE TREATMENT CASE
WATERFLOODING START AT 300.0 DAYS
TREATMENT START AT 1609.0 DAYS (WOR=20.0)
PERMEABILITY REDUCTION IS FACTOR OF 1000

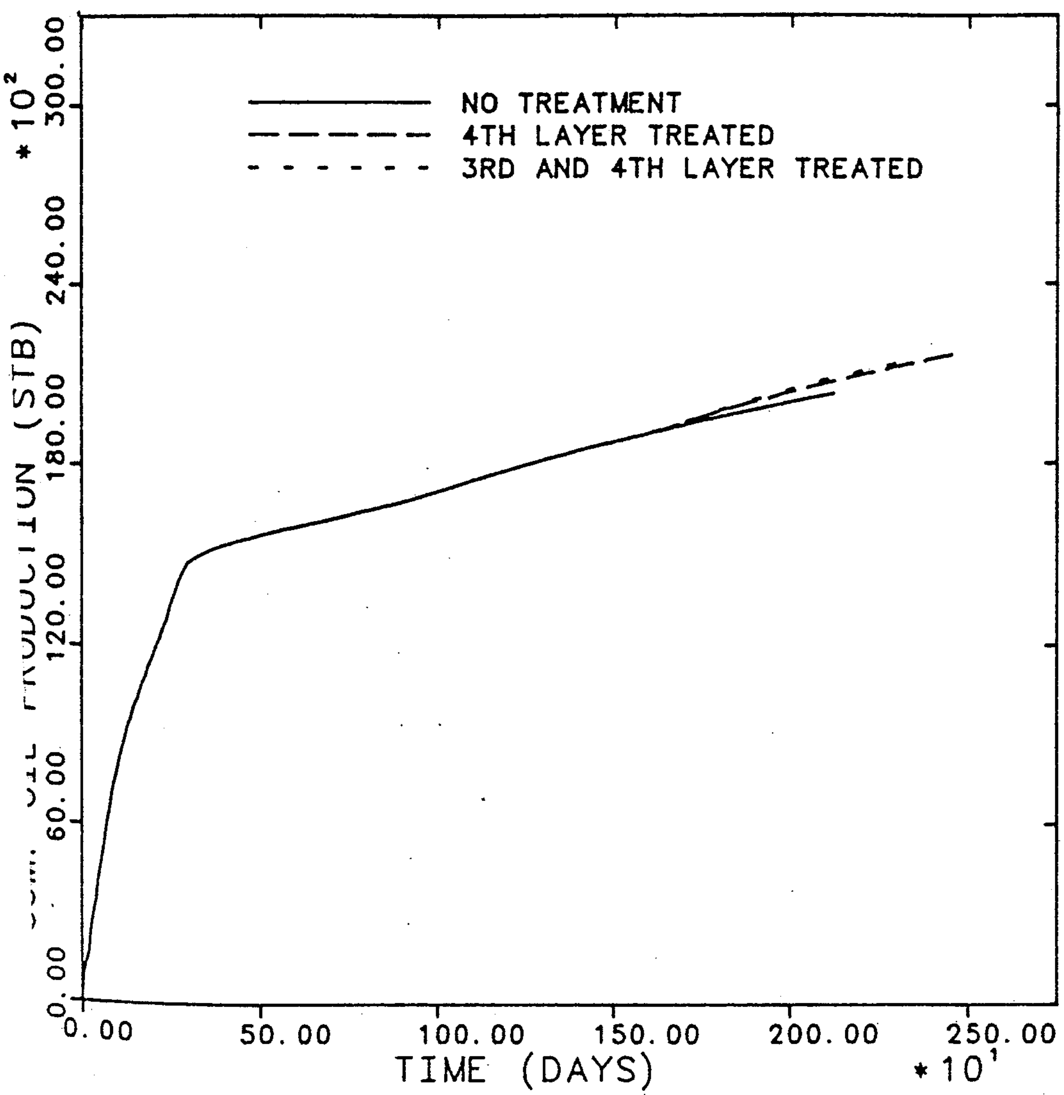

FIG. 42 COMPARISON OF OIL PRODUCTION RATE BETWEEN
TWO TREATMENT SCHEMES AND NONE TREATMENT CASE
WATERFLOODING START AT 300.0 DAYS
TREATMENT START AT 1609.0 DAYS (WOR=20.0)
PERMEABILITY REDUCTION IS FACTOR OF 10

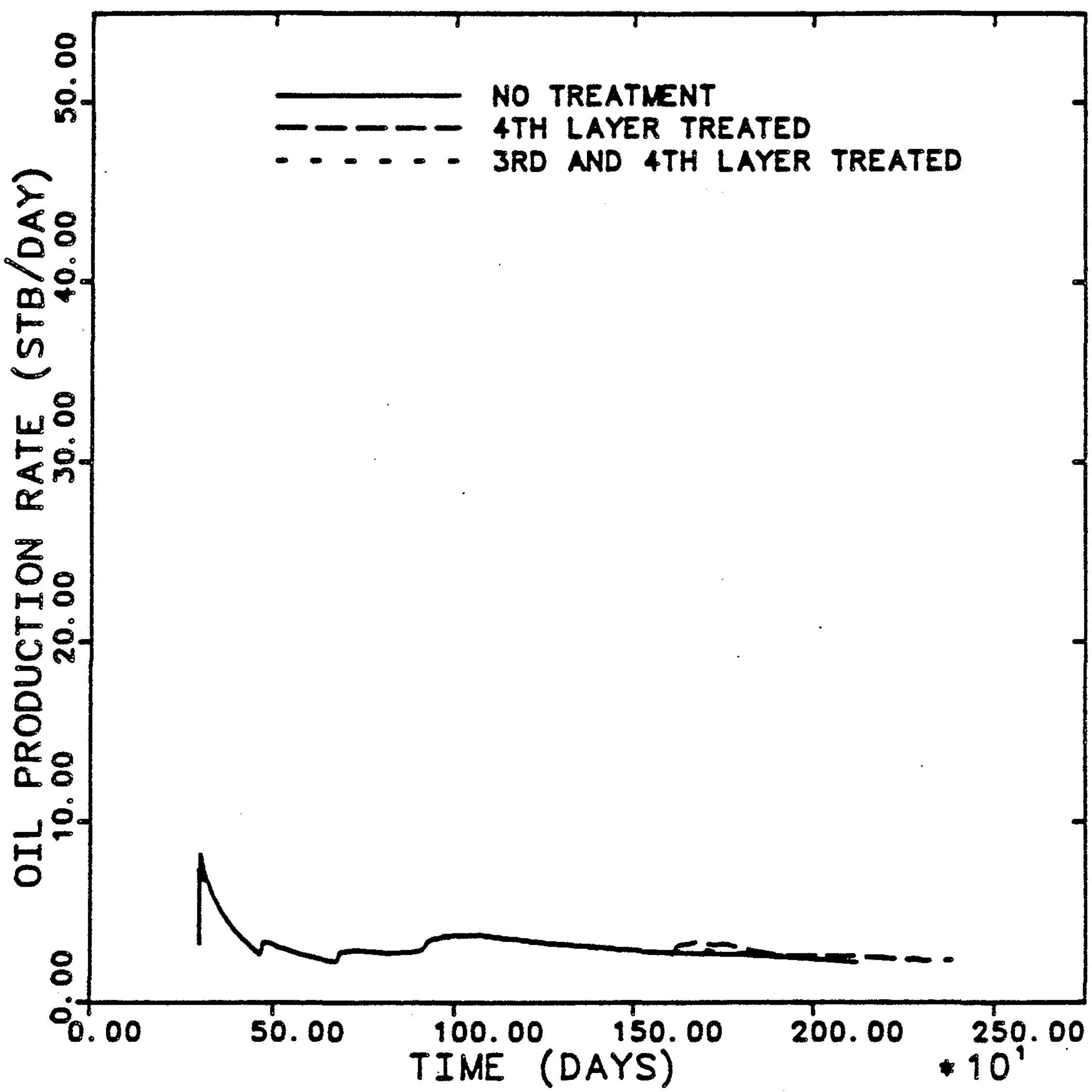

FIG. 43 COMPARISON OF OIL PRODUCTION RATE BETWEEN TWO TREATMENT SCHEMES AND NONE TREATMENT CASE
WATERFLOODING START AT 300.0 DAYS
TREATMENT START AT 1609.0 DAYS (WOR=20.0)
PERMEABILITY REDUCTION IS FACTOR OF 100

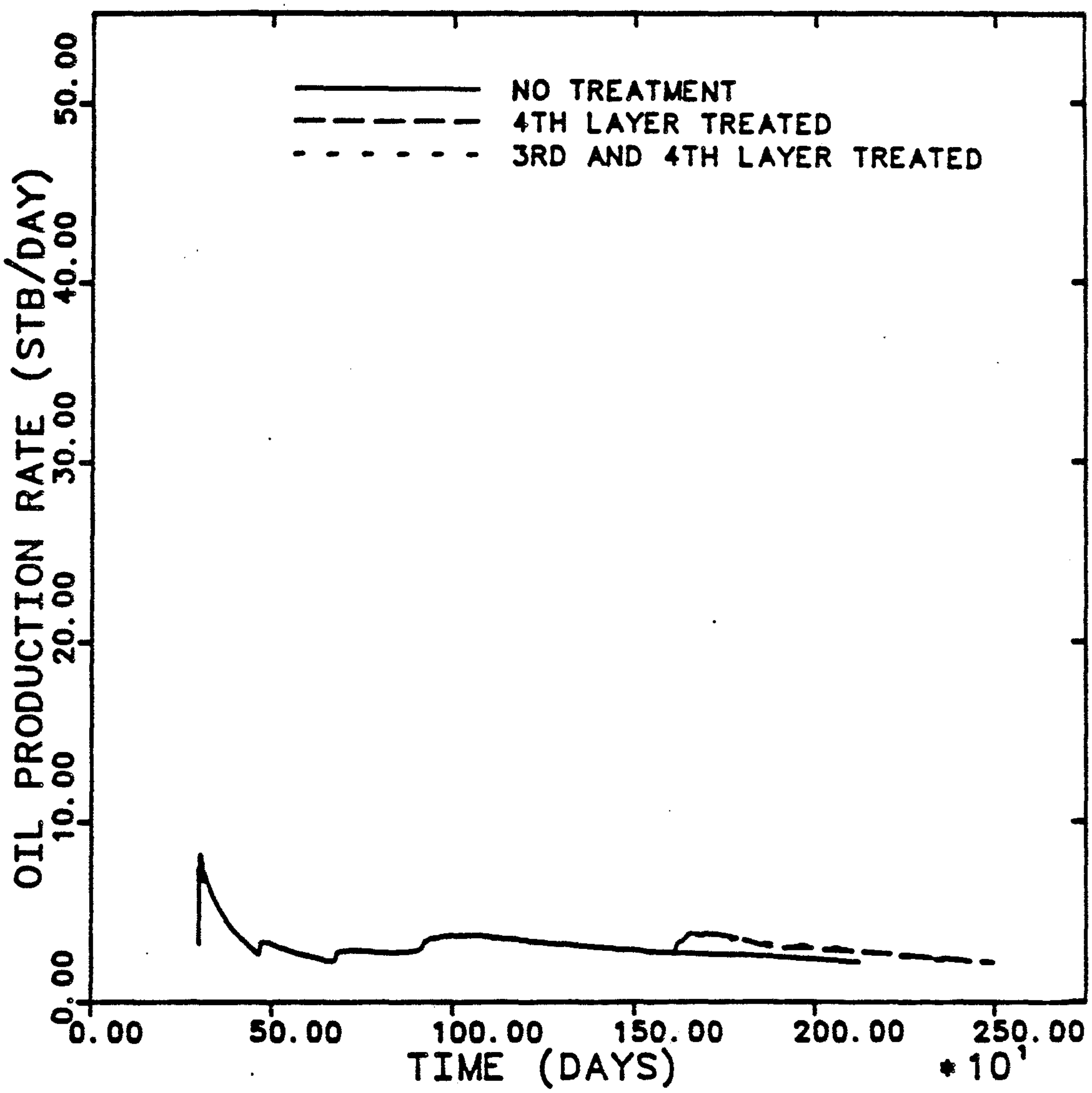

FIG. 44 COMPARISON OF OIL PRODUCTION RATE BETWEEN TWO TREATMENT SCHEMES AND NONE TREATMENT CASE
WATERFLOODING START AT 300.0 DAYS
TREATMENT START AT 1609.0 DAYS (WOR=20.0)
PERMEABILITY REDUCTION IS FACTOR OF 1000

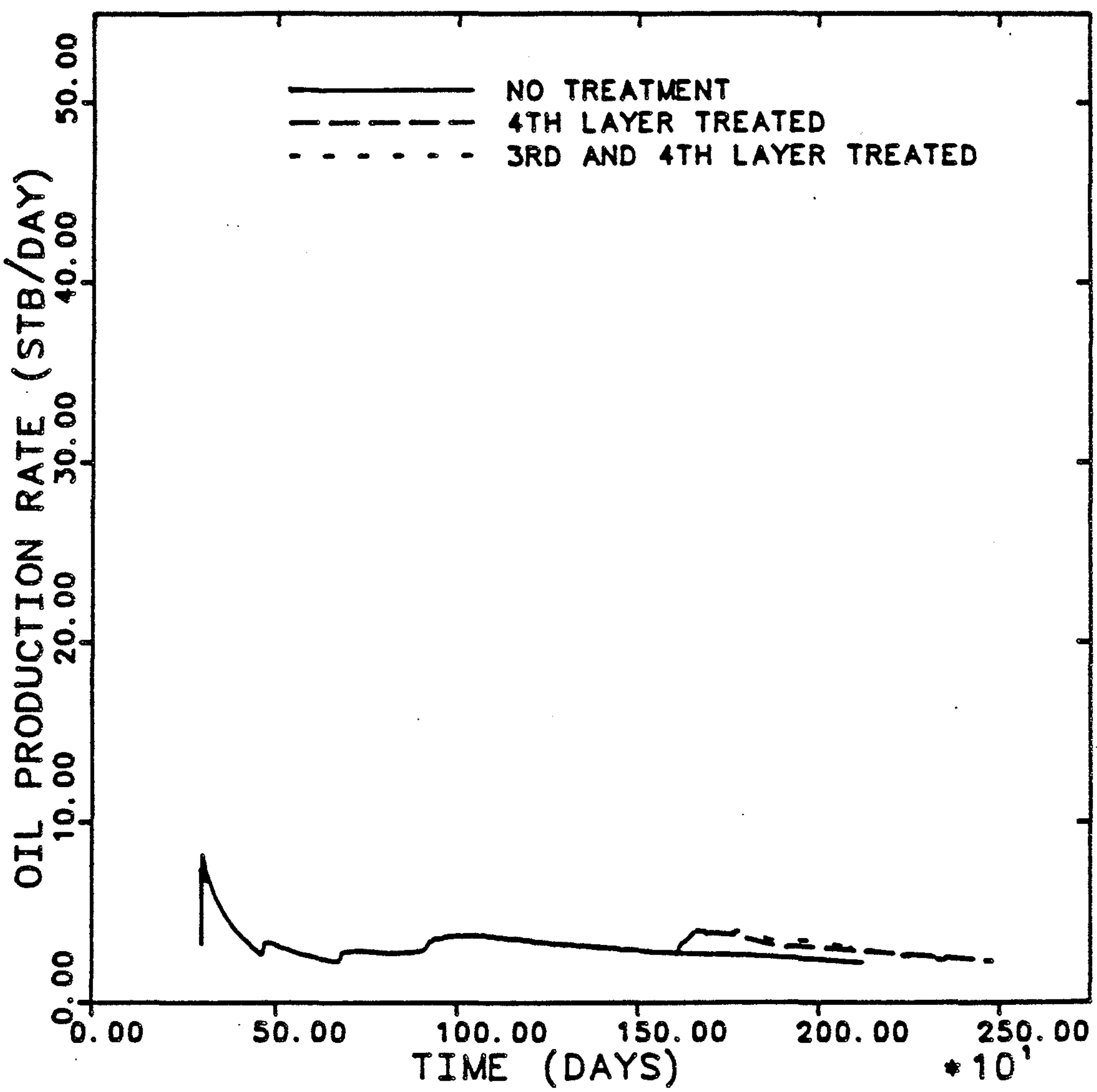

Fig. 45 to 47 present the bottomhole pressure of the injection well after the waterflooding had started at the 300th day. Before the 300th day, the bottomhole pressure shown in these plots was of production well when it had not been converted into injection well. These plots also show that pressure of the injection well resulted from treatment will increase, and the more severe the reduction of permeability is, the higher the injection well pressure becomes.

Fig. 48 to 50 present the average reservoir pressure. They have the same trends as injection well bottomhole pressure .

Fig. 51 to 53 are plots of water oil ratio changes. The water oil ratio decreased and then increased again. The degree of changes depends on the scheme of treatment.

As shown in Table 24, oil recovery increases for each treatment case. When the level of permeability of reduction increased, the oil recovery increment increased as well. However, there is a little sensitivity among the high level permeability reduction cases, and the number of layers being treated plays a significant role in these cases. As seen in Table 24, case 3, a low level permeability reduction with two-layer treatment gains much more oil incremental than case 2, one-layer treatment; but case 4 and case 6, high level permeability reduction with one-layer treatment, gain a larger oil increment than case 5 and case 7. These differences resulted from the redistribution of water injected due to the conformance treatment. For a low level conformance treatment, water can still enter the candidate zones. In the case of one layer (the highest permeability zone of 360 md), the dominant zones for water entry become the layers of 160 md and 102 md, and thus, the sweep in these zones is accelerated. It results in the water oil ratio

FIG. 45 COMPARISON OF BOTTOMHOLE PRESSURE BETWEEN TWO TREATMENT SCHEMES AND NONE TREATMENT CASE
WATERFLOODING START AT 300.0 DAYS
TREATMENT START AT 1609.0 DAYS (WOR=20.0)
PERMEABILITY REDUCTION IS FACTOR OF 10

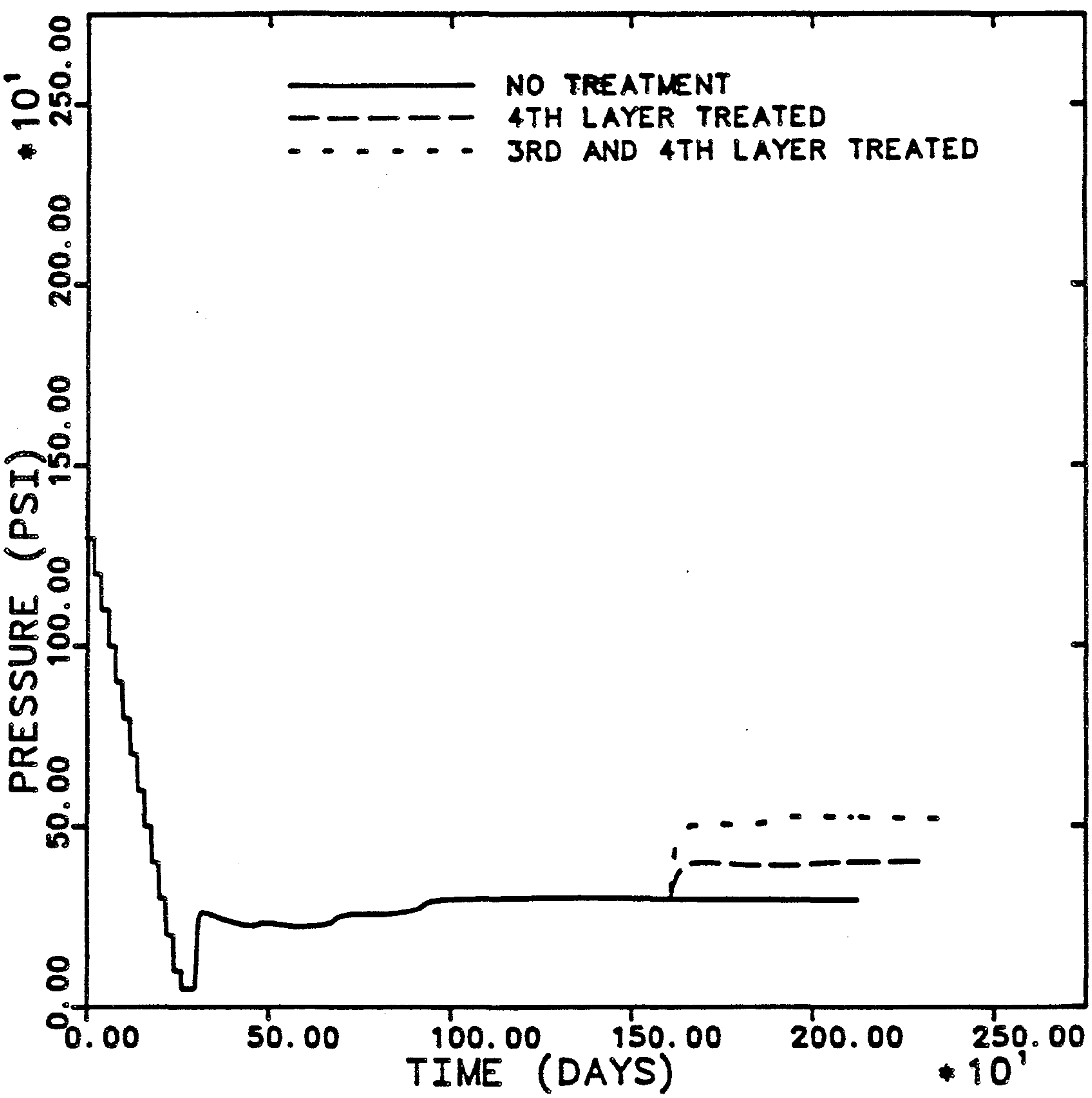

FIG. 46 COMPARISON OF BOTTOMHOLE PRESSURE BETWEEN
TWO TREATMENT SCHEMES AND NONE TREATMENT CASE
WATERFLOODING START AT 300.0 DAYS
TREATMENT START AT 1609.0 DAYS (WOR=20.0)
PERMEABILITY REDUCTION IS FACTOR OF 100

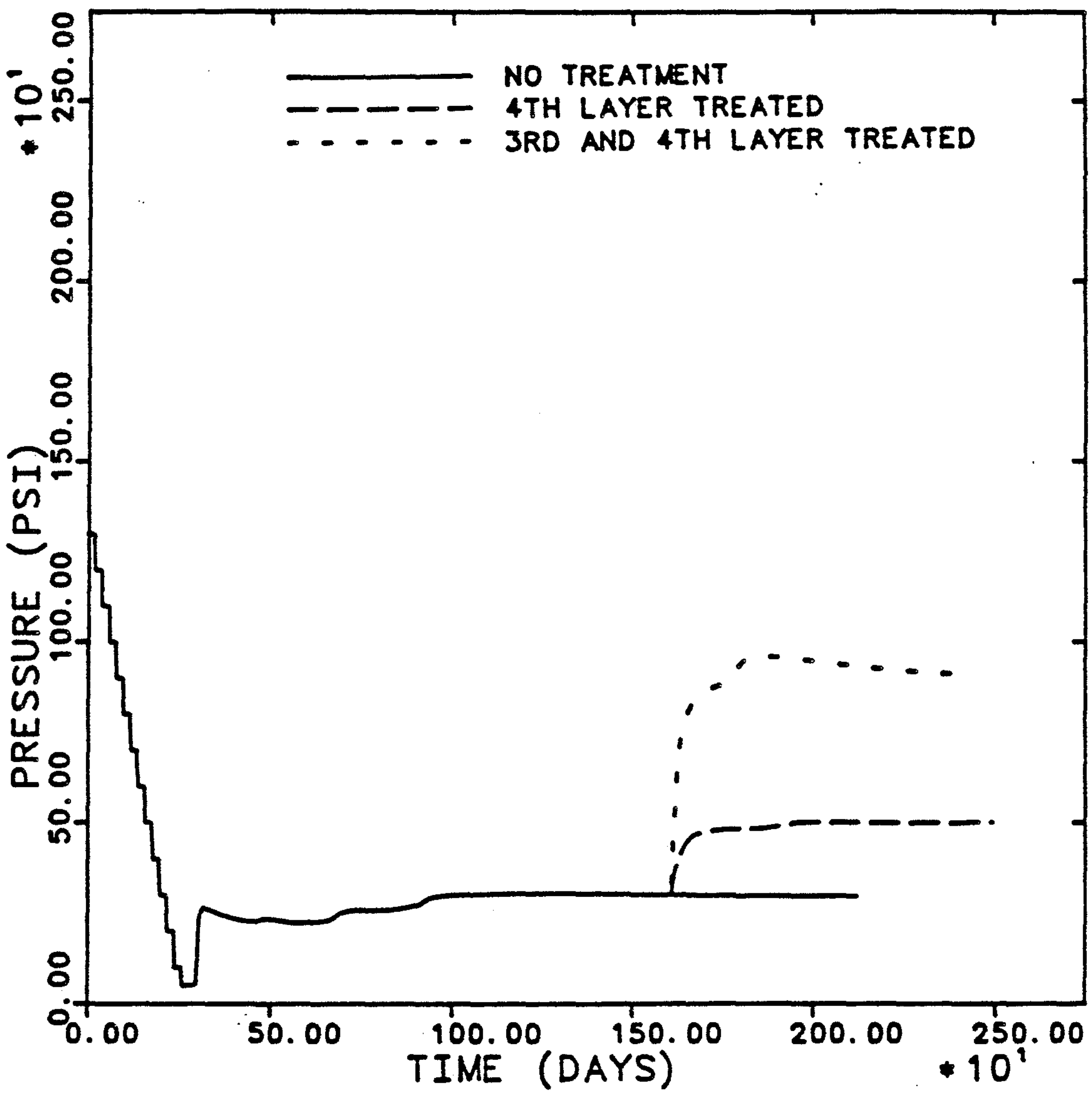

FIG. 47 COMPARISON OF BOTTOMHOLE PRESSURE BETWEEN
TWO TREATMENT SCHEMES AND NONE TREATMENT CASE
WATERFLOODING START AT 300.0 DAYS
TREATMENT START AT 1609.0 DAYS (WOR=20.0)
PERMEABILITY REDUCTION IS FACTOR OF 1000

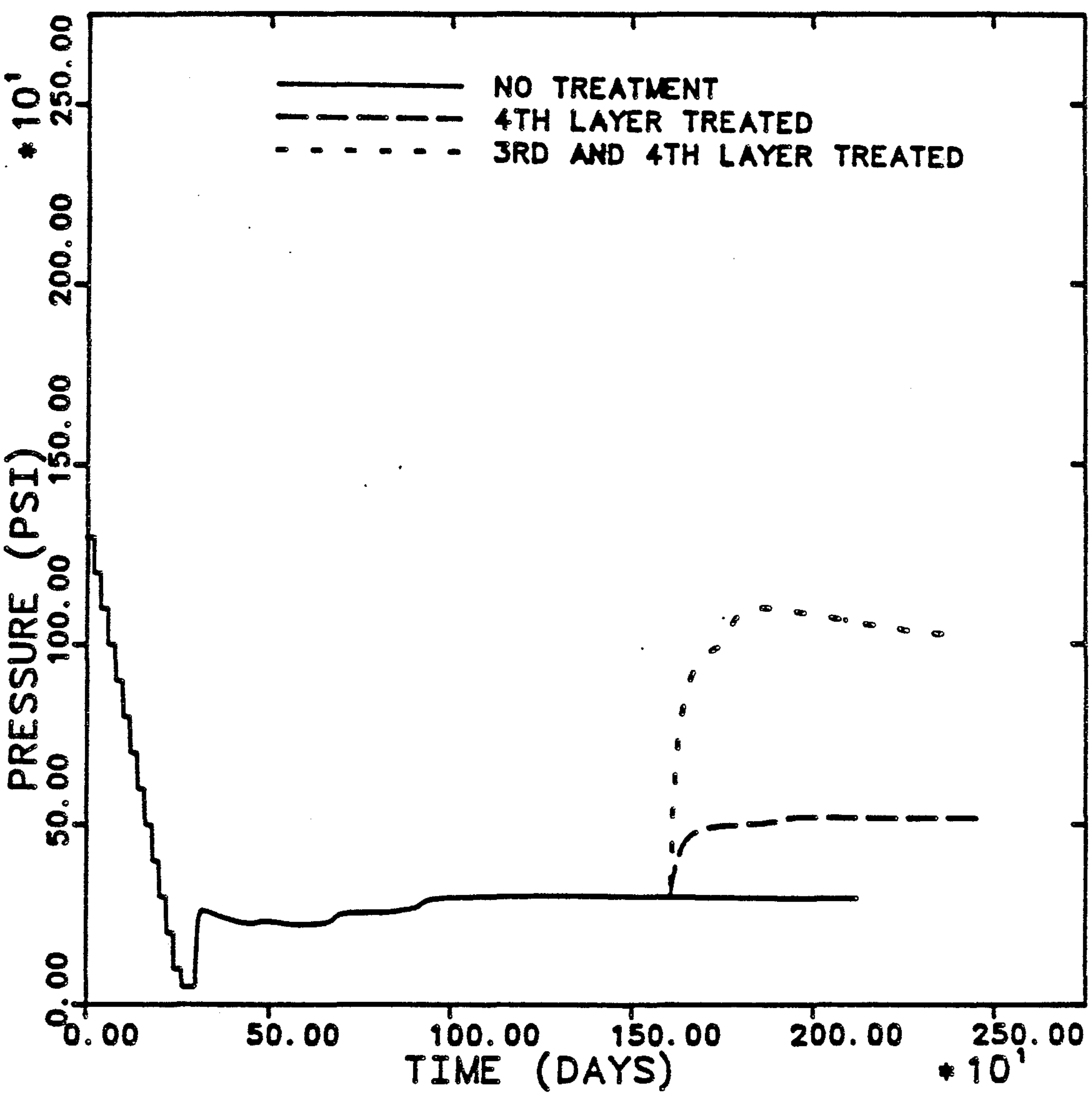

FIG. 48 COMPARISON OF AVERAGE PRESSURE BETWEEN TWO TREATMENT SCHEMES AND NONE TREATMENT CASE
WATERFLOODING START AT 300.0 DAYS
TREATMENT START AT 1609.0 DAYS (WOR=20.0)
PERMEABILITY REDUCTION IS FACTOR OF 10

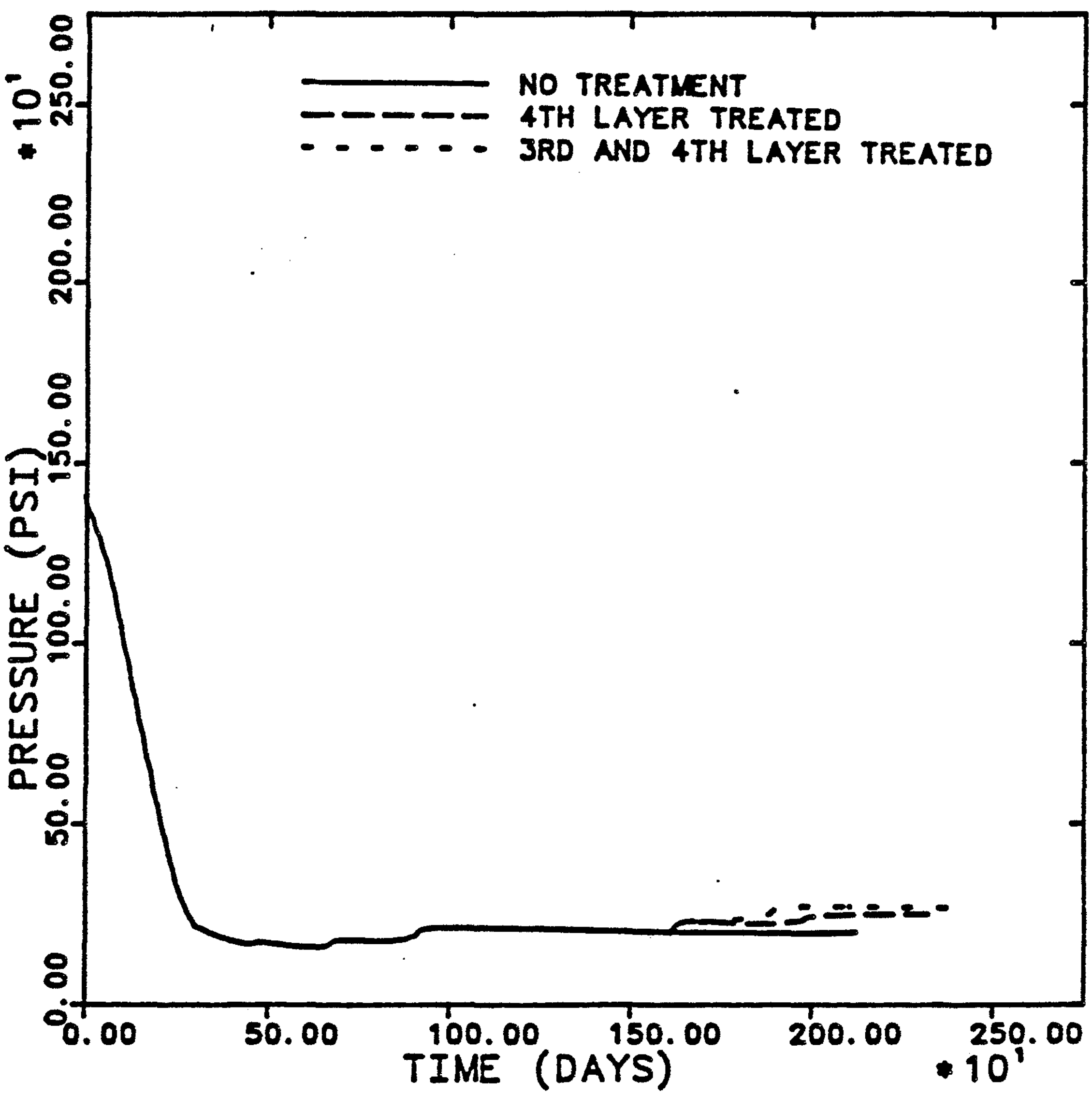

FIG. 49 COMPARISON FO AVERAGE PRESSURE BETWEEN TWO TREATMENT SCHEMES AND NONE TREATMENT CASE
WATERFLOODING START AT 300.0 DAYS
TREATMENT START AT 1609.0 DAYS (WOR=20.0)
PERMEABILITY REDUCTION IS FACTOR OF 100

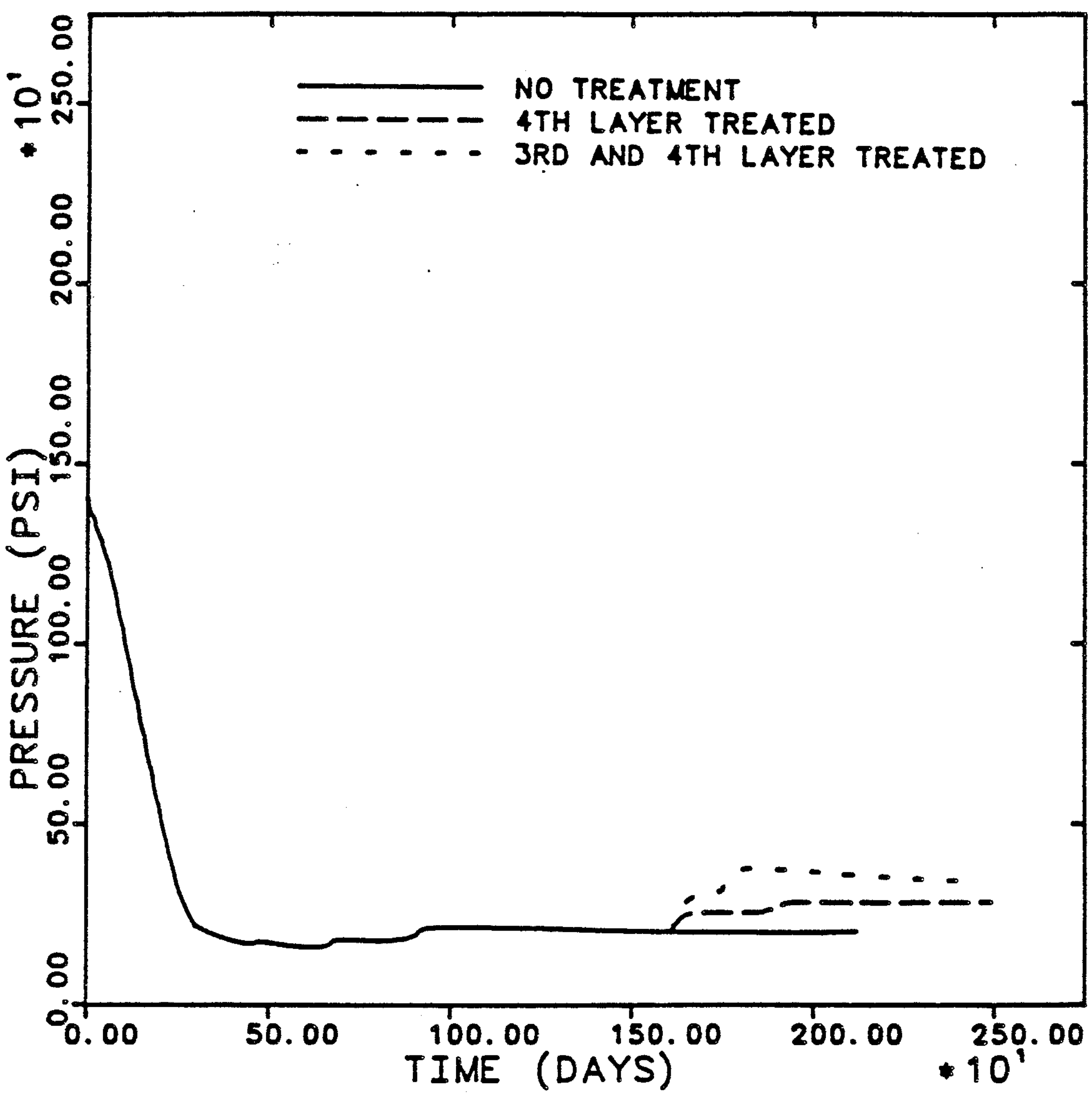

FIG. 50 COMPARISON OF AVERAGE PRESSURE BETWEEN TWO TREATMENT SCHEMES AND NONE TREATMENT CASE
WATERFLOODING START AT 300.0 DAYS
TREATMENT START AT 1609.0 DAYS (WOR=20.0)
PERMEABILITY REDUCTION IS FACTOR OF 1000

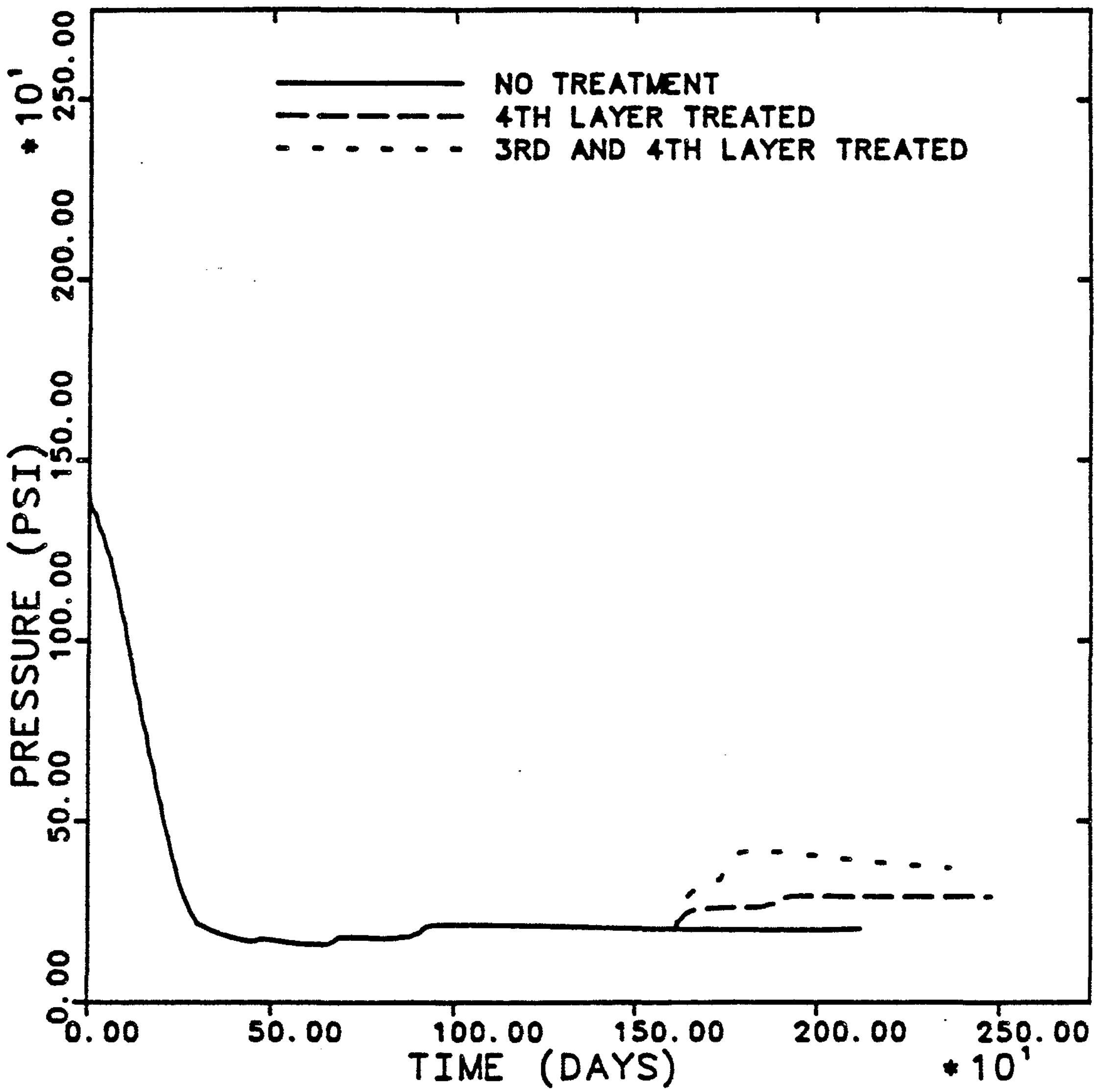

FIG. 51 COMPARISON OF WATER OIL RATIO BETWEEN
TWO TREATMENT SCHEMES AND NONE TREATMENT CASE
WATERFLOODING START AT 300.0 DAYS
TREATMENT START AT 1609.0 DAYS (WOR=20.0)
PERMEABILITY REDUCTION IS FACTOR OF 10

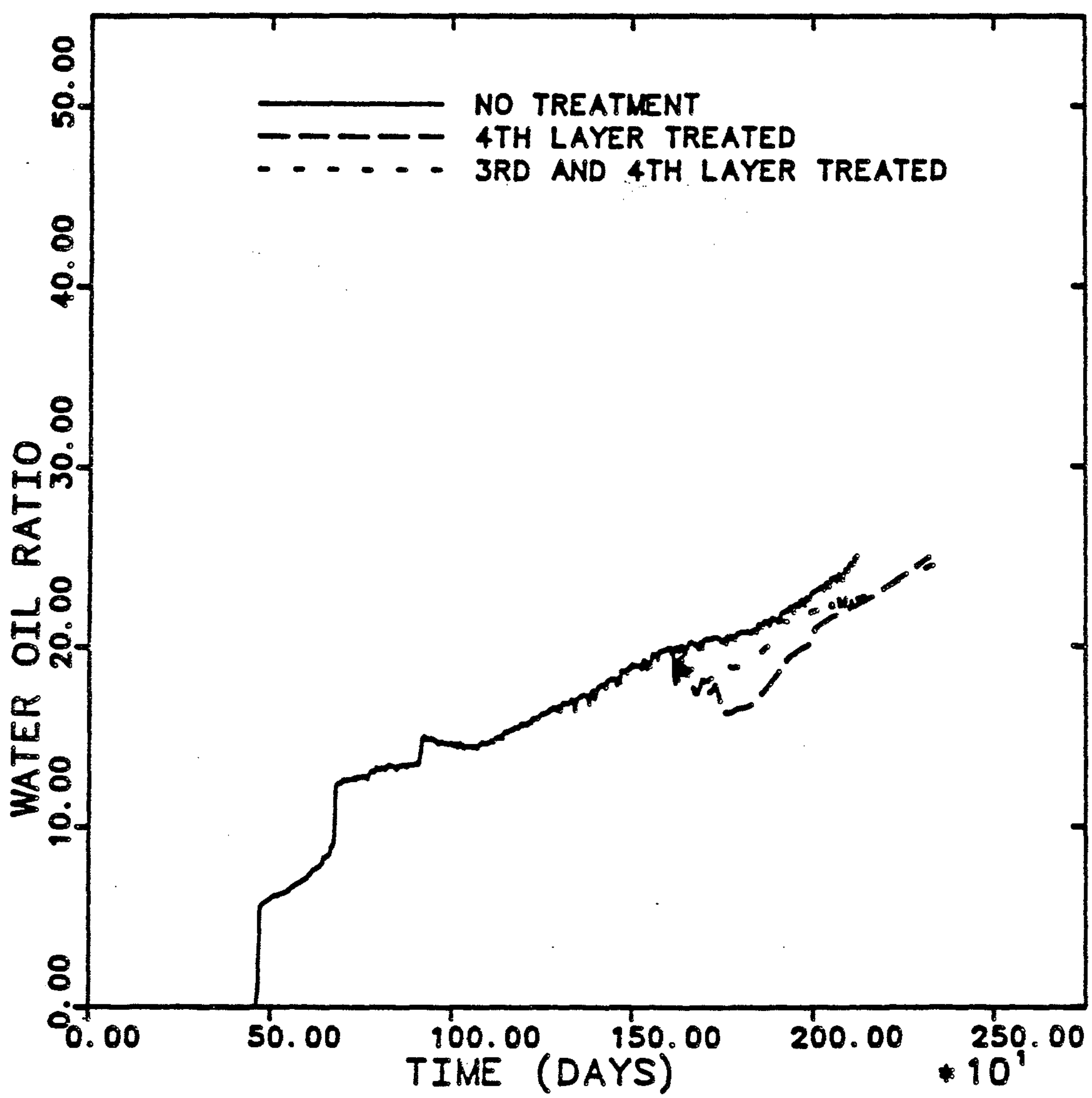

FIG. 52 COMPARISON OF WATER OIL RATIO BETWEEN TWO TREATMENT SCHEMES AND NONE TREATMENT CASE
WATERFLOODING START AT 300.0 DAYS
TREATMENT START AT 1609.0 DAYS (WOR=20.0)
PERMEABILITY REDUCTION IS FACTOR OF 100

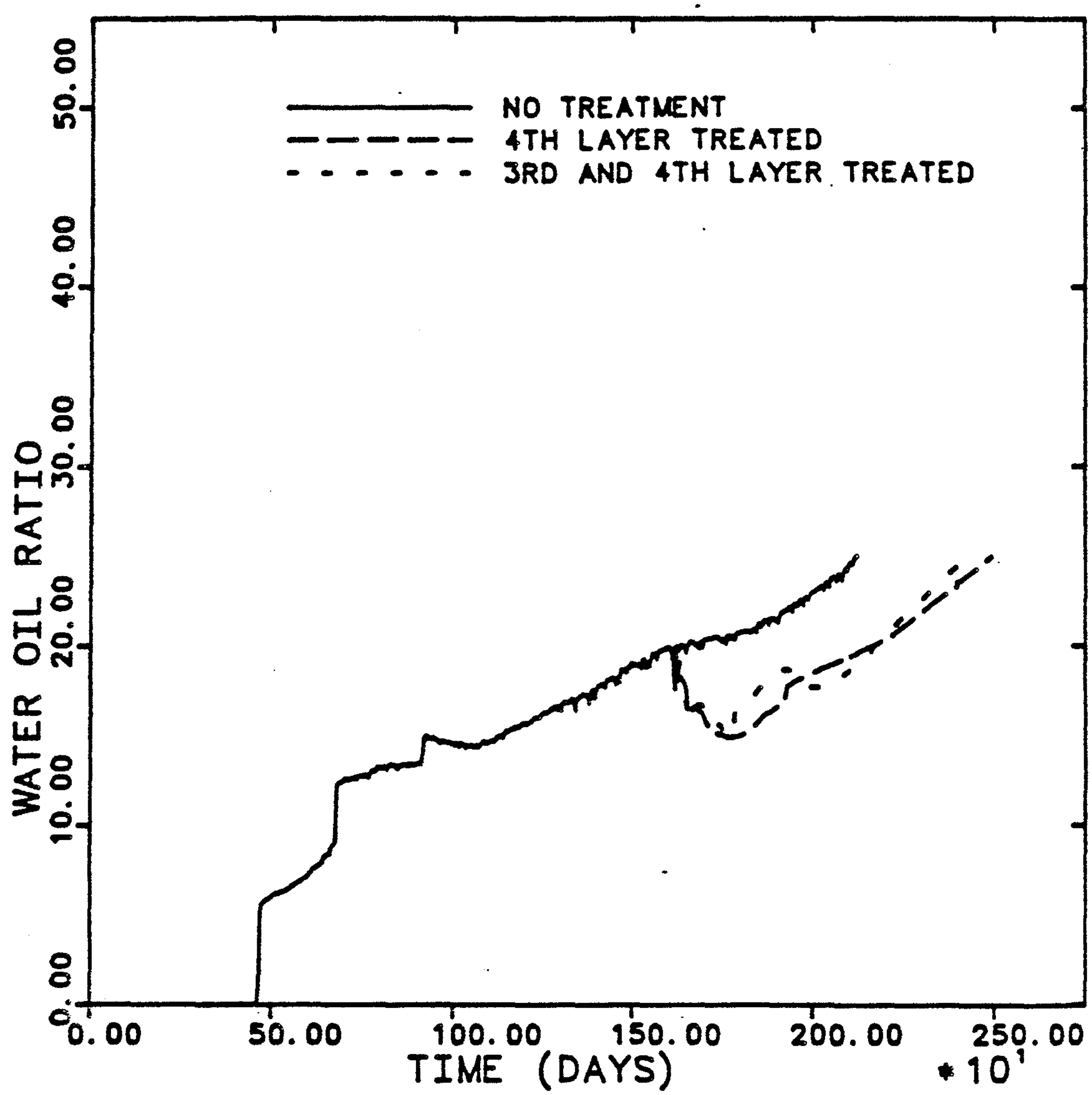

FIG. 53 COMPARISON OF WATER OIL RATIO BETWEEN
TWO TREATMENT SCHEMES AND NONE TREATMENT CASE
WATERFLOODING START AT 300.0 DAYS
TREATMENT START AT 1609.0 DAYS (WOR=20.0)
PERMEABILITY REDUCTION IS FACTOR OF 1000

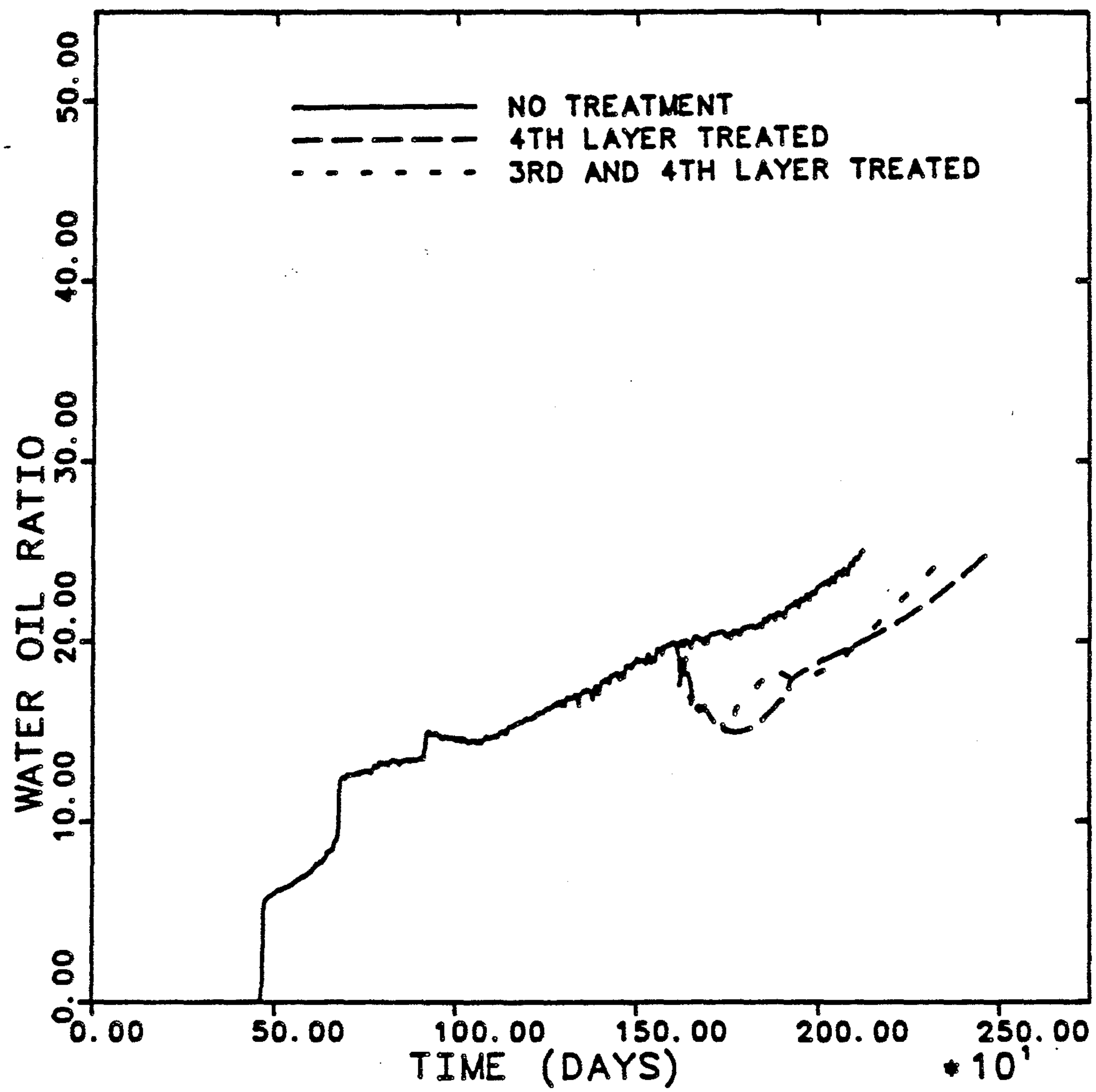

increasing rapidly and oil recovery declining. But, in high level conformance treatment, when two layers are treated, the remaining layers of 26 md and 102 md take in almost all the water. It prevents recovery of some remaining oil in layers of high permeability , and the water oil ratio limit of 25 was reached soon. Therefore, the cases of two-layer treatment with high level permeability reduction gain less oil recovery increment than cases of one-layer treatment. Nevertheless, as far as the amount of injection water is concerned, the two-layer treatment scheme needs less water than one-layer treatment scheme .

In the same table, the rightmost column shows the average rate for injection needed. As we claimed before, to get the rate as prescribed, rate convergence needs to be checked. Without incorporating an iteration method to calculate the rate, we alternatively minimize the rate deviation by setting the pressure change per time step size to 40 psi and obtain a good result. Because the average rate of 59 STB/DAY compared to prescribed rate 60 STB/DAY, the deviation is within an acceptable range. Besides, the average time step size also increased from 0.01 day to 1.0 day.

From this case study, not only can we conclude that this reservoir is a good candidate for conformance treatment, but also we can apply several conclusions attained in Chapter V to confirm the following facts:

(1) This layered reservoir is a good candidate for conformance treatment due to its low vertical permeability.

(2) This layered reservoir needs high level conformance treatment due to its high horizontal permeability contrast.

(3) Though little sensitivity of oil increment exists among the high level conformance treatments, there is a significant difference in water injection.

Besides, we also found that :

(1) To simulate a three-phase fluid flow system, an approach to interpret the relative permeability of medium wetting phase (oil) is needed.

(2) To handle a severe permeability contrast problem like this field case, treating the source terms implicitly can improve the stability of pressure solution and enlarge the time step size from 0.01 day to 1.0 day.

CHAPTER VII

CONCLUSIONS AND RECOMMENDATIONS

The following conclusions have been drawn from this thesis:

(1) The DOE BOAST program, with necessary modifications, was a useful tool for studing vertical conformance treatments.

(2) Two rate allocation methods were examined, with the potential rate allocation method being chosen because it proved to be suitable for layered reservoirs which have small vertical permeability.

(3) Implicitly solving the rate terms in a simulator which treats pressure explicitly can improve the solution stability.

(4) A low level of reservoir crossflow was conducive to high incremental oil recovery from a vertical conformance treatment. Also, significant incremental recovery was obtained in cases with relatively high vertical permeability.

(5) Incremental recoveries from a profile control treatment generally increased as the ratio of the permeability thickness product of the high permeability zone to that of the low permeability zone increased. For some cases with high permeability contrast between zones(50 to 1), this trend was reversed.

(6) Incremental recovery from a vertical conformance treatment increased when the permeability contrast between layers increased.

(7) In cases where a vertical conformance treatment resulted in little or no incremental recovery, smaller volumes of injected water were needed to recover a a given amount of oil in the treated case than in the untreated case. The benefit of this reduced water volume is questionable because of the reduced injectivity of the treated well.

(8) Incremental oil recovery from a vertical conformance treatment was not sensitive to the level of permeability reduction in the treated zone as long as the treated permeability was as low or lower than the permeability of the low permeability reservoir layer.

(9) The layered reservoir investigated in the field case is a good candidate for conformance treatment due to its very low vertical permeability and high horizontal permeability contrast.

The conclusions forementioned are due to permeability reduction that is done arbitrarily. For further investigation of polyacrylamide conformance treatments, this restriction needs to be relaxed -- a realistic placement needs to be modeled. Not only should the simulator be able to take into account the properties of the polymer solution, the effects of degradation and retention of placement , but it should also be extended to simulate a three dimensional reservoir performance.

NOMENCLATURE

Symboles

AB	coefficient of matrix formula for bottom side of grid
AE	coefficient of matrix formula for east side of grid
AN	coefficient of matrix formula for north side of grid
AS	coefficient of matrix formula for south side of grid
AT	coefficient of matrix formula for top side of grid
AW	coefficient of matrix formula for west side of grid
A_g	phase transimissibility of gas
A_o	phase transimissibility of oil
A_w	phase transimissibility of water
B	righthand side vector in matrix formula
B_g	formation volume factor of gas
B_o	formation volume factor of oil
B_w	formation volume factor of water
C_g	gas compressibility
C_o	oil compressibility
C_r	rock compressibility
C_t	total compressibility
C_w	water compressibility
D	depth
E	coefficient of matrix formula for center of grid

FCOEF	modified coefficient
F_k	flow coefficient
f_w	water fractional flow
g	gravity constant
h	layer thickness
k	absolute permeability
$\bar{K}$	dispersion tensor
k_{rg}	relative permeability of gas
kro	relative permeability of oil in three-phase system
k_{row}	relative permeability of oil in water-oil system
k_{rog}	relative permeability of oil in gas-oil system
k_{rw}	relative permeability of water
N_i	flux term of component i
p	pressure
P_{cgo}	capillary pressure of gas to oil
P_{cow}	capillary pressure of oil to water
p_k^w	bottomhole pressure at corresponding kth layer
p_u^w	bottomhole pressure at uppermost layer
q	volumetric flow rate
$q_{\ell k}$	volumetric flow rate for phase ℓ in kth layer
Q_T	total volumetric flow rate
QVG	volumetric flow rate of gas
QVO	volumetric flow rate of oil
QVW	volumetric flow rate of water
R_i	source term for component i
R_s	solution gas oil ratio

r_w	radius of wellbore
s	skin factor
S^*	normalized phase saturation
S_g	gas saturation
S_o	oil saturation
S_{or}	residual oil saturation
S_w	water saturation
S_{wc}	connate water saturation
Δt	difference in time changes
V_B	bulk volume
V_P	pore volume
u	volumetric velocity
u_T	total volumetric velocity .
w_{ij}	mass fraction of component i in phase j
W_i	accumulation term of component i
Δx	grid size in x direction
Δy	grid size in y direction
Δz	grid size in z direction

Greek Symbols

β_w	factor used to determine oil relative permeability in three phase system
β_g	factor used to determine oil relative permeability in three phase system
Υ	specific gravity

λ	mobility
ρ	density
Φ	flow potential

Operators

$\vec{\nabla}$	gradient operator
$\vec{\nabla}\cdot$	divergence operator
$\sum$	summation opreator
∂	partial differentiation
d	total differentiation

Subscripts

i	component index or x-direction node index
j	phase index or y-direction node index
k	z-direction node index
ℓ	phase index
L	total number of layers
M	total number of phases
s	rock surface
sc	standard condition
u	uppermost node
x	x-direction
y	y-direction
z	z-direction

1,2,3	fluid 1,2,3

Superscripts

n	old time level
n+1	new time level
w	wellbore

APPENDIX

The general flow diagram outlining the whole program is :

Nonrecurrent Section

REBOAST.DAT

Initial Run

Read in system dimension

KPHI.DAT

Read in permeability, porosity

Calculate grid block pore volume
and constant part of transimissibility

Read fluid properties and relative
permeability data

INITIAL.DAT

Read in initial condition indicating
the pressure and satuation distribution

Specify the solution method

Recurrent Section

RESTART.DAT

Restart Run

MODKPHI.DAT

Read in permeability changed

REBOAST.DAT

Read in information needed

Recurrent Section

Note : Contents of $\boxed{}$ indicates the datafile to be needed

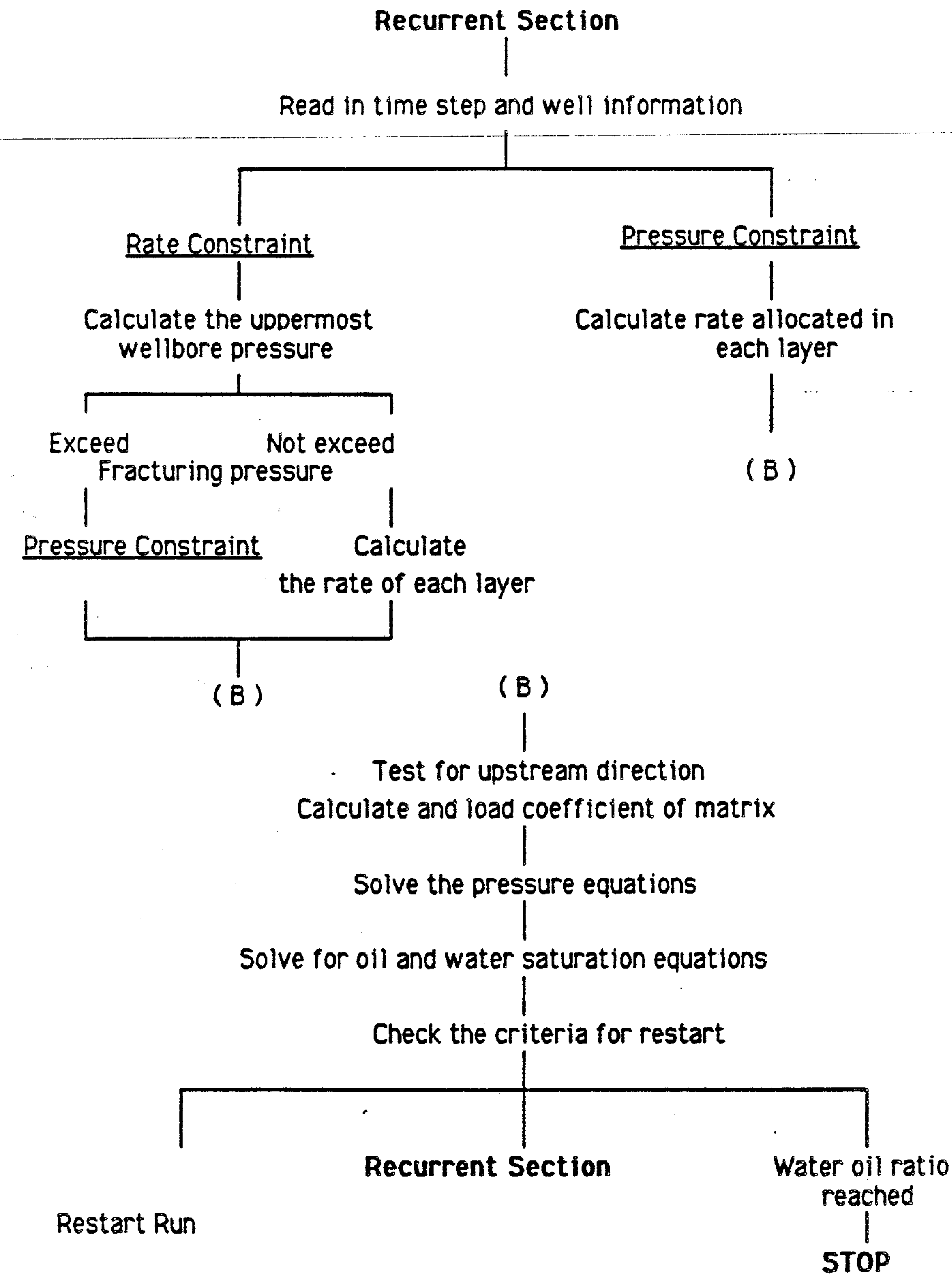
Recurrent Section
Read in time step and well information
Rate Constraint
Pressure Constraint
Calculate the uppermost wellbore pressure
Calculate rate allocated in each layer
Exceed
Not exceed
Fracturing pressure
(B)
Pressure Constraint
Calculate the rate of each layer
(B)
(B)
Test for upstream direction
Calculate and load coefficient of matrix
Solve the pressure equations
Solve for oil and water saturation equations
Check the criteria for restart
Recurrent Section
Water oil ratio reached
Restart Run
STOP

REFERENCES

1. Downs, S. L. and Gohel, M. K.: "Injection Profile Connections-A Review of Workover Techniques-Willard Unit," JPT, Vol.26, May 1974, p.557

2. Felsenthal, Martin, and Gangle, Francis, J.: "A Case Study of Thief Zones in a California Waterflood,"JPT, Vol.27, Nov. 1975, p.1385.

3. Froning, S. P. and Birdwell, B. F.: "Here's How Getty Controls Injectivity Profile in Ventura," Oil and Gas J., Feb.20, 1975, p.60

4. Garland, T. M.: "Selective Plugging of Water Injection Wells," JPT, Dec. 1956, p. 1550-1560

5. Peacock, Robert A.: "What Can Be Done to Improve Waterflooding," SPE 2546 presented at the 44th Annual Fall Meeting, Denver, Colo., Oct. 1969.

6. Sparlin, Derry: "An Evaluation of Polyacrylamides for Reducing Water Production," JPT, Vol. 28, Aug. 1976, p. 906-914

7. Mazzochi, E. F. and Carter, K. M " Channelblock Pilot Application- Weyburn Unit, Saskatchewan," JPT, Vol. 26, September 1974, p.973

8. Abdo, M. K., Chung, H. S. and Phelps, C. H : "Field Experience with Waterflood Diversion by Complexed Biopolymers," SPE/DOE 12642 presented at the SPE/DOE Fourth Symposium on Enhanced Oil Recovery, Tulsa, OK., April 15-18, 1984

9. Robertson, J. O., Jr. and Oefelein, F. H. "Plugging Thief Zones in Water Injection Wells," JPT, Vol. 19, August, 1967, p.999

10. Felber, Betty. J. and Dauben, Dwight L.: "Development of Lignosulfonate Gels for Sweep Improvement," SPE 6206 presented at 51st Annual Fall Meeting, New Orleans, LA Oct. 1976

11. Hess P. H. , Clark, C. O. , Haskin, C. A. , and Hull, T. R. "Chemical Method for Formation Plugging," JPT, Vol. 23, May 1971, p.559

12. Dykstra, H. and Parsons, R .L.: "The prediction of Oil Recovery by Water Flood," Secondary Recovery of Oil in the United States, 2nd ed., API(1950) p.160-174.

13. Schmalz, J. P. and Rahme, H. D. : "The Variation of Waterflood Performance With Variation in Permeability Profile," Prod. Monthly (1950) 15, No.9, p.9-12.

14. Stiles, W. E.: "Use of Permeability Distribution in Waterflood Calculation," Trans, AIME(1949) 186,p.9-13.

15. Miller, M. G. and Lente, M. R.: "Performance of Bodcaw Reservoir, Catton Valley Field Cycling Project: New Methods of Predicting Gas-Condensate Reservoir Performance Under Cycling Operations Compare to Field Data," Drill and Prod, Prac., API (1974) p.128-149.

16. Smith, F. W. : "The Behavior of Partially Hydrolyzed Polyacrylamide Solutions in Porous Media," JPT, Feb. 1970. p.48

17. Dovan, H. T. and Hutchins, R. D. : "Development of a New Aluminum-Polymer Gel System for Permeability Adjustment," SPE/DOE 12641 presented at the SPE/DOE Fourth Symposium on Enhanced Oil Recovery , Tulsa, OK., April 15-18, 1984.

18. Huang, Chyi-Gang, Green, D. W. and Willhite G. P. : "An Experimental Study of the In-Situ Gelation of Chromium (+3)-Polyacrylamide Polymer in Porous Media," SPE/DOE 12638 presented at the SPE/DOE Fourth Symposium on Enhanced Oil Recovery ,Tulsa, OK, April 15-18, 1984 .

19. Ford, W. O., Jr. and Kelldorf, W.F. N.: "Field Results of a Short Setting-Time Polymer Placement Technique," JPT, July 1976, p.749

20. Fitch, J. P. and Canfield, Carl M. : "Field Performance Evaluation of Cross-Linked Polymers to Increase Oil Recovery in the Wilmington Field, California," SPE 5366 Presented at the 45th California Regional Meeting, Ventura, Cal., April 1975.

21. Sandiford, B. B. and Graham, G. A. : "Injection of Polymer Solutions in Producing Wells," AIChe Symposium Series, Vol. 69, No. 127, p.40,1973

22. Routson, W. G. , Neale, M. and Penmton, J. R. " A New Blocking Agent for Waterflood Channeling," SPE 3992 presented at the 47th Annual Fall Meeting, San Antonio, TX, October 1972.

23. Needham, R. B. , Threlkeld, C. B. and Gall, J. W. : " Control of Water Mobility Using Polymers and Multivalent Cations," Paper SPE4747 presented at the Improved Oil Recovery Symposium of the SPE of AIME, Tulsa Okla., April 22-24, 1974.

24. Silva, Luis F. and Faroag Ali, S. M. : "Waterflood Performance in the Presence of Stratification and Formation Plugging," SPE 3556 Presented at the 46th Annual Fall Meeting, New Orleans, La., Oct. 1971

25. BETA II Black Oil Model, Version 2.2, Intercomp Resource Development and Engineering, Inc., July 1980.

26. Fanchi, J.R., Harpole, K.J., Bujnowski, S.W. : "Boast: A Three-dimensional, Three-press Black Oil Applied Simulation Tool," Vol.I and II. U.S. Department of Energy, Sept. 1982.

27. Aziz, K. and Settari, A. : Petroleum Reservoir Simulation , Applied Science Publishers Ltd., London (1979).

28. Nolen, James S. and Berry, D. W. : " A Study of the Reliability of a Semi-Implicit Reservoir Simulator," paper SPE 2981 presented at SPE 45th Annual Fall Meeting, Huston, Tex., Oct. 4-7, 1970.

29. Corey, A. T., Rathjens, C. H., Henderson, J. H. and Wyllie, M. R. J. : "Three-Phase Relative Permeability," Trans., AIME (1956) 207,349

30. Snell, R. W. : " Three-Phase Relative Permeability in an Unconsolidated Sand," J. Inst. of Pet. (1962) 84,80

31. Stone, H. L. : " Probability Model for Estimating Thre-Phase Relative Permeability ," JPT ,(Feb. 1970) p. 214-218.

VITA

Jyun-Syung Tsau was born in Taiwan, Republic of China, on June 22, 1956, the son of Mr. Bing-Shiang Tsau and Mrs. Arsho Jen. In June, 1978, he received his B.S. degree in Mining Engineering from Cheng Kung University at Taiwan. After finishing his military duties in Taiwan, he entered the Chinese Petroleum Corporation in October, 1980. During the following one and half years, he was employed as a Research Assistant Engineer at Exploration & Development Research Center. In December, 1981, he married Su-Hwa Hsu in Taiwan. In January, 1983, he entered the Graduate School of the University of Texas at Austin. His first daughter, Jennifer, was born at Austin in April, 1985.

Permanent Address : 18-2 Alley 4, Lane 781, Ming-Sheng East Road
Taipei, Taiwan
Republic of China

This Thesis was typed by the author on the Macintosh.